

Dissertation zur Erlangung des Doktorgrades
der Fakultät für Chemie und Pharmazie
der Ludwig-Maximilians-Universität München



Design of an Acid Labile Traceless-cleavable Click
Linker for Use in a Novel Protein Transduction Shuttle

vorgelegt von
Kevin Maier
aus Oberzell
2012

Erklärung

Diese Dissertation wurde im Sinne von § 7 der Promotionsordnung vom 28. November 2011 von Herrn Prof. Dr. Ernst Wagner betreut.

Eidesstattliche Versicherung

Diese Dissertation wurde eigenständig und ohne unerlaubte Hilfe erarbeitet.

München, den 30.08.2012

.....

(Unterschrift des Autors)

Dissertation eingereicht am: 13.09.2012

1. Gutachter: Prof. Dr. Ernst Wagner
2. Gutachter: Prof. Dr. Christian Plank

Mündliche Prüfung am: 17.10.2012

Meiner Familie

Indes sie forschten, röntgten, filmten, funkten,

entstand von selbst die köstlichste Erfindung:

der Umweg als die kürzeste Verbindung zwischen zwei Punkten.

Erich Kästner

1 Table of Contents

1	Table of Contents.....	5
2	Introduction	11
2.1	Macromolecular therapy - a brief survey	11
2.2	Barriers in macromolecular therapy.....	13
2.3	Nucleic acid versus protein delivery	17
2.4	Strategies for transporting proteins into the cytosol of living cells	19
2.5	Biological cleaveable crosslinkers	21
2.6	Aims of the thesis	23
2.6.1	Establishment of a cellular test system for protein delivery.....	23
2.6.2	Protein delivery with defined polycations	24
2.6.3	Development of a new traceless cleavable linker for protein delivery ...	25
3	Materials	27
3.1	Chemicals.....	27
3.2	Reagents.....	27
3.2.1	Dyes.....	27
3.2.2	Peptides.....	27
3.2.3	Linkers	27
3.3	Solvents.....	28
3.4	Buffers.....	28
3.5	Solutions.....	28
3.6	Cell culture material.....	28

Table of Contents	6
3.7 Cell lines.....	29
3.8 Bacteria strains.....	29
3.9 Nucleic acids	29
4 Methods	30
4.1 General chemical procedures.....	30
4.1.1 ¹ HNMR and ¹³ CNMR	30
4.1.2 Mass spectroscopy	30
4.1.3 CD spectroscopy.....	30
4.1.4 UV-Vis spectroscopy.....	31
4.1.5 Fluorescence spectroscopy	31
4.1.6 Chromatography	31
4.1.7 Dynamic light scattering (DLS).....	32
4.2 Synthesis.....	32
4.2.1 Synthesis of watersoluble hemicyanine alkyne dye	32
4.2.2 Synthesis of azide hemicyanine dye	34
4.2.3 Synthesis of N-propargyl maleimide	36
4.2.4 Synthesis of N-Succinimidyl-3-(2-pyridyldithio)-propionate (SPDP) ...	36
4.2.5 Synthesis of MAM linker	38
4.2.6 Synthesis of AzMMMan linker.....	39
4.2.7 Synthesis of PentyneMMMan linker.....	40
4.3 Cloning, heterologous expression and purification of nlsEGFP and HIV-TAT-nlsEGFP.....	42
4.4 Modification of proteins with crosslinkers	43
4.4.1 Modification with SPDP.....	43
4.4.2 Modification of nlsEGFP with succinimidyl-4-(<i>N</i> -maleimidomethyl)cyclohexane-1-carboxylate (SMCC)	44
4.4.3 Modification of nlsEGFP with MAM linker	44

4.4.4	Modification of HSA with PentyneMMan linker.....	44
4.4.5	Modification with AzMMMan linker.....	45
4.5	Coupling of carriers, dyes and PEG to the proteins.....	46
4.5.1	Coupling of G3 PPI to nlsEGFP via EDC.....	46
4.5.2	Coupling of G3 PPI to nlsEGFPx5SPDP via a reducible disulfide bond	47
4.5.3	Coupling of 386 to nlsEGFPx5SPDP	47
4.5.4	Coupling of 386 to β -galactosidasex8SPDP	48
4.5.5	Coupling of 386 to SMCC-nlsEGFP	48
4.5.6	Coupling of 386 to AzMMMan-nlsEGFP	48
4.5.7	Coupling of TMR labelled- 386 to AzMMMan-nlsEGFP	48
4.5.8	Coupling of 386 to AzMMMan- β -galactosidase	49
4.5.9	Coupling of poly(ethylene glycol) (PEG)	49
4.5.10	Coupling of alkyne hemicyanine dye to AzMMMan-HSA.....	50
4.5.11	Coupling of phosphine dye DyLight 488 to AzMMMan-HSA.....	50
4.5.12	Coupling of azide dye to PentyneMMan-HSA.....	51
4.5.13	Coupling of folic acid and melittin to AzMMMan-EGFP	51
4.5.14	Coupling of transduction oligomer 71 to MAM-EGFP	52
4.6	Characterization of new acid labile crosslinkers	52
4.6.1	Determination of the degree of protein modification.....	52
4.6.2	Determination of the acid catalyzed release of linker from the protein..	53
4.6.3	Serum stability assay	53
4.6.4	Release of PEG from HSA conjugate	54
4.6.5	Release kinetics of TMR-labeled PEG from HSA conjugate.....	54
4.6.6	Acid catalyzed release of nlsEGFP from 386-DBCO -AzMMMan-nlsEGFP.....	55
4.7	Biological characterization of the synthesized conjugates.....	56
4.7.1	General procedures	56

Table of Contents	8
4.7.2 Protein transductions	57
4.7.3 Endocytosis inhibition	59
4.7.4 Cell viability assay.....	59
4.7.5 Activity test of modified β -galactosidase	59
4.7.6 Erythrocyte leakage assay	60
5 Results	61
5.1 nlsEGFP as a model protein.....	61
5.1.1 Cloning, heterolog expression and purification of nlsEGFP and TAT-nlsEGFP.....	62
5.1.2 Microinjection of nlsEGFP and TAT-nlsEGFP.....	64
5.2 Protein transduction with TAT-nlsEGFP	66
5.3 Cationic lipid mediated protein delivery	68
5.4 Dendrimer based Protein Transduction	68
5.4.1 Synthesis of G3 PPI-nlsEGFP	68
5.4.2 Protein transduction with G3 PPI-nlsEGFP.....	70
5.4.3 Microinjection of G3 PPI-nlsEGFP	72
5.5 Protein transduction with G3PPI coupled to nlsEGFP over a bioreversible bond.....	73
5.5.1 Synthesis of G3PPI-SS-nlsEGFP	73
5.5.2 Protein transduction using G3PPI-SS-nlsEGFP.....	75
5.6 Protein transduction using the structure defined oligomer 386	77
5.6.1 Synthesis of reducible 386 modified nlsEGFP	77
5.6.2 Protein transduction with 386 -SS-nlsEGFP	79
5.6.3 Transduction of 386 -SS- β galactosidase	85
5.7 Development of acid labile, traceless heterobifunctional click linkers for protein delivery.....	88
5.7.1 Synthesis of MAM linker	88

Table of Contents	9
5.7.2 Acid lability of MAM linker	89
5.7.3 Synthesis of AzMMMan linker.....	91
5.7.4 Synthesis of water soluble alkyne hemicyanine dye	92
5.7.5 Modification of proteins with AzMMMan.....	93
5.7.6 Synthesis of PentyneMMMan crosslinker	106
5.7.7 Acid lability of PentyneMMMan linker	107
6 Discussion.....	109
6.1 Establishing of a cellular test system for protein delivery	109
6.2 Development of a sequence defined carrier system for protein delivery ...	110
6.3 Design of a traceless-cleavable linker for protein delivery.....	114
7 Summary.....	117
8 Abbreviations	119
9 Appendix.....	124
9.1 Plasmid Maps and Base Sequences.....	124
9.1.1 pc1068-pRHGPCNA	124
9.1.2 pET 23a(+).	128
9.1.3 pET 23a(+)-SV40nls-EGFP	131
9.1.4 pET 23a(+)-SV40nls-EGFP-HIVTAT.....	134
9.2 Amino Acid Sequences	137
9.2.1 SV40nls-EGFP.....	137
9.2.2 SV40nls-EGFP-HIVTAT.....	137
9.2.3 β -galactosidase.....	137
9.3 Analytic spectra	139
9.3.1 Alkyne hemicyanine dye	139
9.3.2 AzMMMan linker	140
9.3.3 PentyneMMMan linker	143
10 References	147

Table of Contents	10
11 Publications	159
11.1 Original papers.....	159
11.2 Book chapters	159
11.3 Poster presentations	160
12 Acknowledgements.....	161

2 Introduction

2.1 Macromolecular therapy - a brief survey

Today most of the drugs prescribed belong to a group of molecules smaller than 500 Da (1). In most cases, these small molecules can be obtained through direct chemical synthesis. Due to their small sizes and their partition coefficient, they are usually able to freely diffuse through the plasma membrane bilayer and get to their site of action. In general small molecules share a common mode of action. They are usually blocking the active site of a target molecule, either by covalent coupling or just by intermolecular interaction. Due to lack of specificity this often causes unwanted side effects and in consequence toxicity occurs. In contrast macromolecules, e.g. nucleic acids or proteins, in most cases exhibit high specificity for their target molecule. This is rooted in their complex structure. The complexity does not only reduce the risk of unwanted interactions, but primarily it opens the door for a large set of functionalities that cannot be mimicked by small molecules (2). Macromolecules, of rather high molecular weight and often multiple charged, are in most cases not able to overcome the cytoplasmic membrane. Because of this reason the application of macromolecular drugs is mainly limited to therapeutics, whose site of action is located extracellular or on the cell surface (3-7). The first clinical used macromolecular therapeutic was insulin which was extracted from bovine pancreas in 1922 by Lilly (8). Problems, like availability of pancreases for purification, high costs and immunological reactions of some patients hindered a widespread use. Although these problems could not be solved at this time, this successful application slowly shifted the focus of drug development from small molecules to macromolecular compounds. In the following 40 years many endogenous proteins with therapeutic potential have been identified (9, 10). But it took the development of recombinant DNA technique and modern biotechnology which enabled easy and cheap production of large amounts of recombinant proteins, leading to the explosion of the biopharmaceutical market. Aside low costs and easy scale up, recombinant produced proteins have got several therapeutic advantages compared to other protein sources. Due to the transcription and translation of the exact human gene, they lower the risk of immunogenic responses and often have got higher specific activity. Up to date nearly 100 recombinant proteins are approved by the FDA for clinical use (2). Plenty

of diseases, e.g. cystic fibrosis or Duchenne muscle dystrophy are the result of a mutation in a protein encoding gene. The growing knowledge in genetics and biotechnology also opened the door for gene therapy, a concept of treating such diseases on their molecular origin. The basic idea of gene therapy, replacing the deficient gene with a functional copy, arose during the 1960s and 1970s, when the first evidences for uptake of exogenous DNA in mammalian cells have been found (11, 12). From this point of time things went on quite fast. The first approved human gene therapy trial was performed by Rosenberg and colleagues in 1989. They used retroviruses to introduce a gene encoding for resistance to neomycin into human tumor-infiltrating lymphocytes prior to reinfusion into patients with advanced melanoma (13). Despite some severe backlashes, up to date more than 1700 clinical studies on human gene therapy are either in process or even have been finished (Gene Therapy Clinical Trials Database). Besides DNA, diverse other nucleic acids, like antisense RNAs (14), messenger RNAs (15), 2'-O-alkyl RNAs (16), aptamers (17), phosphorothioate DNAs (PS-DNA) (18), inosine-cytosine RNAs (polyIC) (19), decoy oligonucleotides (20), and LNAs (21) are in the clinical trial phase or are already used in macromolecular therapy. Among these nucleic acid based techniques, siRNA mediated RNA interference is rising particular hope, as it can be used for both up- (22) and down- regulation of a gene. Since Tuschel and coworkers (2001) showed that synthetic siRNAs can down regulate gene expression in mammalian cells (23) and Andrew Fire together with Craig Mello won the Nobel Prize (2006) for their work on RNA interference, more than 30 clinical trials on siRNA mediated RNA interference have been started (24). All nucleic acid based therapies inherence the risk of potential interaction of the delivered macromolecular drug with the DNA of the target cell. In worst case, this can lead to severe damage of the treated organism (25).

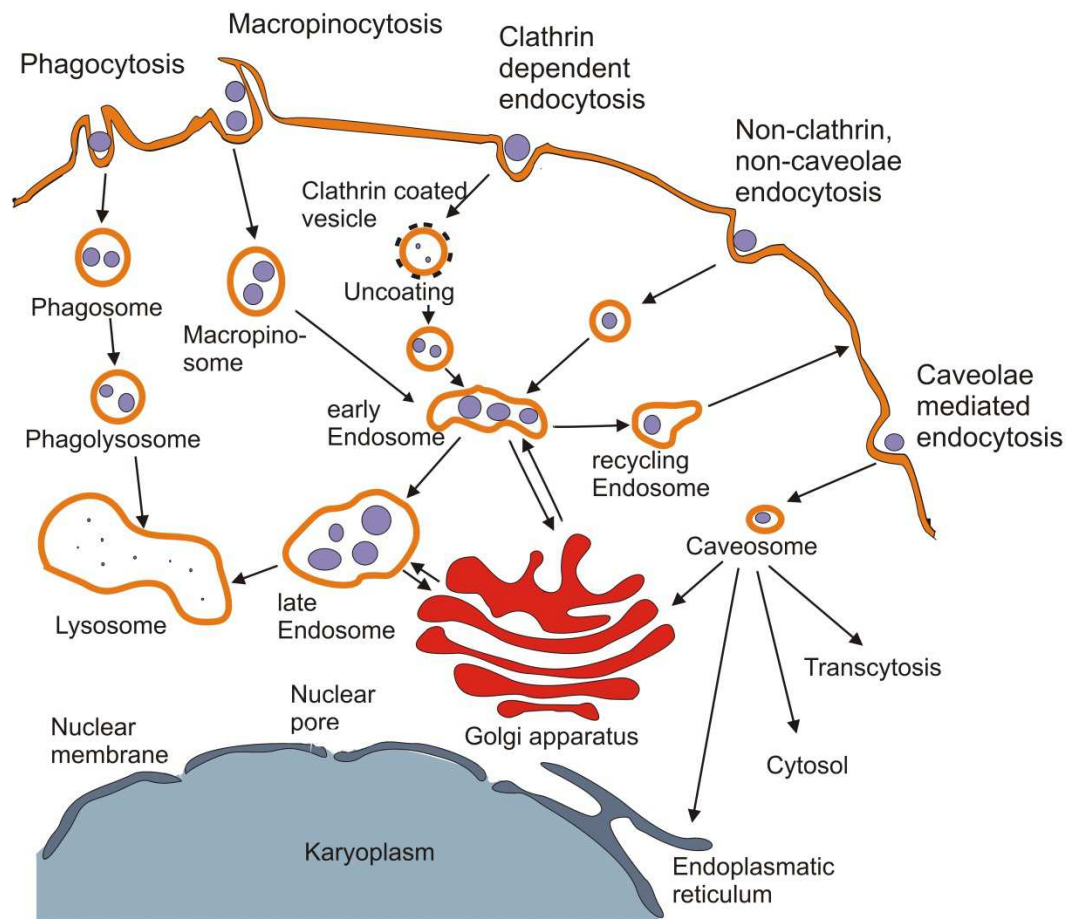
Intracellular delivery of active proteins supplementing dysfunctional cellular proteins is an encouraging alternative to gene therapy (26, 27). It is expected to be a safe approach, lacking the potential malignant transformation of viral gene therapy (28). Protein transduction presents the most straight forward plan of attack for healing plenty of diseases caused by mutated or wrong folded proteins (29). The first protein observed, having the ability to translocate through the intact phospholipid bilayer, was the HIV-1 TAT protein (30, 31). In the meantime, it has been discovered that natural homeoproteins such as the *Antennapedia* homeobox can cross cell

membranes and internalize into cells as part of their physiological function (32) and numerous homeoprotein-derived natural and artificial transduction peptides have been identified. (33-36) Thus, the intracellular delivery of active proteins, named 'protein transduction', now is considered as an interesting option and alternative to gene therapy, substituting for dysfunctional cellular proteins (27, 29, 37). After this observation in 1988, it took almost another 20 years until the first clinical trials using this new technique started. Clinical trials include treatment of various diseases, e.g. dermal scar therapy, psoriasis, pulmonary fibrosis, hyperhidrosis. Altogether up to date over 20 Phase 1 and Phase 2 clinical trials were performed and more than 2000 patients have been treated with drugs, delivering peptides or proteins into cells (38). A Phase 2a clinical trial in the treatment of Lateral Canthal Lines showed significant efficacy versus a placebo. The therapeutic is based on a Botulinum Toxin Type A protein, which is delivered by a protein transduction domain (PTD). Moreover the drug appears to be well tolerated. Although protein transduction technology is still in its infancy, it raises hope in the development of new macromolecular drugs for the treatment of numerous diseases caused by dysfunctional cellular proteins. Although tremendous progress was made in the last decade, all of the macromolecular therapy techniques, except the extracellular operative ones, share a common difficulty – without effective delivery into the cell their therapeutic use is very limited.

2.2 Barriers in macromolecular therapy

On the long rocky road to the site of action, the macromolecular drug has to overcome many hurdles. So many different critical steps have to be addressed. First problem is to decide what's the right administration form of a certain macromolecular drug. Oral application of a macromolecular drug in most cases does not make sense, as the therapeutic would be rapidly degraded inside the intestinal tract. One possibility to get an adequate quantity of the drug to the target is local injection, followed by passive diffusion of the macromolecular medicate. Presumably the treatment of age related macula degeneration with siRNA represents the most spectacular example of this administration form (39). Major disadvantage of this method is that far not all tissues and cells can be reached. Most inner organs as well as tumor tissue have got strong blood circulation and therefore are good accessible through direct intravenous injection. Once inside the blood flow the macromolecular

drug is confronted with a hostile environment. The macromolecular drug is threatened with degradation by proteases, nucleases, phagocytotic cells of the immune system and many more. One possibility to reduce interaction with these components is PEGylation of the macromolecular therapeutic. Polyethylene glycol (PEG) is a uncharged, hydrophilic polymer which was shown to reduce immunogenicity and enhances circulation live of proteins (40). Also unspecific interaction of DNA polyplexes with blood components could be minimized through this way (41). Next hindrances that have to be mastered are clearance by liver and kidney which presents a particular problem in delivery of macromolecules (42). In this case again PEGylation can be used to increase size, as the kidney allows clearance mainly of particles below 8 nm. Next step is the extravasation of the therapeutic to the target cell through the extra cellular matrix. Especially for electrostatic DNA or siRNA polyplex formulations this represents a critical step that may be limiting effective drug delivery (43). Macromolecules, whose site of action is on the cell surface, e.g. surface receptor ligands (44) or antibodies binding to extracellular target (45) have already reached their final destination on this stage. For macromolecular drugs acting in the cytosol the major delivery problems are just starting at this point. Now they have to overcome the biological barrier of the cytoplasmic membrane, a phospholipid bilayer structure whose primary natural function is to prevent the uncontrolled cell entrance of such big and charged molecules (molecular weight cut-off around 600 Da) (46).

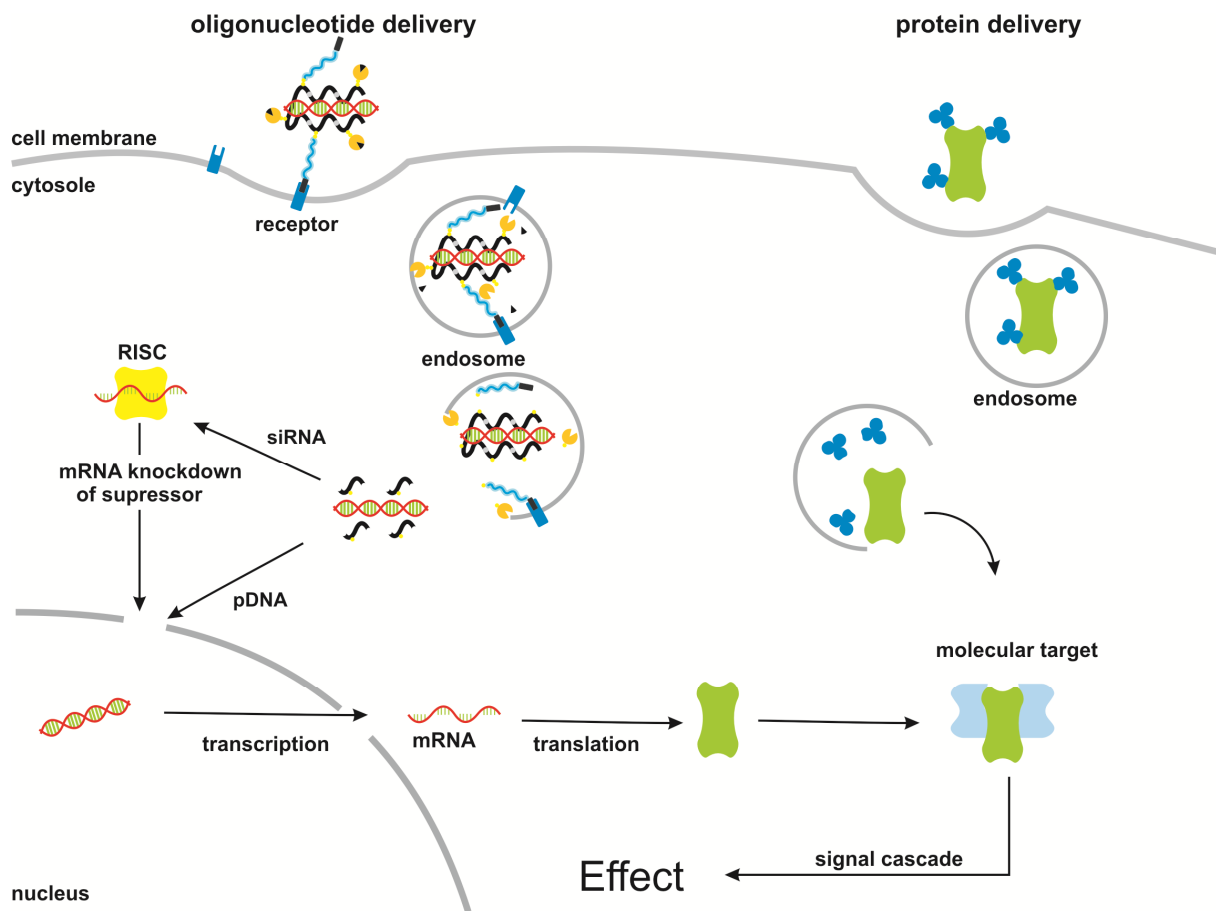


Scheme 2.1: Illustration of uptake pathways for macromolecular drugs and further processing of the internalized vesicles. Except caveolae mediated endocytosis, all other cellular entries lead at least partly to fusion of the vesicles with lysosomes and therefore to acidic degradation of the cargo.

Endocytosis is a natural occurring process that allows the directed uptake of molecules, for example Fe^{3+} . Iron is internalized after binding of iron loaded transferrin to the transferrin receptor (47). Macromolecular drugs can use this cellular feature to penetrate into the target cell, when ligands like Transferrin (48), Folate (49), EGF (50), RGD (51), B6 (51) or GE11 (52) are associated to their surface. Literature describes, as illustrated in Scheme 2.1, at least five different ways of endocytosis: phagocytosis, clathrin-mediated endocytosis, macropinocytosis, caveolae-mediated endocytosis, and clathrin-caveolae-independent endocytosis (53). Targeted uptake occurs mainly via clathrin mediated endocytosis (54). Also unspecific binding of a macromolecular drugs to the cell, e.g. via electrostatic interaction can lead to internalization. In this case all pathways can be involved (55, 56). Except caveolae mediated endocytosis, all other cellular entries lead at least partly to fusion of the vesicles with lysosomes and therefore to acidic degradation of the internalized macromolecules (57). To prevent this, the therapeutic has to escape

from endo-lysosomal degradation. As most macromolecular drugs are not able to disrupt the endosome membrane themselves, a second molecule providing this feature is needed. In case of DNA polyplexes this often is the cationic polymer polyethylenimine (PEI). PEI polymers possess protonable primary, secondary or tertiary amines, with a pK_a between five and seven which can buffer acidification of the late endosomes by taking up protons. This buffering goes along with concurrent influx of chloride to maintain charge neutrality and results in an increased ionic strength inside the endosome. To balance this, water is accumulating passively inside the endosome. Therefore the pressure inside the endosome increases more and more until the membrane bursts and the content of the endosome is released into the cytosol (58). Lipid based carriers present another possibility to destabilize the endosome membrane and promote release of the entrapped therapeutic (59-61). A third well known strategy to promote endosomal release is the use of lytic, membrane disrupting peptides, for example melittin. Melittin the main active compound in bee venom inserts into the phospholipid bilayer where it forms pores and leads to membrane disruption (62). As the lytic properties are not pH specific, melittin is also interacting with other membranes and therefore exhibits quite high toxicity. In contrast to melittin the lytic influenza peptide develops its lytic activity through a change in conformation which occurs after acidification. Because of this property it is a great reagent for enhancing endosomal release (63). Although some chemicals, e.g. Chloroquine, can prevent endosomal acidification and therefore enhance endosomal escape, their inherent toxicity excludes therapeutic applications (64-66). Although after endosomal release most drugs have reached their destination, they have to get rid of all modifications to develop their natural behavior. Some therapeutics, like DNA or transcription factors, need to be further translocated subcellularly to the nucleus, their site of action. Subcellular nuclear transport presents a major bottleneck in DNA delivery (67). Proteins exposing their nuclear localization signal are translocated into the nucleus by binding of the cytosolic, heterodimer carrier protein importin. Importin binding is resulting in a GTP driven active transport through the nuclear pore complex (68).

2.3 Nucleic acid versus protein delivery



Scheme 2.2: Illustration of differences and similarities in further processing, after cellular uptake of nucleic acids and proteins (Scheme partly adapted from David Schaffert (69)).

Intracellular delivery of active proteins supplementing dysfunctional cellular proteins is an encouraging alternative to gene therapy (26, 27). First difference of nucleic acid and protein delivery is the different stability of the naked molecules in plasma. For example Houk et al. showed that naked linear DNA has got an half-life of only 11 minutes in isolated rat plasma (70), whereas proteins have got an half-life of up to a few hours (71). Protein transduction presents the most straight forward plan of attack for healing plenty of diseases caused by mutated or wrong folded proteins (29). A DNA molecule delivered into the cell is acting as a kind of prodrug, because it has to be further processed by the cell to develop its therapeutic effect. First the DNA has to be transcribed into mRNA and the mRNA has to be translated into the protein to get the active compound (Scheme 2.2). Up-regulation of a gene encoding for a certain protein via RNAi technique is even more complicate. In this case the siRNA must knockdown the translation of mRNA encoding for a suppressor protein of the

accordant gene. This leads to enhanced transcription and therefore translation of the desired gene (22). Delivery of mRNA is again a step closer. In this case the internalized mRNA is active in the cytosol and just has to get transcribed to result in the corresponding active protein (72). Aside that protein delivery has got several other advantages compared to nucleic acid delivery. It is expected to be a safe approach, lacking the potential malignant transformation of viral gene therapy (28). In addition protein transduction technology offers the possibility to transport proteins into the cytosol, containing artificial or D-amino acids, which are considered to be less immunogenic (62) and more stable towards intracellular degradation. Harris and coworkers have shown that shortening of the amino acid sequence and replacement of L-amino acids through their D-AA analog raises half-life time of Somatostatin from a few minutes up to 1.5 hours (73). A well-known bottleneck in nucleic acid delivery, the transport of the DNA into the nucleus (74), which is indispensable for target gene expression, is easily bypassed. Most proteins have got their site of action inside the cytosol. Nevertheless some therapeutic proteins like transcription factors also have to be subcellularly transported into the nucleus to get active. But in contrast to DNA this is much easier, just because of the smaller size of proteins. The nuclear pore complex has got a diameter of around 8 nm which allows passive diffusion of molecules up to 40 kDa into the nucleus. Bigger proteins are only transported into the nucleus through an energy dependent process, when they are bearing an exposed nuclear targeting sequence (68). One big drawback of protein delivery in comparison to gene therapy is that especially for enzymes their tertiary conformation is essential for the activity. This tertiary structure may be disturbed by coupling carrier molecules for example CPPs. Typically nucleic acids like plasmid DNA is forming a stable polyplex with most cationic carrier molecules, held together by electrostatic interactions. In contrast complexation of proteins, because of the lower density of negative charges on the surface, affords in most cases covalent coupling of the carrier molecule to the protein cargo. Kataoka and coworkers presented another smart technique to overcome this problem. They substituted the positive charges of lysine residues in proteins through negative ones by reaction with citraconic anhydride, thus charge density is high enough for non-covalent complexation (75). Another major difference may be for some cases an advantage and for other ones a disadvantage. In contrast to protein transduction, cells transduced with DNA are expressing the encoded protein, dependent on the used promoter, quite a long time

(76). Protein delivery is a short termed treatment, because the internalized proteins are degraded by proteases after a while. To sum up nucleic acid as well as protein delivery has its special features and offers specific advantages over the other one.

2.4 Strategies for transporting proteins into the cytosol of living cells

Proteins have to overcome the biological barrier of the cytoplasmic membrane to get into the cytosol. As already mentioned this phospholipid bilayer structure was designed from nature for preventing the uncontrolled entering and exiting of such big, charged molecules. For pure in-vitro studies, it is possible to use physical methods, like microinjection or electroporation, to promote an uptake of the desired peptide or protein (77, 78). With the help of a microinjector the cytoplasmic membrane of individual cells is perforated with a thin glass capillary and the protein is directly injected into the cytosol. Because of the big effort only a few cells can be addressed with this technique and in addition quite a great amount of the cells do not survive this treatment. Electroporation in contrast to microinjection is a technique which is also applicable for in vivo application (79). An externally applied electrical field is temporarily changing the conformation of membrane properties, resulting in an increase in membrane permeability. During this short time interval proteins can overcome the phospholipid bilayer. In opposite to these rather brute physical methods, for moderate biological techniques having the potential for broad therapeutic application, in most cases a carrier molecule is needed. On the rocky road into the cytosol, the transduction carrier has to prevent the cargo from extracellular degradation and transport it piggyback over the biological barrier of the cytoplasmic membrane. Once inside the cell the carrier-cargo complex has to escape from endo-lysosomal degradation. Afterwards the carrier should release its cargo in the cytosol to warrant activity of the protein. A perfect carrier system has to address all this critical steps and furthermore exhibit low cytotoxicity. In the last decades many efforts have been made to create such a perfect carrier system. In 2010 Voelkel et al. presented a technology for protein delivery, where they transported GFP into the cytosol of living cells using murine retroviral particles as carrier system (80). Quite a similar system were they used lentivirus derived virus like particles (VLPs) was

developed by Frederico and coworkers (81). Major drawback of these virus based systems is the presence of reverse transcriptase and integrase in the particles which causes the potential risk of conversion of RNAs into DNA and integration of DNA into the chromosome of the transduced cell (82). Dai and colleagues used single walled carbon nanotubes (SWNT) for the delivery of streptavidin and cytochrome c in a number of different cell lines (83-85). Aside carbon nanotubes, also another inorganic carriers, e.g. mesoporous silica nanoparticles (MSN) and gold nanoparticles were successfully used to deliver proteins into cells (86-88). Major drawback of this carriers based on inorganic compounds is that the protein is attached to their surface, where it is not protected against proteases and in many cases the shuttles exhibit low endosomal escape. Most commercial available carriers for protein delivery are based on cationic lipids (89-91). Liposomes are supposed to enter cells via two different mechanisms, endocytosis or fusion of the liposome with the cell membrane (92). Later uptake mechanism offers the advantage that the cargo is not internalized in endosomes but is rather directly discharged into the cytosol. Main disadvantage is the low stability of most cationic lipid based vectors under serum containing conditions that hampers effective protein uptake (93). The first protein observed that was naturally able to translocate through the intact phospholipid bilayer was the HIV-1 TAT protein (30, 31). In the meantime, it has been discovered that natural homeoproteins such as the *Antennapedia* homeobox can cross cell membranes and internalize into cells as part of their physiological function (32) and numerous homeoprotein-derived natural and artificial transduction peptides have been identified. (33-36). Thus, the intracellular delivery of active proteins, named 'protein transduction', now is considered as an interesting option and alternative to gene therapy, substituting for dysfunctional cellular proteins (27, 29, 37). The most common method used for protein delivery is the use of short positively charged peptides, so called protein transduction domains (PTDs) (27, 94-96). These PTDs can be grouped in two major classes, natural ones like Penetratin (96, 97) or HIV-TAT (27) and artificial ones e.g. oligoarginines (98). Protein transduction domains (PTDs) or also called cell penetrating peptides (CPPs) in general are tagged to the cargo protein by genetic engineering. Especially in cases where the active center of an enzyme is located near the carboxy- or amino-terminus this tags can disturb functionality. The internalization pathway of these fusion proteins is discussed controversial. Some studies suggest macropinocytosis (97, 99) others predicate it is

a mixture between different mechanisms (100). At least uptake means may be dependent on the used CPP, cell line, concentration and cargo (101, 102). The efficiency of the following step, the retrograde transport out of the endosome is very low for most PTDs (103, 104). Altogether the efficiency of this technique seems to be dependent on cell line and cargo size (98, 101). Okuyama et al. engineered a synthetic carrier system that is mimicking an alpha helix found in some PTDs. Covalent coupling of this small molecule based carriers (SMoCs) to the DNA replication licensing repressor protein geminin showed an antiproliferative effect on human cancer cells (105). Aside PTD mediated protein delivery the use of cationic polymers, e.g. polyethylenimine is a widely used strategy for protein transduction (75, 106-109). Cationic polymers like polyethylenimine often are very effective carriers, but are lacking of precise structure and often show high toxicity dependent on the molecular weight of the used polymer (110). Up to date protein delivery still lacks of an all-purpose carrier system. Each of the presented technologies has got its limitations. Some technologies show cell type dependence (98) or others are bordered to certain cargo proteins (111).

2.5 Biological cleaveable crosslinkers

Today plenty of different protein crosslinkers are on the market. They are used for many different applications, e.g. for analysis of protein structure and subunits, formation of protein- protein conjugations, immobilization of proteins on solid phase, PEGylation, formation of crosslinks between nucleic acids and proteins, analysis of protein interactions, preparation of immunogens or for the construction of immunotoxins. For some applications it is of favor that the bond between the crosslinked molecules is reversible and can be cleaved under certain conditions. Also for this acquirement linkers are available. Linkers containing internal esters, e.g. the ethylene glycolbis(succinimidylsuccinate) (EGS) can be cleaved by incubation with hydroxylamine (112, 113). Introduction of diol containing groups that can be cleaved by periodate is also a very common technique in crosslinker development (114, 115). Base labile crosslinkers based on sulfone groups present another group of commercial linkers (116-118). Although all these presented linkers are cleavable under conditions which are compatible for most proteins, they do not allow a cleavage under such mild chemical conditions compatible with a living biological

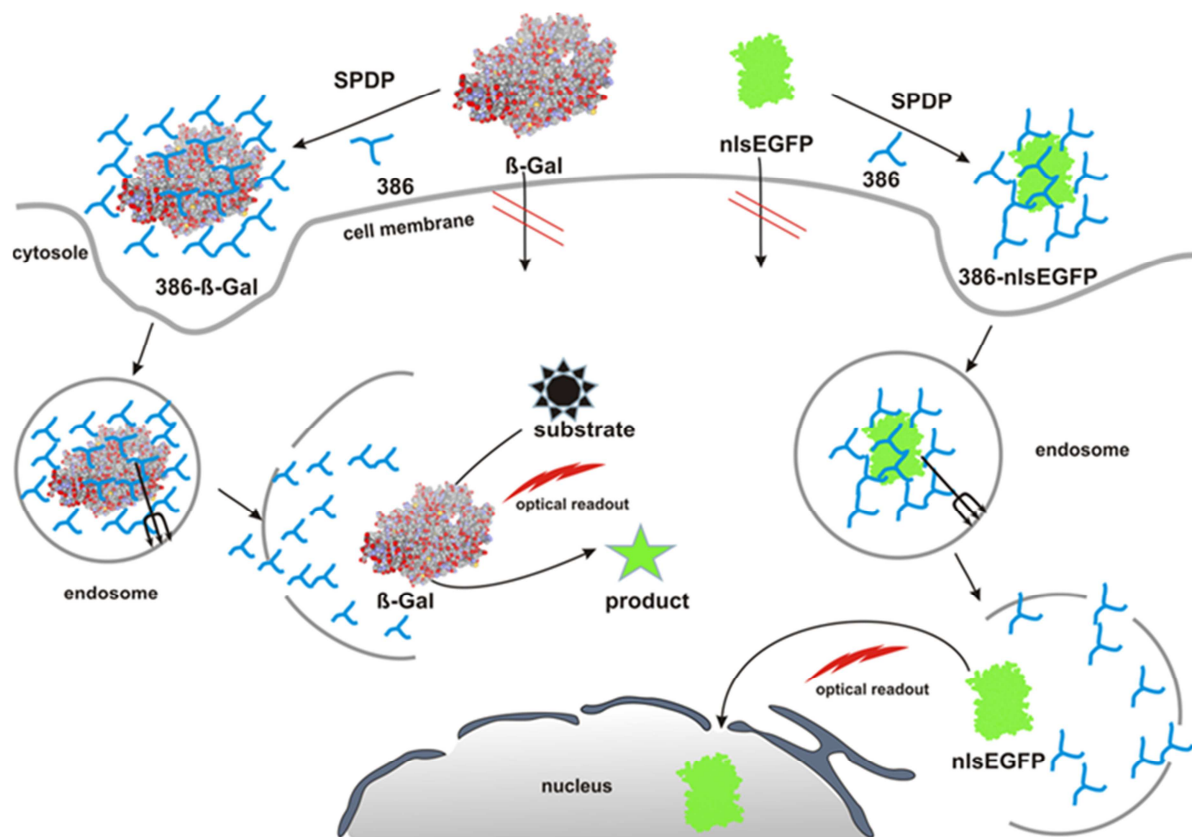
system. Furthermore for intracellular macromolecular drug delivery it is of advantage to have a chemical dynamic linker triggered by tiny changes in chemical microenvironment. During the delivery process the chemical microenvironment changes with the further transport of the macromolecular drug to another cellular compartment. The linker should respond to this tiny chemical changes in the required manner. For example the linker should be stable in the extracellular matrix, before cellular uptake and after internalization the bond between carrier and cargo should be cleaved. Nearly all commercial available crosslinkers providing this feature are based on bioreducible disulfide bonds (119-122). The most famous under this type of linkers is the heterobifunctional crosslinker (SPDP), which was developed by Carlson et al. in 1978 (119). One end is built up from an amine reactive succinimidylester that can be reacted with the amine group of lysine containing proteins, resulting in a stable amide bond. The other functional group is a 2-pyridyldithio group which allows reaction with sulfhydryl containing molecules (e.g. cysteine residues of proteins or peptides), forming a disulfide bond. This disulfide bond is stable in a non-reducing environment, for example in the extracellular matrix. Under mild reducing conditions in contrast, (e.g. caused by glutathione levels in the cytosol), it is cleaved (123, 124). An additional feature of SPDP is that the cleavage of the 2-pyridyldithio group causes a change in the spectral properties and therefore it is quite easy to determine the amount of linker coupled to the desired molecule. For this reasons SPDP became the most used linker in macromolecular drug delivery (123, 125-127). Photo-cleavable linkers present another strategy that allows controlled cleavage of the bond between two crosslinked molecules (128-130). Ottl and coworkers developed a hetrobifunctional linker, which contains a photoreactive o-nitrobenzyl group (129). Upon light stimulus the linker is cleaved. Photocleavable linkers are applicable mainly for in vitro uses, because deeper tissues can hardly be addressed. Knorr et al. presented a homobifunctional acetone ketal cross-linker in 2008 that capitalizes from the differences in pH in different cellular compartments or tissues (131). The inherent acetal group is cleaved under mild acidic conditions, which are typical for tumor tissue (132) or early endosomes (133), whereas the linker is quite stable under physiological pH of 7.4. All cleavable linkers presented have in common that they are not cleaved off completely. After cleavage a small relict of the linker remains bound to the molecule of interest. For some applications like protein delivery this might be a drawback, e.g. the active site of an enzyme could be sterically blocked by this

fragment. Blätter et al. created a heterobifunctional, acid labile linker in 1984 that is based on maleic anhydride. This linker is cleaved off traceless from the molecule of interest upon acidification (134). Major drawback of this linker is that it requires quite low pH values to be cleaved. A linker especially developed for protein delivery was presented by Dowdy and colleagues in 2010 (27). It is based on nitrilotriacetic acid (NTA) coordinated copper that is strongly binding to hexahistidine-tagged macromolecules like peptides and proteins. This affinity is lost after a pH drop to 5 which can be found as already mentioned in late endosomes. Major drawback of this linker is that exclusively the histidine bearing end of the protein can be modified and therefore no real encapsulation is possible. Up to date still no perfect linker system for protein delivery is available.

2.6 Aims of the thesis

2.6.1 Establishment of a cellular test system for protein delivery

Aim of this thesis was to establish a test system for protein delivery. The test systems should enable easy and fast qualitative proof of successful protein internalization. The protein should be of average size and exhibit a typical isoelectric point (pI). Furthermore it should be possible to evaluate the percentage of transfected cells, as well as the amount of protein that was taken up by the cells. As a “golden standard”, one corresponding model protein should be established bearing a very common PTD like HIV-TAT peptide. This CPP should be fused to the model protein by genetic engineering. This standard protein transduction technology should serve as a reference test method, to evaluate and compare the efficiency of different developed carrier systems. One of the major bottle necks for protein delivery is, as already mentioned endosomal release. The test model ought to demonstrate easy, if the cargo is released out from the endosome and is behaving naturally inside the cytosol, e.g. through successful subcellular transport. Furthermore the test system should be able to evidence that biologic activity of a transported enzyme is maintained. A model of such a test system is illustrated in Scheme 2.3.



Scheme 2.3: Illustration documenting the concept of the planned protein delivery test system. 386 is a precise oligo(ethane amino)amide carrier. SPDP is a protein crosslinker.

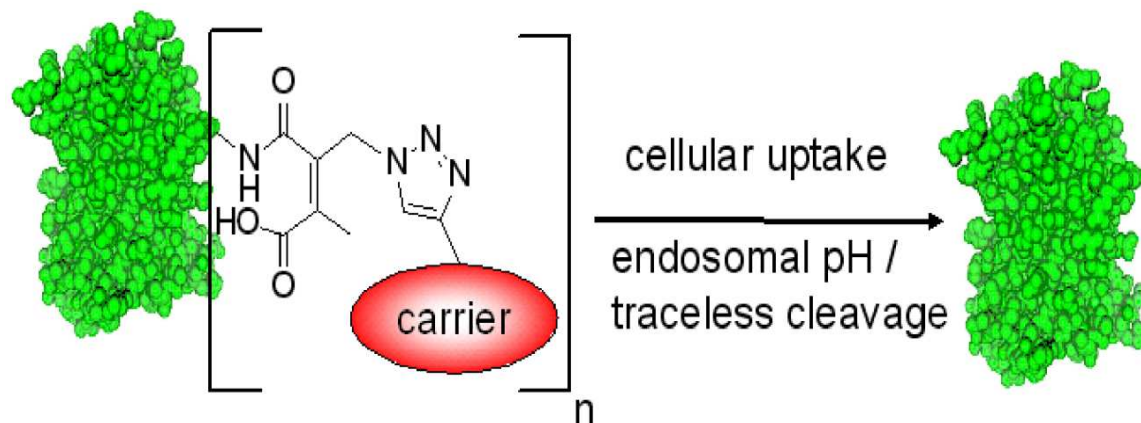
2.6.2 Protein delivery with defined polycations

The most widespread technique for delivery of proteins is the use of CPP as carrier system (27, 94-96). As already mentioned such delivery is of low efficiency especially since endosomal escape is very low (103, 104). At least efficiency seems to be limited to certain cell lines and cargos. For that reason an efficient delivery system that is applicable for a huge amount of proteins on many different cell lines should be developed. In contrast to PTDs an artificial polycation should be used as carrier system. Up to date for protein transduction mostly PEI has been used as a polycationic carrier (75, 106-109). PEI is a highly efficient carrier but it is a polymer that lacks of defined, precise chemical structure and exhibits quite high toxicity. For this thesis a structure defined, precise oligo(ethane amino)amide carrier should be used. These carriers were developed recently in our lab for the delivery of siRNA and DNA (59). The oligo(ethane amino)amide carriers are based on natural and synthetic amino acids and were synthesized with solid phase supported chemistry. Because of their low molecular weight they exhibit low toxicity. Nevertheless they show high

transduction efficiency in case of nucleic acid delivery. This high transduction efficiency, aside of the good complexation properties and the ability to form stable polyplexes, might be a result of their endosome destabilizing properties. Because of these promising results in nucleic acid delivery, the carriers should be tested for their ability to transport proteins into the cytosol of living cells.

2.6.3 Development of a new traceless cleavable linker for protein delivery

Aside the establishment of a test system for successful protein delivery and the development of a new protein transduction technology, the synthesis of a linker designed for intracellular protein delivery was the major aim of this thesis. The new linker should fulfill following requirements for protein delivery. The bond between carrier and cargo should be stable under physiological conditions that means especially under serum containing conditions at pH 7.4. After uptake the linker should be cleaved off traceless form the cargo to release an unmodified natural protein. This desired feature is demonstrated in Scheme 2.4. The linker cleavage should be triggered by the pH drop in the endosome. At a pH of around 5 the linker should release the carrier from the cargo completely. Furthermore the linker system should allow the complete encapsulation of the protein with the carrier molecule. In recent years click chemistry reactions, especially the copper catalyzed 1,3-dipolar cycloaddition (CuAAC) and the Staudinger ligation, became useful tools for conjugating biomolecules (49, 135-137). Both reactions have great advantages compared to other linking strategies, like high efficiency and bioorthogonality. The new linker should enable the use of these click chemistry reactions for covalent modification of the cargo protein with the carrier.



Scheme 2.4: Illustration of the linker concept. Scheme (138) is showing the linker coupling a carrier over CuAAC to nlsEGFP. Furthermore all major desired properties of the new linker are displayed: heterobifunctionality, bioorthogonality, using click chemistry, complete encapsulation, acid lability, traceless cleavage.

3 Materials

3.1 Chemicals

All used chemicals, unless noted otherwise, were purchased from Sigma-Aldrich and used without further purification.

3.2 Reagents

3.2.1 Dyes

Dylight 488 a phosphine containing dye for copper free click chemistry coupling over Staudinger ligation was purchased from Thermo Fisher Scientific (Schwerte, Germany). Tetramethylrhodamine-5-maleimide was bought from Sigma-Aldrich (Munich, Germany).

3.2.2 Peptides

Cystein modified melittin (Mel) with following sequence CIGA VLKV LTTG LPAL ISWI KRKR QQ, in all D conformation, was ordered from IRIS biotech (Marktredwitz, Germany). The N-terminal cysteine was introduced as an amine and the C-terminal amino acid as carboxylic acid.

3.2.3 Linkers

The copper free click chemistry linkers DBCO-PEG4-maleimide and DBCO-NHS were purchased from Jena Bioscience (Jena, Germany). The heterobifunctional SMCC crosslinker was ordered from Pierce Biotechnology (Bonn, Germany).

3.3 Solvents

DCM, MeOH, THF were purchased from Merck (Darmstadt, Germany). CHCl_3 , n-hexane, n-heptane, DMSO, ACN, Et_2O were obtained from Sigma Aldrich (Munich, Germany). All solvents were purified by distillation and dried before use. Water was used after purification and deionization. Deuterated solvents were bought from Sigma Aldrich.

3.4 Buffers

PBS buffer was prepared with following mixture: NaCl 137 mM, KCl 2.7 mM, $\text{Na}_2\text{HPO}_4 \times 2 \text{H}_2\text{O}$ 2mM, pH 7.4. If another pH value is stated it was adjusted with aqueous 1M HCl or NaOH solution.

3.5 Solutions

Click solution A was freshly prepared by dissolving CuBr (1 mg, 7 μmol) in DMSO/tert-ButOH (70 μl , 3/1, v/v). Click solution B was prepared by dissolving Tris[(1-benzyl-1H-1,2,3-triazol-4-yl)methyl]amine (TBTA, 2.7 mg, 5 μmol) in DMSO/tert-ButOH (3/1, v/v) (100 μl). Click solution C was freshly prepared by mixing click solution A and click solution B (1/2, v/v).

3.6 Cell culture material

All cell culture consumables (flasks, dishes, well plates) were purchased from NUNC (Langenselbold, Germany) or TPP (Trasadingen, Switzerland). Growth media, as well as FCS, Glutamine, Penicillin/Streptomycin were ordered from Invitrogen (Karlsruhe, Germany).

3.7 Cell lines

All cell lines were purchased from the American Type Culture Collection (ATCC, Wesel, Germany). The used cell lines are listed in Table 3.1.

Table 3.1: Used cell lines

Name	Description	ATCC number
HeLa	human cervix adenocarcinoma cell line	CCL-2
Neuro2A	murine neuroblastoma cell line	CCL-131
NIH/3T3	murine fibroblast cell line	CRL-1658
KB	human nasopharyngeal epidermoid carcinoma cell line	CCL-17

3.8 Bacteria strains

Chemical competent *E. coli* protein expression strain BL21(DE3)plysS was purchased from Novagen (Merck4biosciences, Darmstadt, Germany).

E. coli strain DH5 α was bought from Invitrogen (Karlsruhe, Germany) and was used for plasmid amplification.

3.9 Nucleic acids

The plasmid pRHGPCNA containing a gene encoding for a nuclear localization sequence (derived from SV 40 large T antigen) bearing nlsEGFP fusion protein was kindly provided by M. Cristina Cardoso (TU Darmstadt, Germany). For heterolog protein expression the plasmid pET 23a (+) vector from Novagen (Merck4biosciences, Darmstadt, Germany) was used.

Primers with following base sequences were used:

- a) For nlsEGFP amplification following oligonucleotides were purchased from Eurofins MWG (Ebersberg, Germany):

forward: 5'-GTTGATGAATTCCCGAAGAAGAAGCGCAAAGTA-3`;

reverse: 5`-TCAACTAAGCTTCTTGTAAGCTCGTCCATGCC-3`.

- b) For introducing the HIV-TAT PTD sequence following oligonucleotides were ordered from Eurofins MWG (Ebersberg, Germany)

Sense:

5`AGCTTGGTTATGGGCGCAAAAACGCCGTCAGCGCCGTCGGGGCC3`

Antisense:

5`TCGAGGCCCGACGGCGCTGACGGCGTTTTTTGCGCCATAACCA 3`

4 Methods

4.1 General chemical procedures

4.1.1 ¹H-NMR and ¹³C-NMR

The ¹H-NMR and ¹³C-NMR spectra were recorded at room temperature using a JNMR-GX (400 MHz, Joel) or a JNMR-GX 500 (500 MHz) with a coupling constant of 0.3 Hz. All spectra were recorded without TMS as internal standard and thus spectra were calibrated to the residual proton signal of the deuterated solvent. For the measurements 10-100 mg sample were used. Spectra were analyzed using the NMR software MestreNova (MestreLab research) or NUTS (Acron NMR).

4.1.2 Mass spectroscopy

Mass spectra were recorded on a Thermo Finnigan MAT 95 or on a Jeol MStation.

4.1.3 CD spectroscopy

nlsEGFP was diluted in phosphate buffer (50mM, pH 7.5, 1mg/ml). Spectra were recorded on a Jasco J810 CD and ORD spectrometer. **386**-DBCO-AzMMMan-

nlsEGFP was dialyzed against citric acid-phosphate buffer (0.1 M, pH 5) at 37°C overnight to cleave off the transduction oligomer **386**. This was followed by another dialysis step against phosphate buffer (50mM, pH 7.5, 1 mg/ml) for 12 hours. The dialysis was performed using a 14000 MWCO dialysis membrane from Carl Roth (Karlsruhe, Germany). The protein was concentrated to 1 mg per ml with Amicon Ultra centrifugal filter units (MWCO=10,000).

4.1.4 UV-Vis spectroscopy

Protein, linker concentrations, etc. were determined by measuring UV-Vis absorbance at different wavelengths. For these measurements a Genesys 10 S UV-Vis spectrophotometer (Thermo Scientific, Bonn, Germany) was used.

4.1.5 Fluorescence spectroscopy

For fluorescence spectroscopy a Varian Cary Eclipse (Darmstadt, Germany) fluorescence spectrophotometer was used. Proteins were diluted in PBS buffer (pH 7.3).

4.1.6 Chromatography

4.1.6.1 HPLC

HPLC runs were performed either on a GE Healthcare ÄKTA Basic system or on a Bio-Rad (München, Germany) BioLogic FPLC station. The Äkta system is built up from a P-900 dual-pump, a UV-900 three channel UV-detector and F-950 fraction collector. The system was controlled by the appropriate UNICORN software (version 4.11). The BioLogic Workstation is containing two pumps, 6 valves, a conductivity meter and an external UV-detector. The system is operated by the BioLogic version 1.3 software. A fraction collector model 2180 also from Bio-Rad was used.

4.1.6.2 Dry column vacuum chromatography (DCVC)

Dry column vacuum chromatography was done as described by Pederson and colleagues (139).

4.1.6.3 Flash Column Chromatography (FCC)

Flash chromatography was performed as described by Still and coworkers (140). As stationary phase silica gel with a mean diameter between 0.035 and 0.073 mm was used. Column height and diameter were varied according to sample size and the required resolution.

4.1.6.4 Thin layer chromatography (TLC)

Silica gel coated aluminium plates were used for thin layer chromatography. Detection method was UV-detection at 254 nm.

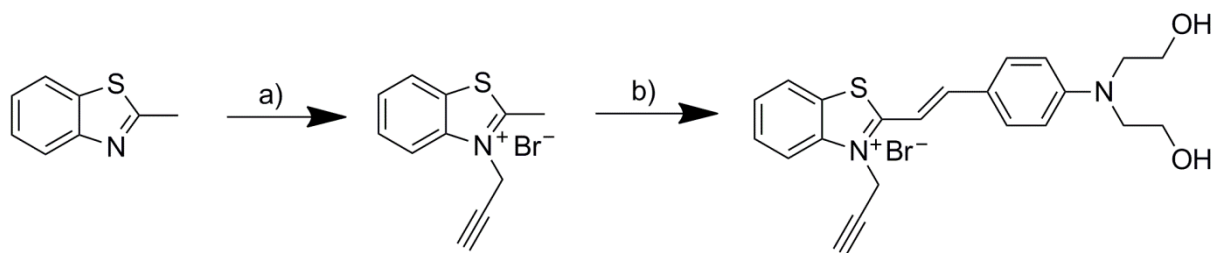
4.1.7 Dynamic light scattering (DLS)

Particle size and zeta potential of the transduction shuttles was measured by dynamic laser-light scattering using a Zetasizer Nano ZS (Malvern Instruments, Worcestershire, UK). Modified proteins were measured in HEPES buffer (20mM, pH 7.4) at a concentration of 5 mg/ml.

4.2 Synthesis

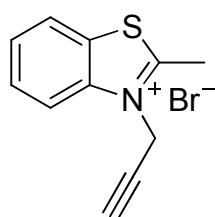
4.2.1 Synthesis of watersoluble hemicyanine alkyne dye

The watersoluble hemicyanine dye (E)-2-(4-(bis(2-hydroxyethyl)amino)styryl)-3-(prop-2-yn-1-yl)benzo[d]thiazol-3-ium bromide was synthesized in a very straightforward two step reaction from methylbenzothiazole as precursor. First step is a nucleophilic substitution followed by a condensation of the product with 4-N,N-bis(2-hydroxyethyl)aminobenzaldehyde.



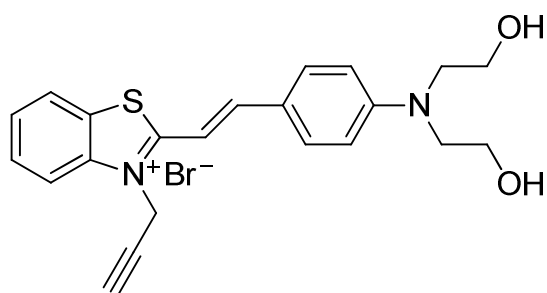
Scheme 4.1: Synthesis strategy of watersoluble hemicyanine alkyne dye. (E)-2-(4-(bis(2-hydroxyethyl)amino)styryl)-3-(prop-2-yn-1-yl)benzothiazol-3-ium bromide

4.2.1.1 Synthesis of 2-methyl-3-prop-2-ynyl-benzothiazol-3-ium bromide



This compound was prepared analogously as described elsewhere (141). Briefly: Methylbenzothiazole (12.0 g, 0.1 mol) was given to a solution of propargyl bromide (5.0 g, 34 mmol) in acetonitrile (20 mL) under vigorously stirring. Subsequently the reaction mixture was refluxed for 24 h. Afterwards the reaction mixture was allowed to cool to room temperature, and the precipitate was collected. This gave the desired product as a grey solid (5.8 g, 21% yield); $^1\text{H NMR}$ (500 MHz, DMSO D_6) δ 8.5 (d, $J = 8.1$ Hz, 1H), 8.38 (d, $J = 8.5$ Hz, 1H), 7.95 (t, $J = 8$ Hz, 1H), 7.83 (t, $J = 7.8$ Hz, 1H), 5.78 (d, $J = 2.5$ Hz, 2H), 3.85 (t, $J = 2.5$ Hz, 1H), 3.27 (s, 3H).

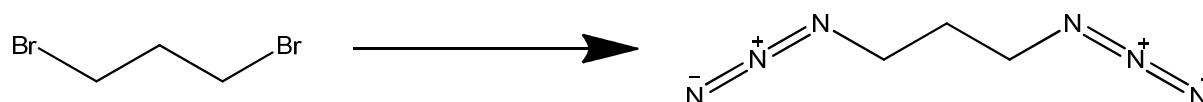
4.2.1.2 Synthesis of 2-[2-(4-dihydroxyethylamino-phenyl)-vinyl]-3-prop-2-ynyl-benzothiazol-3-ium bromide



4-N,N-bishydroxyethyl aminobenzaldehyde (0.5 g, 2.39 mmol) and 2-methyl-3-prop-2-ynyl-benzothiazol-3-ium bromide (641 mg, 2.39 mmol) were diluted in ethanol (20 ml) and refluxed for 2 h. Afterwards the solvent was removed in a rotary evaporator. The residue was purified by DCVC (dry column vacuum chromatography). First the column was washed with ethylacetate/methanol (9:1, v/v) followed by a washing step with acetone/methanol (9/1, v/v) and elution using acetone/water (1:1, v/v). Most of the acetone was removed by evaporation and the residue was lyophilized. This gave a dark purple fluffy solid (0.86 g, 78 % yield). MS (FAB⁺, 8 kV) calcd for C₂₂H₂₃N₂O₂S [M]⁺ 379.50, found 379.5. ¹H NMR (500 MHz, [d₆]DMSO) 8.30 (d, J = 7.82 Hz, 1H), 8.12 (m, 2H), 7.90 (d, J = 8.71 Hz, 2H), 7.80 (t, J = 7.98 Hz, 1H), 7.68 (m, 2H); 6.93 (d, J = 9.11 Hz, 2H), 5.77 (s, 2H), 4.90 (s, 2H), 3.72 (t, 1H), 3.62 (m, 8H).

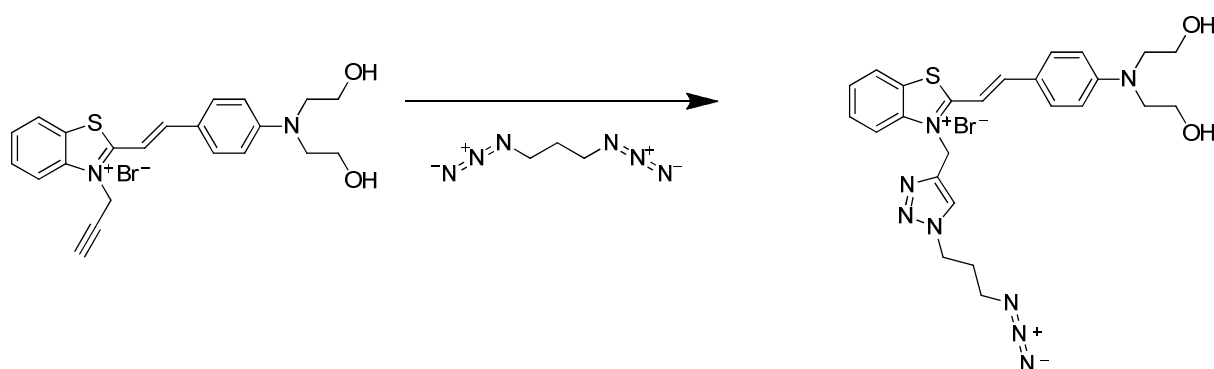
4.2.2 Synthesis of azide hemicyanine dye

4.2.2.1 Synthesis of propane diazide



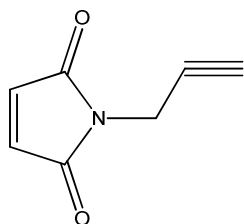
This synthesis was done after a procedure described by Ciampi et al. (142). Briefly: 1,3-dibromopropane (5.0 g, 24.8 mmol) was diluted in DMF (80 mL). Sodium azide (5.0 g, 76.9 mmol) was added in one portion under argon. The reaction mixture was heated to 65° C and the reaction was continued for 48 h under argon. Afterwards the reaction mixture was cooled to room temperature and diluted with diethyl ether (200 mL). The resulting suspension was washed with water (20 mL) and two times with brine (50 mL) and then dried over NaSO₄. Removal of sodium sulfate by filtration and subsequent evaporation gave yellow oil. The crude product was further purified using column chromatography (silica gel) with elution by hexane to give propane diazide as colorless oil (2.5 g, 80,11%). ¹H NMR (300 MHz, CDCl₃) δ: 1.80 (q, 2H), 3.35 (t, 4H, J = 6.5 Hz).

4.2.2.2 Synthesis of azide hemicyanine dye by CuAAC



Alkyne hemicyanine dye (2-[2-(4-Dihydroxyethylamino-phenyl)-vinyl]-3-prop-2-ynyl-benzothiazol-3-ium bromide) (25 mg, 54 μmol) was diluted in DMSO (1ml). Propane diazide was added in one portion (540 μmol , 110 mg). Reaction was started by addition of click solution C (30 μl). Preparation of click solution is described in section 3.5. The reaction mixture was stirred 2 hours at 80° C. After cooling to room temperature the mixture was precipitated in MTBE (50 ml) three times. The residue was purified by DCVC. First the column was washed with ethylacetate/MetOH (9:1, v/v) followed by a washing step with acetone/methanol (9/1, v/v) and elution using acetone/water (1:1, v/v). Most of the acetone was removed by evaporation and the residue was lyophilized. This gave a dark purple fluffy solid (39.8 mg, 63 %). MS (FAB⁺, 8 kV) calcd for C₂₅H₂₉N₈O₂S [M]⁺ 505.52, found 505.2. ¹H NMR (500 MHz, [d₆]DMSO) 8.30 (d, J = 7.82 Hz, 1H), 8.12 (m, 2H), 7.90 (d, J = 8.71 Hz, 2H), 7.80 (t, J = 7.98 Hz, 1H), 7.68 (m, 2H); 6.93 (d, J = 9.11 Hz, 2H), 6.38 (s, 2H), 4.90 (s, 2H), 4.42 (t, 2H), 3.62 (m, 8H), 3.37 (m, 2H), 1.81 (m, 2H).

4.2.3 Synthesis of N-propargyl maleimide

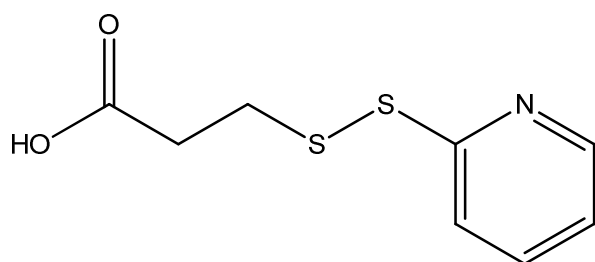


N-Propargyl maleimide was synthesized quite similar as described elsewhere (143). In short: A saturated aqueous solution of sodium bicarbonate (40 ml), propargylamine (330 μ l, 4.84 mmol) was dissolved and cooled on an ice bath. Afterwards N-(methoxy carbonyl) maleimide (751 mg, 4.81 mmol) was added in portions over 20 min under vigorous stirring. This mixture was stirred for 30 min at 0° C, followed by 45 min at room temperature. Subsequently the product was extracted with CH₂Cl₂ (3 \times 50 mL). The organic phase was dried over Na₂SO₄ and the crude product was purified by silica gel column chromatography with using EtOAc/heptane (1:2) as solvent. Evaporation of the solvent gave colorless oil (279 mg, 43% yield). ¹H NMR (500MHz, CDCl₃): 6.76 (s, 2H); 4.30 (d, *J* = 2.5 Hz, 2H); 2.22 (t, *J* = 2.5 Hz, 1H).

4.2.4 Synthesis of N-succinimidyl-3-(2-pyridyldithio)-propionate (SPDP)

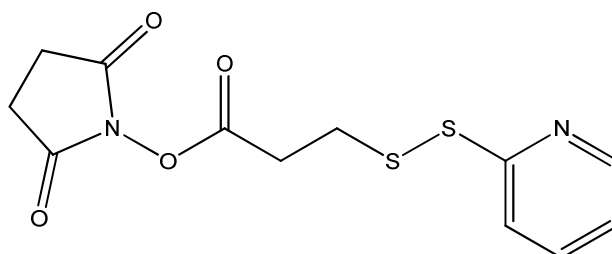
SPDP was synthesized quite similar to the method described elsewhere (144). All modifications are announced in the following section.

4.2.4.1 Synthesis of 3-(Pyridin-2ylsulfanyl)-propionic acid



Dithiopyridine (3.77 g, 17.11 mmol) was diluted in 30 ml EtOH and 0.4% acetic acid. A solution of 3-mercaptopropionic acid (0.9 g, 8.48 mmol, 737 μ l) in 20 ml EtOH and 0.4 % acetic acid was added dropwise over one hour. 2 hours later the solvent was removed on an evaporator. The resulting oil was purified by DCVC using basic alumina as stationary phase (diameter 4 cm, h=7 cm). After the column was preconditioned with CHCl_3 and loaded, the crude product was washed with $\text{CHCl}_3/\text{MeOH}$ 8/2 until the collected fractions were colorless. Afterwards the product could be eluted by addition of 4% acetic acid to the former solvent mixture. Fractions were collected and the solvent was removed by evaporation (1.67 g, 91%). ^1H NMR (500 MHz, $[\text{CD}_3\text{OD}]$) 8.40 (ddd, $J = 4.9/1.8/0.9$ Hz, 1H), 7.77-7.89 (m, 2H), 7.20-7.26 (m, 1H); 3.04 (t, $J = 6.9$ Hz, 2H), 2.71 (t, $J = 6.8$ Hz, 2H).

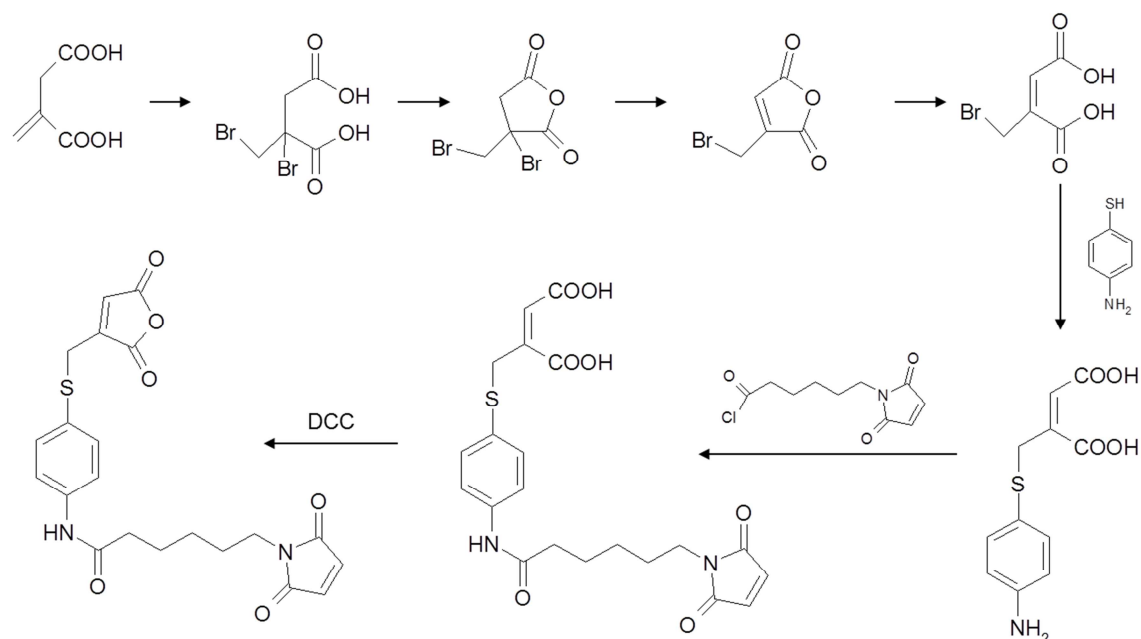
4.2.4.2 Synthesis of SPDP



3-(Pyridin-2ylsulfanyl)-propionic acid (1.643 g, 7.634 mmol) was dissolved in dry CH_2Cl_2 . N-hydroxysuccinimide (1.0 g, 8.68 mmol) was added in one portion. After the suspension was completely dissolved, N,N'-Dicyclohexylcarbodiimide (DCC) (1.7505 g, 8.688 mmol) was added. 4 hours later the side product Dicyclohexylurea (DCU) was filtered off and the solvent was removed by evaporation. The yellowish solid was

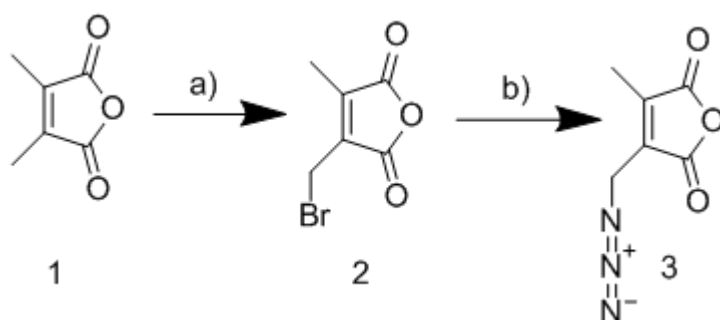
purified by DCVC (diameter 4 cm, h=7 cm) using silica gel as stationary phase and a gradient of 0-15% MeOH in CH₃Cl (50 ml fractions). After recrystallization in EtOH the pure product, a white solid was obtained (1.48 g, 62%). ¹H NMR (500 MHz, [CDCl₃]) 8.48-8.51 (ddd, J = 4.7/1.3/1.2 Hz, 1H), 7.64-7.69 (m, 2H), 7.09-7.14 (m, 1H); 3.09 -3.15 (m, 2H), 3.04 -3.09 (m, 2H), 2.84 (s, 4H).

4.2.5 Synthesis of MAM linker



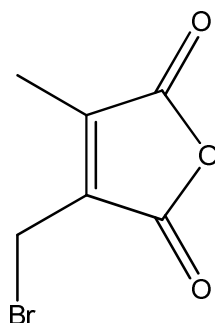
The synthesis of MAM linker (6-(2,5-dioxo-2,5-dihydro-1H-pyrrol-1-yl)-N-(4-(((2,5-dioxo-2,5-dihydrofuran-3-yl)methyl)thio)phenyl)hexanamide) was done according to the method of Blättler et al. (134).

4.2.6 Synthesis of AzMMMan linker



The azidomethyl-methylmaleic anhydride linker (AzMMMan) was synthesized from dimethylmaleic anhydride as precursor very straightforward in two simple reaction steps: a) radical substitution with N-bromosuccinimide resulting in 2, followed by b) Finkelstein reaction with sodium azide.

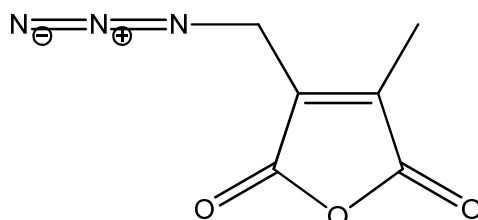
4.2.6.1 Synthesis of 3-(Bromomethyl)-4-methyl-2,5-furandione



This compound was synthesized according to the procedure described elsewhere (145) with minor modifications. Dimethylmaleic anhydride (5.04 g, 50 mmol), N-bromosuccinimide (14.24 g, 100 mmol), and benzoyl peroxide (200 mg, 0.83 mmol) were dissolved in carbon tetrachloride (250 mL). This mixture was gently refluxed for 5 h in a 500 mL round-bottom flask. Afterwards the reaction mixture was allowed to cool to room temperature and an additional amount of benzoyl peroxide (200 mg, 0.83 mmol) was added. The refluxing was continued 5 h more. After cooling to room temperature the residue was filtered and washed two times with carbon tetrachloride (25 mL). Subsequently the organic phase was washed two times with water (100 mL) and brine (100 mL). The organic layer was dried over Na₂SO₄ and concentrated in vacuo to result in yellow oil. This oil was first purified by chromatography on a silica gel column and eluted with a mixture of petroleum ether/ethyl acetate (8:2). Finally

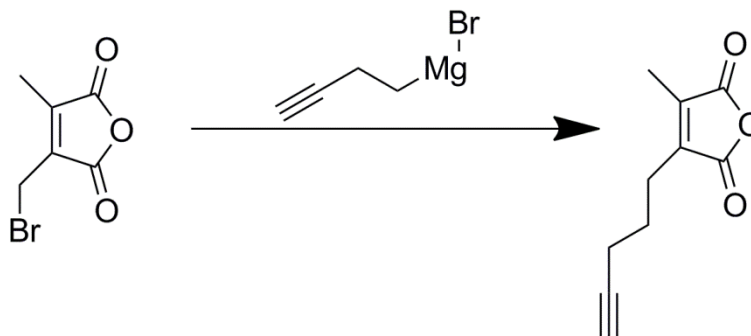
the residue was distilled under high vacuum (120-125° C, 2 mm) to get pure product (3.9 g, 56% yield). ¹H NMR (400 MHz, CDCl₃) 4.17 (s 2H), 2.17 (s 3H).

4.2.6.2 Synthesis of 3-(Azidomethyl)-4-methyl-2,5-furandione



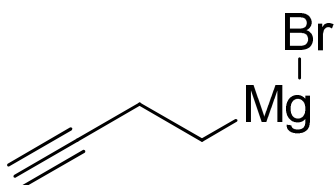
3-(Bromomethyl)-4-methyl-2,5-furandione (310.5 mg, 1.5 mmol) was dissolved in acetone (10 ml). Sodium azide (97.5 mg, 1.5 mmol) was added in one portion. The suspension was stirred over night at room temperature. After filtering the solvent was evaporated. The remaining oil was dissolved in ethyl acetate (20 ml) and washed with water (20 ml). Afterwards the organic layer was washed with 20 ml brine and dried over Na₂SO₄. Concentration in vacuo, followed by chromatographic purification over a silica gel column using hexane/ethyl acetate (7:3) as mobile phase gave pure product (220 mg, yield 88%). ¹H NMR (500 MHz, CDCl₃) 4.29 (q, J = 1.01 Hz, 2H), 2.17 (t, J = 1.01 Hz, 3H). ¹³C NMR (100 MHz, [d₆] acetone) δ 9.09, 43.15, 137.23, 144.51, 165.24, 165.93. IR ν_{max} 2101, 1759, 1679 cm⁻¹. MS (70 eV, DEI⁺) calcd for C₆H₅N₃O₃ [M]⁺ 167.12, found 166.99.

4.2.7 Synthesis of PentyneMMan linker



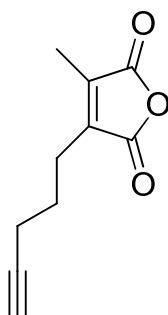
The 3-methyl-4-(pent-4-yn-1-yl)furan-2,5-dione linker (PentyneMMan) was synthesized from 3-(Bromomethyl)-4-methyl-2,5-furandione anhydride by a Grignard reaction with 3-butynyl-1-magnesium bromide.

4.2.7.1 Synthesis of 3-butynyl-1-magnesium bromide



This reaction was done analog as described elsewhere (146). Briefly: First the reaction flask was charged with ZnBr_2 (120 mg, 4 mol %, 0.53 mmol) and Mg (650 mg). Afterwards the flask was heated under vacuum and flushed with argon. Now diethylether (10 mL) and propargyl bromide (1.0 mL, 13 mmol) in Et_2O (8 mL) were added dropwise over a period of 40 minutes. Subsequently after the addition, exothermic reaction started and the mixture was cooled to 0°C (ice water). The mixture was stirred at the same temperature for further 1 h. This gave a greenish supernatant and pulverized Mg precipitates. The concentration of the supernatant was 0.52 M. This was determined by titration using methyl orange as an indicator (74% yield).

4.2.7.2 Synthesis of 3-methyl-4-pentynyl-furan-2,5-dione



3-(Bromomethyl)-4-methyl-2,5-furandione anhydride (410 mg, 2 mmol) and CuI (38 mg, 0.2 mmol) were dissolved in Et_2O (10 mL). Now HMPA (4 ml) was added. The reaction flask was flushed with argon. Reaction was started by dropping in a solution of 3-butynyl-1-magnesium bromide (0.52 M) from the reaction described above. Reaction was continued for 15 minutes over an ice bath. Now the reaction mixture was allowed to warm to room temperature and stirring was continued overnight. The resulting pink suspension was diluted with Et_2O (15 mL). Subsequently sulphuric acid (4 M, 10 ml) were added. The precipitations dissolve and the solution is turning

brown. The water phase was extracted three times with Et₂O (15 mL). Afterwards the combined organic phases were washed two times with water (20 mL) and then with brine (20 ml). Now the organic phase was dried with Na₂SO₄ filtered and solvent was removed by evaporation. The crude product purified over DCVC (diameter 4 cm, h=7 cm) with a step gradient from 0-50% EtAc in n-hexane (2.5 % steps, 20 ml fractions). After the solvent was removed colorless oil was obtained (113 mg, 32 %). TLC: R_f = 0.44 (n-heptane/EtAc =3/1). ¹H NMR (500 MHz, CDCl₃) 2.56 (m, 2H), 2.19 (m, 2H), 2.05 (s, 3H), 1.962 (m, 2H), 1.77 (m, 2H) ¹³C NMR (100 MHz, CDCl₃) δ 9.56, 18.023, 23.20, 25.86, 69.85, 82.66, 141.54, 143.52, 165.68, 165.99. IR v_{max} 3291, 2937, 2118, 1762, 1699, 1624 cm⁻¹. MS (70 eV, DCI⁺) calcd for C₁₀H₁₀O₃ [M]⁺ 178.18, found 179.1.

4.3 Cloning, heterologous expression and purification of nlsEGFP and HIV-TAT-nlsEGFP

The plasmid containing a gene for EGFP, tagged with a nuclear localization sequence (derived from SV 40 large T antigen), was kindly provided by M. Cristina Cardoso (TU Darmstadt, Germany). The coding region of the plasmid was amplified with PCR reaction using following primers:

forward: 5'-GTTGATGAATTCCCGAAGAAGAAGCGCAAAGTA-3';

reverse: 5'-TCAACTAAGCTTCTTGTAAGCTCGTCCATGCC-3'.

This gene was cloned into Novagen pET 23a (+) vector (Merck4biosciences, Darmstadt, Germany). By the common calciumchloride method, this plasmid was transformed into E. coli BL21(DE3)plysS (Novagen, Merck4biosciences, Darmstadt, Germany). Under constant shaking in TB medium (37° C), the cells were grown to an optical density of 0.75 (600nm). Protein expression was induced with isopropyl β-D-1-thiogalactopyranoside (Biomol, Hamburg, Germany) (final concentration 1mM) and expression was continued for another 16 hours. After ultrasonic cell lysis the nlsEGFP was purified by nickel chromatography using a gradient from binding buffer (50 mM sodium hydrogenphosphate, 300 mM sodium chloride, 20 mM imidazole) to elution buffer (50 mM sodium hydrogenphosphate, 500 mM sodium chloride, 250 mM imidazole). The protein was dialysed over night at 4° C against PBS buffer (pH 7.3)

using a dialysis membrane (14000 MWCO) from Carl Roth (Karlsruhe, Germany). Finally the nlsEGFP was concentrated with Amicon Ultra centrifugal filter units (MWCO 10,000). Transformation, protein expression and purification of the PTD bearing homolog were done in the same way. Following primers encoding for HIV-TAT sequence were annealed and cloned into the vector described above.

Sense: 5`AGCTTGGTTATGGGCGCAAAAACGCCGTCAGCGCCGTCGGGGCC3`
Antisense: 5`TCGAGGCCCGACGGCGCTGACGGCGTTTTTTTGCGCCATAACCA
3`

4.4 Modification of proteins with crosslinkers

4.4.1 Modification with SPDP

4.4.1.1 Modification of nlsEGFP with SPDP

nlsEGFP (3 mg, 0.095 μmol) was diluted in PBS buffer (1 ml; pH 7.3, 1 mM EDTA). Then SPDP (Succinimidyl 3-(2-pyridyldithio) propionate) was dissolved in DMSO (50 μl ; 1.14 μmol) and added to above protein solution. After incubation (2 h; 20°C), not conjugated linker was removed by size exclusion chromatography (Sephadex G25 superfine) using PBS buffer (pH 7.3, 1 mM EDTA) as mobile phase. The modified protein was concentrated with Amicon Ultra centrifugal filter units (MWCO=10,000; Millipore (Billerica, MA)). Protein concentration was quantified by measurement of the absorbance at a wavelength of 488 nm using an extinction coefficient of 55000 $\text{M}^{-1}\text{cm}^{-1}$. The ratio of linker to protein could be calculated, after reducing a sample of the modified protein with DTT (dithiothreitol) and determination of the change in absorbance (343 nm; 8080 $\text{M}^{-1}\text{cm}^{-1}$).

4.4.1.2 Modification of β -galactosidase with SPDP

β -galactosidase (3 mg, 0.026 μmol) was diluted in PBS buffer (1 mL; pH 7.3, 1 mM EDTA). Then SPDP (succinimidyl 3-(2-pyridyldithio)propionate) was dissolved in DMSO (50 μl ; 0.775 μmol) and added to above protein solution (30-fold molar excess compared to β -galactosidase). After incubation (2 h; 20° C), unconjugated linker was removed by size exclusion chromatography (Sephadex G25 superfine) using PBS

buffer (pH 7.3, 1 mM EDTA) as mobile phase. The modified protein was concentrated with Amicon Ultra centrifugal filter units (MWCO 10,000; Millipore (Billerica, MA)). The protein concentration was determined at 280 nm using a molar extinction coefficient of $210000 \text{ M}^{-1}\text{cm}^{-1}$. The ratio of linker to protein could be calculated, after reducing a sample of the modified protein with DTT (dithiothreitol) and determination of the change in absorbance (343 nm; $8080 \text{ M}^{-1}\text{cm}^{-1}$).

4.4.2 Modification of nlsEGFP with succinimidyl-4-(*N*-maleimidomethyl) cyclohexane-1-carboxylate (SMCC)

nlsEGFP (2 mg, 0.063 μmol) was diluted in PBS buffer (1 ml, pH 7.3) and SMCC (0.3 mg, 0.951 μmol) dissolved in DMSO (50 μl) was added. After an incubation time of 2 hours at room temperature, the reaction mixture was passed through a Sephadex G 25 superfine size exclusion column. The purified protein was concentrated with Amicon Ultra centrifugal filter units (MWCO 10,000).

4.4.3 Modification of nlsEGFP with MAM linker

nlsEGFP (5 mg, 0.158 μmol) was dissolved in Hepps Puffer (950 μl , 0.5 M, pH 9.0). Afterwards MAM linker (5 mg, 11.66 μmol) was diluted in DMSO (50 μl) and dropped slowly to the protein solution. Incubation (2 h) under constant stirring (20° C) was followed by removal of non-coupled linker. This was performed by size exclusion chromatography using PBS buffer (pH 8.0) as mobile phase. The modified protein was concentrated with Amicon Ultra centrifugal filter units (MWCO 10,000; Millipore (Billerica, MA)). The concentration of the modified nlsEGFP was quantified by measuring the absorbance (488 nm) using an extinction coefficient of $55000 \text{ M}^{-1}\text{cm}^{-1}$.

4.4.4 Modification of HSA with PentyneMMan linker

Human serum albumin (5 mg, 0.075 μmol) was dissolved in 500 μl Hepps buffer (0.5 M, pH 9.0). Then PentyneMMan linker (5 mg, 0.028 mmol) was diluted in acetonitrile

(50 μ l) and slowly dropped into the protein solution. After incubation for 2 h under constant stirring at room temperature not conjugated linker was removed by size exclusion chromatography using PBS buffer (pH 8.0) as mobile phase. The modified protein was concentrated with Amicon Ultra centrifugal filter units (MWCO 10,000; Millipore (Billerica, MA)). The concentration of the modified HSA was quantified by measurement the absorbance at a wavelength of 280 nm using an extinction coefficient of $41440 \text{ M}^{-1}\text{cm}^{-1}$.

4.4.5 Modification with AzMMMan linker

4.4.5.1 Modification of Melittin

Melittin peptide (2 mg, $2893.6 \text{ g mol}^{-1}$, 0.691 μ mol) was dissolved in a mixture of acetonitrile and Hepps buffer (0.5 M, pH 9.0) (1/2 v/v, 1 ml). Immediately after hydrolysis, N-ethylmaleimide (1 μ mol, 0.125 mg) dissolved in acetonitrile (50 μ l) was added. After 10 minutes at room temperature AzMMMan crosslinker (7.5 mg, 45 μ mol) was added and aggitated for 2 hours at 20° C. The reaction buffer was diluted in PBS buffer (add 5 ml, pH 8.5) and concentrated via ultrafiltration (Vivaspin2, Vivascience, Hannover, Germany MWCO 1000). Thereafter the reaction mixture was passed over a SEC G25 size exclusion column using 2.5 mM ammonium carbonate buffer (pH adjusted to 8.0) as eluent. The peptide containing fraction was lyophilised.

4.4.5.2 Modification of HSA

Human serum albumin (5 mg, 0.075 μ mol) was dissolved in 500 μ l Hepps buffer (0.5 M, pH=9.0). Then AzMMMan (5 mg, 0.03 mmol) was diluted in acetonitrile (50 μ l) and slowly, dropped into the protein solution. After incubation for 2 h under constant stirring at room temperature not conjugated linker was removed by size exclusion chromatography using PBS buffer (pH 8.0) as mobile phase. The modified protein was concentrated with Amicon Ultra centrifugal filter units (MWCO 10,000; Millipore (Billerica, MA)). The concentration of the modified HSA was quantified by measurement the absorbance at a wavelength of 280 nm using an extinction coefficient of $41440 \text{ M}^{-1}\text{cm}^{-1}$.

4.4.5.3 Modification of nlsEGFP

The conjugation was performed analogous to the method described above for the modification of HSA. Briefly: nlsEGFP 5 mg (0.158 μmol) was dissolved in Hepps Puffer (950 μl , 0.5 M, pH 9.0). Afterwards AzMMMan linker (5 mg, 0.03 mmol) was diluted in acetonitrile (50 μl) and dropped slowly to the protein solution. Incubation (2 h) under constant stirring (20° C) was followed by removal of non-coupled linker. This was performed by size exclusion chromatography using PBS buffer (pH 8.0) as mobile phase. The modified protein was concentrated with Amicon Ultra centrifugal filter units (MWCO 10,000; Millipore (Billerica, MA)). The concentration of the modified nlsEGFP was quantified by measuring the absorbance (λ 488 nm) using an extinction coefficient of 55000 $\text{M}^{-1}\text{cm}^{-1}$.

4.4.5.4 Modification of β -galactosidase

The conjugation was performed very similar to the method described above for the modification of HSA. Briefly: β -Gal 5 mg (0.043 μmol) was dissolved in Hepps Puffer (975 μl , 0.25 M, pH 8.5). Afterwards AzMMMan linker 3 (5 mg, 0.03 mmol) was diluted in acetonitrile (25 μl) and dropped slowly to the protein solution. Incubation (2 h) under constant stirring (20° C) was followed by removal of non-coupled linker. This was performed by size exclusion chromatography using PBS buffer (pH 8.0) as mobile phase. The modified protein was concentrated with Amicon Ultra centrifugal filter units (MWCO 10,000; Millipore (Billerica, MA)). The concentration of the modified β -Gal was quantified by measuring the absorbance (λ 280 nm) using an extinction coefficient of 210000 $\text{M}^{-1}\text{cm}^{-1}$.

4.5 Coupling of carriers, dyes and PEG to the proteins

4.5.1 Coupling of G3 PPI to nlsEGFP via EDC

G3 PPI (50 mg, 0.03 mmol) was diluted in H_2O (1ml). After complete dissolution pH was adjusted to 5.0 with water diluted hydrochloric acid (1 M). nlsEGFP (1 mg) diluted in 100 μl PBS buffer was added. The reaction was started by the addition of

EDC (N-(3-Dimethylaminopropyl)-N'-ethylcarbodiimide hydrochloride, final concentration 0.1 mg/ml) and continued under constant stirring at room temperature for 16 hours. The dendrimer modified nlsEGFP was purified over size exclusion chromatography using PBS buffer (pH 7.4) as mobile phase. Afterwards the product was concentrated using Amicon Ultra centrifugal filter units (MWCO 10,000).

4.5.2 Coupling of G3 PPI to nlsEGFPx5SPDP via a reducible disulfide bond

G3 PPI was diluted in PBS buffer (10 mg, 6 μ mol, 1 ml). pH was adjusted to 7.4 with water diluted hydrochloric acid (1 M). SPDP (8 μ mol) diluted in 100 μ l DMSO was added in one portion. After reaction for 2 hours at room temperature the protected thiol group was reduced by the addition of DTT (0.01 mmol, 1.5 mg) and further stirring for 30 minutes. The reaction product was purified over size exclusion chromatography using 0.01 M HCl as mobile phase and subsequently lyophilized. SPDP modified nlsEGFP (1 mg, 0.0317 μ mol) was diluted in Hepps buffer (1 ml, 0.5 M pH 8.0) and 10-fold molar excess of thiol bearing G3 PPI dendrimer (compared to covalently bound linker) (0.32 μ mol, 0.54 mg) was added and reacted for one hour. The reaction product was purified over SEC using PBS buffer (pH 7.4) as mobile phase.

4.5.3 Coupling of 386 to nlsEGFPx5SPDP

SPDP modified nlsEGFP (1 mg, 0.0317 μ mol) was diluted in Hepps buffer (1 ml, 0.5 M pH 8.5) and 2-fold molar excess of oligomer **386** (compared to covalently bound linker) (0.32 μ mol, 1.95 mg, 39 μ l) which was pre-dissolved in water (50 mg/ml), was added for the modification of nlsEGFP. Thereafter pH was adjusted to 7.5 with aqueous HCl (1 M). The product was purified, after 1 hour incubation (20° C) by Amicon Ultra centrifugal filter units (MWCO 10,000; \times 3 washing steps with PBS buffer, 1 mM EDTA, pH 7.3).

4.5.4 Coupling of **386** to β -galactosidase₈SPDP

SPDP modified β -galactosidase (1 mg, 0.0086 μ mol) was diluted in Hepps buffer (1 ml, 0.5 M pH 8.5) and 5-fold molar excess of oligomer **386** (compared to covalently bound linker) (0.34 μ mol, 2.1 mg, 42 μ l) which was pre-dissolved in water (50 mg/ml), was added for the modification of nlsEGFP. Thereafter pH was adjusted to 7.5 with aqueous HCl (1 M). The product was purified, after 1 hour incubation (20° C) by Amicon Ultra centrifugal filter units (MWCO 10,000; \times 3 washing steps with PBS buffer, 1 mM EDTA, pH 7.3).

4.5.5 Coupling of **386** to SMCC-nlsEGFP

SMCC modified nlsEGFP (1 mg, 0.032 μ mol) was diluted in Hepps buffer (1 ml, 0.5 M pH 8.5). Then a dilute aqueous solution (30 μ l, 50 mg/ml) of oligomer **386** (M_w 6165.9 g mol^{-1}) was added (0.24 μ mol). The pH was adjusted to 7.5 with aqueous HCl (1 M). After incubation for 1 hour at room temperature the product was isolated by Amicon Ultra centrifugal filter units (MWCO 10,000) (\times 2 washing steps with PBS buffer pH 7.3).

4.5.6 Coupling of **386** to AzMMMan-nlsEGFP

Oligomer **386** (1.5 mg, 0.24 μ mol, containing within the sequence three mol equivalent cysteine mercapto groups) was diluted in Hepps buffer (1 ml, 0.5 M, pH 8.5). Subsequently dibenzylcyclooctyne-PEG4-maleimide (0.49 mg, 0.72 μ mol) diluted in DMSO (100 μ l) was added. Afterwards the pH was adjusted to 8.0. This mixture was given in one portion to AzMMMan-nlsEGFP (1 mg, 0.032 μ mol) diluted in Hepps buffer (1 ml, 0.5 M, pH 8.0). After 4 hours at 20°C non-conjugated polymer was removed by centrifugation steps with Amicon Ultra centrifugal filter units (MWCO 10,000) (\times 2 washing steps with PBS buffer pH 7.3).

4.5.7 Coupling of TMR labelled-**386** to AzMMMan-nlsEGFP

386 (20 mg, 3.244 μ mol) was dissolved in DMSO (400 μ l) and TMRM (1.56 mg, 3.244 μ mol), dissolved in DMSO (400 μ l) was added. After one hour at room

temperature, dibenzylcyclooctyne-PEG4-maleimide (4.38 mg, 6.48 μmol) diluted in DMSO (200 μl) was added and stirred for one hour. This was dropped slowly under stirring to AzMMMan-nlsEGFP (10 mg diluted in 10 ml 0.5 M Hepps buffer pH 8.5). After 4 hours at 20° C non-conjugated polymer was removed by centrifugation steps with Amicon Ultra centrifugal filter units (MWCO 10,000) ($\times 2$ washing steps with PBS buffer pH 7.3).

4.5.8 Coupling of 386 to AzMMMan- β -galactosidase

Oligomer **386** (1.5 mg, 0.24 μmol , containing within the sequence three mol equivalent cysteine mercapto groups) was diluted in Hepps buffer (1 ml, 0.5 M, pH 8.5). Subsequently DBCO-PEG4-maleimide (0.49 mg, 0.72 μmol) diluted in DMSO (100 μl) was added. Afterwards the pH was adjusted to 8.0. This mixture was given in one portion to AzMMMan- β -Gal (1 mg, 0.0086 μmol) diluted in Hepps buffer (1 ml, 0.5 M, pH 8.0). After 4 hours at 20° C non-conjugated polymer was removed by centrifugation steps with Amicon Ultra centrifugal filter units (MWCO 10,000) ($\times 2$ washing steps with PBS buffer pH 7.3).

4.5.9 Coupling of poly(ethylene glycol) (PEG)

4.5.9.1 Coupling of PEG 5000 to AzMMMan-nlsEGFP

Poly(ethylene glycol) methyl ether thiol (average M_w 5000 g/mol, 2 mg, 0.4 μmol) was dissolved in PBS buffer (80 μl , pH 8.0). Subsequently N-propargyl maleimide (0.4 μmol) diluted in acetonitrile (20 μl) was added. This mixture was dropped into AzMMMan-HSA (0.5 mg, 7.5 nmol) diluted in PBS (900 μl , pH 8.0). The click reaction was initiated by adding click solution C (30 μl). Click solution C was freshly prepared as described in section 3.5. After incubation for 3 h at 20° C the product was purified via ultrafiltration (Amicon Ultra centrifugal filter units (MWCO 10,000), $\times 2$ washing steps with PBS buffer pH 8.0).

4.5.9.2 Coupling of TMR labelled PEG to AzMMMan-nIsEGFP

PEG dithiol (Mw 8000, 10 mg, 1.25 μmol) was dissolved in DMSO (800 μl) and Tetramethylrhodamine-5-maleimide (TMRM) (0.6 mg, 1.25 μmol), dissolved in DMSO (100 μl) was added. After one hour at room temperature, N-propargyl maleimide (0.17 mg, 1.25 μmol) diluted in DMSO (100 μl) was added and stirred for one hour. 200 μl of this solution was dropped slowly under stirring to AzMMMan-HSA (1 mg, 0.015 mol, diluted in 1.8 ml PBS buffer pH 8.0). The click reaction was started by addition of click reaction c (30 μl). Click solution C was freshly prepared as described in the section buffers and solutions. After 4 hours at 20° C, non-conjugated PEG polymer and dye were removed by centrifugation steps with Amicon Ultra centrifugal filter units (MWCO 10,000) ($\times 2$ washing steps with PBS buffer pH 7.3), yielding the TMR-PEG-HSA conjugate.

4.5.10 Coupling of alkyne hemicyanine dye to AzMMMan-HSA

AzMMMan-HSA (5 mg, 0.075 μM) was diluted in PBS buffer (1.5 ml, pH 8.0). Alkyne dye (0.375 mg, 0.99 μmol) was diluted in DMSO (50 μl) and dropped into the protein solution. Reaction was started by addition of click solution C (30 μl). Click solution C was freshly prepared as described in the section buffers and solutions. After 3 h of incubation at 20° C the reaction batch was purified with Amicon Ultra centrifugal filter units (MWCO 10,000) (two washing steps with PBS buffer pH 8.0), followed by an additional purification step over size exclusion chromatography using PBS buffer (pH 8.0) as mobile phase.

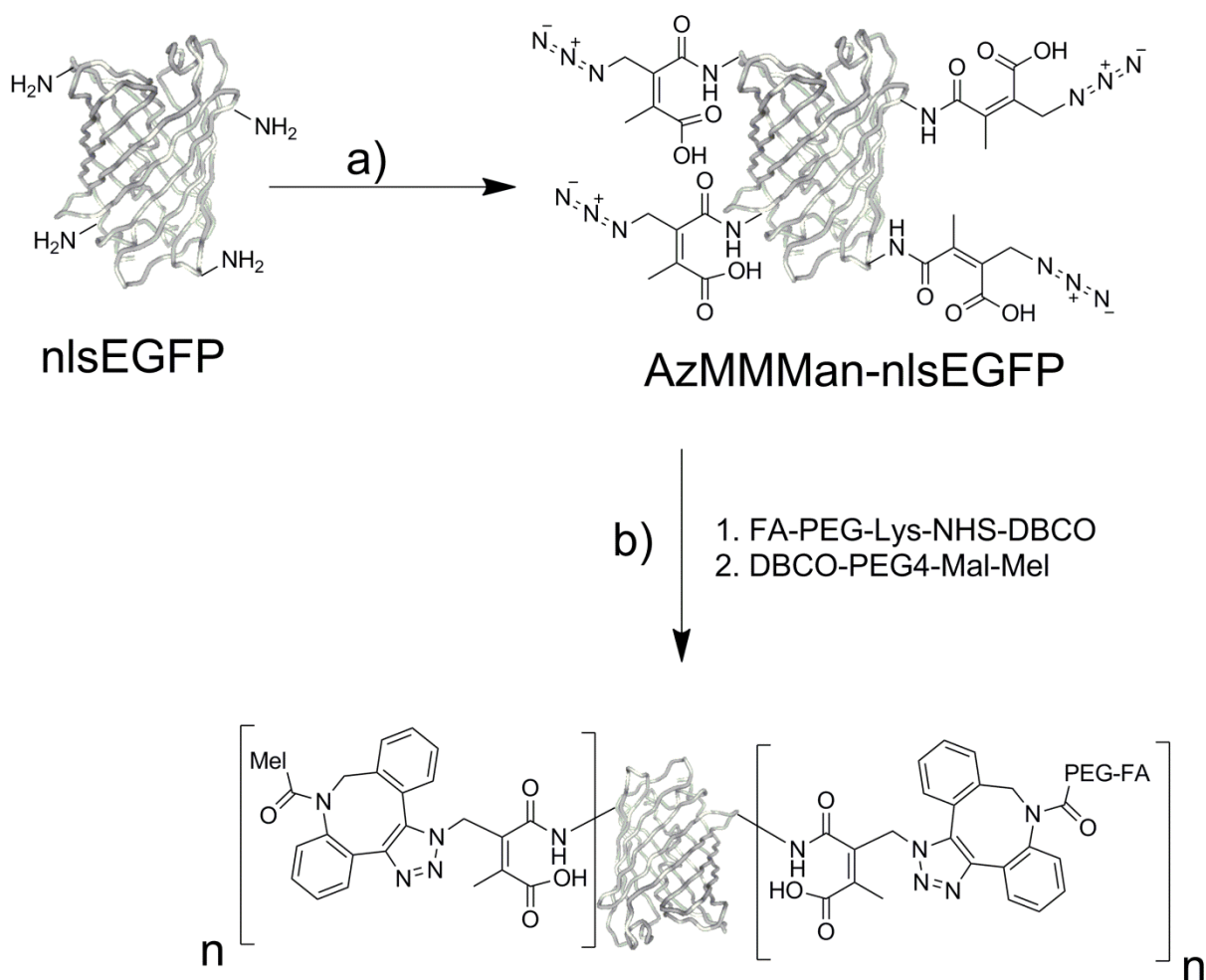
4.5.11 Coupling of phosphine dye DyLight 488 to AzMMMan-HSA

DyLight 488, a phosphine containing dye (Thermo Fisher Scientific, Germany) (0.1 mg, 0.09 μmol) was dissolved in DMSO (20 μl). This was added to AzMMMan-HSA (2 mg, 0.03 μmol , diluted in 230 μl PBS buffer pH 8.5) resulting in an end concentration of 8 mg protein/ml. After 4 h incubation at 37° C the labeled HSA was purified over SEC (G25 superfine) with PBS buffer (pH 8.5) as eluent.

4.5.12 Coupling of azide dye to PentyneMMan-HSA

PentyneMMan-HSA (5 mg, 0.075 μ M) was diluted in PBS buffer (1.5 ml, pH 8.0). Azide dye (0.375 mg, 0.64 μ mol) was diluted in DMSO (50 μ l) and dropped into the protein solution. Reaction was started by addition of click solution C (30 μ l). Click solution C was freshly prepared as described in the section buffers and solutions. After 3 h of incubation at 20° C the reaction batch was purified with Amicon Ultra centrifugal filter units (MWCO 10,000) (two washing steps with PBS buffer pH 8.0), followed by an additional purification step over size exclusion chromatography using PBS buffer (pH 8.0) as mobile phase.

4.5.13 Coupling of folic acid and melittin to AzMMMan-EGFP



Scheme 4.2: Synthesis of a polycation-free protein transduction shuttle.

Folic acid-PEG-lysine (5 mg, 2.9 μ mol) was diluted in 400 μ l of a 1/1 mixture of Heppps (0.25 M, pH 8.5) and DMSO. After dissolution DBCO-NHS ester (2.9 μ mol,

1.25 mg) diluted in DMSO (100 μ l) was added. The reaction was continued for 2 hours and the mixture was purified by dialysis against PBS buffer (pH 8.5) over night. A dialysis membrane with a MWCO of 1000 Da (Carl Roth (Karlsruhe, Germany)) was used. Afterwards it was filled up to 1ml with PBS (pH 8.5). Melittin (0.5 mg, 0.169 μ mol) was diluted in PBS containing 30% acetonitrile (200 μ l). Now dibenzylcyclooctyne-PEG4-maleimide (0.11 mg, 0.169 μ mol) diluted in DMSO (50 μ l) was added dropwise and stirred for 30 minutes. Meanwhile AzMMMan-nlsEGFP (1 mg, 0.032 μ mol) was diluted in PBS buffer (1 ml, pH 8.5). To the protein solution was added a threefold surplus of the folic acid conjugate (0.1 μ mol, 35 μ l) and reacted for two hours at room temperature. Thereafter a 5 fold excess of the melittin conjugate was added (0.16 μ mol, 236 μ l) and reaction was continued for another two hours. Later the modified protein was purified over size exclusion chromatography SEC G25 superfine with PBS buffer (pH 8.5) as eluent.

4.5.14 Coupling of transduction oligomer 71 to MAM-EGFP

MAM modified nlsEGFP (1 mg, 0.032 μ mol) was diluted in Hepps buffer (1 ml, 0.5M pH 8.5). Then a dilute aqueous solution of transduction oligomer **72** (M_w 2247.25 g mol^{-1}) was added (0.064 μ mol). The pH was adjusted to 7.5 with aqueous HCl (1 M). After incubation for 1 hour at room temperature, precipitated protein was separated by centrifugation. The supernatant was purified by dialysis against PBS buffer (pH 7.4, MWCO 15000 Da) over night.

4.6 Characterization of new acid labile crosslinkers

4.6.1 Determination of the degree of protein modification

Samples of HSA (M_w 66478 g mol^{-1} , 5 mg, 0.075 μ M) were reacted with the azido-dimethylmaleic anhydride linker (compound **3**, Scheme 5.8) as described above. But this time varying amounts of AzMMMan diluted in acetonitrile (50 μ l) were added (end concentrations of 2.0, 1.8, 1.6, 1.4, 1.2, 1.0, 0.8, 0.6, 0.4, 0.2 mM). After purification the AzMMMan modified HSA (compound **4**, Scheme 5.8) was reacted with an excess of the water soluble alkyne dye (0.375 mg, 0.99 μ mol) as described above to result in compound **7** (Scheme 5.8). The amount of AzMMMan groups

incorporated in HSA could be determined by quantifying the amount of dye coupled to the protein. This was done by following procedure. A sample of the labeled HSA was taken and the dye was cleaved off from the protein by incubation in an equal volume acetate buffer (0.5 M, pH 3.0) for 5 hours at 37° C. Thereafter the solution was neutralized with Tris buffer (1 M, pH 9.0) and the absorbance of the dye was measured at a wavelength of 530 nm (ϵ 35000 M⁻¹ cm⁻¹). After purification over a size exclusion column with PBS (pH 7.3) as eluent, the protein concentration was determined by measuring the HSA absorbance at 280 nm using an extinction coefficient of 41440 M⁻¹cm⁻¹.

4.6.2 Determination of the acid catalyzed release of linker from the protein

This experiment was done similar to the method described above for the determination of AzMMMA groups incorporated into HSA. Dye labelled HSA (compound 7, Scheme 5.8) was acidified to the required pH with acetic acid and incubated in the same volume of citric acid-phosphate (0.1 M) buffer. Thus samples having final pH values of 8.5, 7.3, 6.0, 5.0 and 4.0 were obtained. These samples were incubated at 37° C. At different time points samples were withdrawn. The amount of released dye was determined, after purification over a size exclusion column, by measuring the absorbance of the dye still coupled to the protein. For the comparative release between dye coupled via Staudinger Ligation and dye linked via CuAAc the incubation was done at 20° C for 16 h. The amount of Dylight was determined using an extinction coefficient of 70000 M⁻¹cm⁻¹ at a wavelength of 493 nm.

4.6.3 Serum stability assay

For the serum stability assay experiments were done following the same procedure as described above in 4.6.2. After incubation against PBS buffer (pH 7.4) containing 30% fetal bovine serum at 37 °C for different time intervals samples were withdrawn purified and analyzed. Each experiment was done in triplicates.

4.6.4 Release of PEG from HSA conjugate

Polyethylene glycol modified HSA (compound **8**, Scheme 5.8) was dialyzed against citric acid-phosphate buffers of different pH values (0.1 M, pH: 8.5, 7.3, 6.0, 5.0, 4.0) for 16 hours at 37° C using a 14000 MWCO dialysis membrane from Carl Roth (Karlsruhe, Germany). Afterwards the solutions were neutralised using sodium hydroxide (1 M). Samples of protein (about 20 µg) were loaded on a 12.5% SDS-PAGE gel. The gel ran for 2 hours at 160 V. After electrophoresis the gel was stained with comassie solution (45/45/10 water/methanol/acetic acid and 0.5% comassie brilliant blue G250). Then the gel was washed several times with an aqueous solution of acetic acid (7.5% v/v) and ethanol (20% v/v).

4.6.5 Release kinetics of TMR-labeled PEG from HSA conjugate

To determine the detailed release kinetics, PEG was labeled with Tetramethylrhodamine-5-maleimide (TMRM). Briefly: PEG dithiol (Mw 8000, 10 mg, 1.25 µmol) was dissolved in DMSO (800 µl) and TMRM (0.6 mg, 1.25 µmol), dissolved in DMSO (100 µl) was added. After one hour at room temperature, N-propargyl maleimide (0.17 mg, 1.25 µmol) diluted in DMSO (100 µl) was added and stirred for one hour. 200 µl of this solution was dropped slowly under stirring to AzMMMan-HSA (1 mg, 0.015 mol, diluted in 1.8 ml PBS buffer, pH 8.0). The click reaction was started by addition of click reaction C (30 µl). Click solution C was freshly prepared as described in section 3.5. After 4 hours at 20° C, non-conjugated PEG polymer and dye were removed by centrifugation steps with Amicon Ultra centrifugal filter units (MWCO 10,000) (×2 washing steps with PBS buffer pH 7.3), yielding the TMR-PEG-HSA conjugate. The release kinetic experiment with this conjugate was performed as described above in section 4.6.2 (release of alkyne dye from conjugate). Absorption was measured at a wavelength of 543 nm.

4.6.6 Acid catalyzed release of nlsEGFP from 386-DBCO - AzMMMan-nlsEGFP

4.6.6.1 Qualitative release

Samples of **386**-DBCO-AzMMMan-nlsEGFP (compound **9**, Scheme 5.8) were acidified to pH 5 by dialysis against citric acid-phosphate buffer (0.1 M, pH 5) at 37° C overnight. The dialysis was performed using a 14000 MWCO dialysis membrane from Carl Roth (Karlsruhe, Germany). After that time the protein solution was neutralized using Tris buffer (1 M, pH 9.0). Afterwards protein samples (about 20 µg) were loaded on a SDS-PAGE gel (12.5%) and run at 160 V for 2 hours. After electrophoresis the gel was stained with comassie solution (45/45/10 water/methanol/acetic acid, v/v/v, and 0.5% w/v comassie brilliant blue G250). Then the gel was washed several times with an aqueous solution of acetic acid (7.5% v/v) and ethanol (20% v/v).

4.6.6.2 Release kinetics

To determine the full release kinetic of **386**-AzMMMan-nlsEGFP conjugates (compound **9**, Scheme 5.8) the oligomer **386** was labeled with one equivalent tetramethylrhodamine-5-maleimide (TMRM) before coupling. Briefly: **386** (20 mg, 3.244 µmol) was dissolved in DMSO (400 µl) and TMRM (1.56 mg, 3.244 µmol), dissolved in DMSO (400 µl) was added. After one hour at room temperature, dibenzylcyclooctyne-PEG4-maleimide (4.38 mg, 6.48 µmol) diluted in DMSO (200 µl) was added and stirred for one hour. This was dropped slowly under stirring to AzMMMan-nlsEGFP (conjugate **5**, Scheme 5.8) (10 mg diluted in 10 ml 0.5 M Hepes buffer, pH 8.5). After 4 hours at 20° C non-conjugated polymer was removed by centrifugation steps with Amicon Ultra centrifugal filter units (MWCO 10,000) (x2 washing steps with PBS buffer, pH 7.3). The release kinetic experiment (see Figure 5) was performed as described above for the release of alkyne dye from conjugate **7** (Scheme 5.8). Absorption was measured at a wavelength of 543 nm.

4.7 Biological characterization of the synthesized conjugates

4.7.1 General procedures

4.7.1.1 Cell culture

The used cell lines are listed in Table 3.1. All cultured cells were grown at 37° C in 5% CO₂ humidified atmosphere. HeLa and Neuro2A cells were grown in DMEM (1 g/l glucose) supplemented with 10% FCS and 100 U/ml penicillin and streptomycin (100 µg/ml). 3T3 murine fibroblasts cells were grown in Dulbecco's modified Eagle's medium (DMEM), supplemented with FCS (10%), glucose (4 g/l), stable glutamine (4 mM), sodium pyruvate (1 mM), penicillin (100 U/mL), and streptomycin (100 µg/mL). KB cells were cultured in RPMI media without folic acid.

4.7.1.2 Flow cytometry (FACS)

3T3, HeLa or Neuro2A cells were seeded in 6-well plates (250000 cells/well). After transfection and washing as described in the transfection section 4.7.2, cells were detached with trypsin/EDTA, diluted with growth media containing 10% FCS, harvested by centrifugation and taken up in phosphate-buffered saline with 10% FCS. Flow cytometry was performed using a Cyan ADP flow cytometer (Dako, Hamburg, Germany). The cellular fluorescence was assayed by excitation of nlsEGFP or C12-FDG at 488 nm and detection of emission at 510 nm. To discriminate between viable and dead cells as well as for exclusion of doublets, cells were appropriately gated by forward/sideward scatter, pulse width and counterstained with propidium iodide. 10000 gated cells per sample were collected. Data was recorded with SummitT software (Summit, Jamesville, NY). Evaluation was done using FlowJo software (Treestar, Ashland, Oregon, USA).

4.7.1.3 Fluorescence microscopy and phase contrast microscopy

For fluorescence microscopy observation, the nuclei of the cells were stained by pipetting Hoechst Dye 33342 (1 µg/ml) into the cell culture media. 10 minutes later the cells were watched on an Axiovert 200 fluorescence microscope from Zeiss (Jena, Germany). A 40x phase 1 objective or a 63x magnification DIC oil immersion objective (Plan-APOCHROMAT) and appropriate filter sets for analysis of EGFP and Hoechst fluorescence were used. Data were analyzed and processed by AxioVision LE software (Zeiss, Jena, Germany). For phase contrast microscopy, also an Axiovert 200 microscope from Zeiss (Jena, Germany) was used. Pictures were taken using a 10x magnification phase 1 contrast objective.

4.7.1.4 Microinjections

Microinjections of nlsEGFP, HIV-TATnlsEGFP or carrier modified nlsEGFP were performed with a Femtojet microinjector and an Injectman NI2 micromanipulator (Eppendorf). HeLa cells were plated onto sterile glass bottom culture dishes. On the day of transfection cells have reached a fluency of 70%. A spinning disk confocal microscope (BFI Optilas, Dietzenbach, Germany) was used for microinjection. Proteins were injected with a concentration of 0.5 mg/ml in PBS buffer.

4.7.2 Protein transductions

Protein transductions were done similar for all transfections independent of used cell line, or used transduction oligomer. Just the used protein concentrations were different.

4.7.2.1 Transduction of nlsEGFP

For fluorescence microscopy, 24 h prior to transfection 20000 cells (HeLa, KB, Neuro2A, 3T3) were seeded in 8 well Nunc chamber slides (Thermo Scientific, Braunschweig, Germany). Before transfection, medium was replaced with fresh medium. Subsequently the oligomer modified nlsEGFP was pipetted into cell culture media (10% FCS). After two hours incubation time the cells were washed with PBS

buffer (pH 7.3), containing 500 IU heparin per ml. Afterwards fresh medium was added and 2 hours later the cells were examined under the microscope.

For FACS experiments, 24 h prior to transfection 250000 cells were seeded in 6 well plates. Before transfection, medium was replaced with fresh medium containing 10% FCS. Subsequently the oligomer modified nlsEGFP was pipetted into the cell culture media. After incubation (usually 120 min, except for the uptake vs. time experiment 15; 30; 60; 120; 180 min) cells were washed two times with PBS buffer (pH 7.3; 500 IU heparin/ ml).

4.7.2.2 Transduction of β -galactosidase

Transfection was done quite similar as described above for nlsEGFP. Neuro2A or HeLa cells were seeded in 6 well plates (250000 cells per well; one day before transduction) and transfected with different concentrations **386**- β -galactosidase for two hours.

For X-Gal staining, a method which was previously described was used (147). After transduction, cells were washed with PBS (containing 500 IU heparin per ml and subsequently fixed with glutaraldehyde (1.25% (v/v)). Following two additional washing steps with PBS, X-gal staining solution (50 mM Tris/HCl, pH 7.5; 5 mM potassium ferrocyanate, 5 mM potassium ferricyanate, 15 mM sodium chloride, 1 mM magnesium chloride, 0.1% Triton and 0.5 mg/mL X-gal) was added and incubated for three hours (37° C). Afterwards the cells were washed once more with PBS and analyzed with a phase contrast microscope.

For quantitative FACS analysis C12-FDG (Invitrogen, Karlsruhe, Germany) substrate was used. 250000 Neuro 2A or HeLa cells were seeded in 6 well plates the day before transfection. Transduction was done by pipetting **386**- β -galactosidase into the growth media. After two hours incubation the cells were washed two times with PBS buffer, supplemented with 500 IU heparin per ml. Afterwards the cells were covered with fresh growth media containing 2.0 μ M C12-FDG. After incubation for 45 minutes, the cells were washed again with PBS and evaluated by flow cytometry.

4.7.3 Endocytosis inhibition

This experiment was performed as described elsewhere (148), with minor modifications. Briefly: 250000 cells were seeded in 6 well plates. Before transfection, medium was replaced with fresh medium containing 1 mM amiloride (inhibitor for macropinocytosis), 5 $\mu\text{g}/\text{mL}$ chlorpromazine (inhibitor for clathrin-mediated endocytosis), or 2.5 mM β -cyclodextrin (inhibitor for caveolae-mediated endocytosis). After 30 minutes incubation, the oligomer modified nlsEGFP was pipetted into the cell culture media (0.5 μM). Another 120 min later, cells were washed two times with PBS buffer (pH 7.3, 500 IU heparin per ml) and subsequently analyzed via flow cytometry or fluorescence microscopy.

4.7.4 Cell viability assay

The metabolic activity of transfected cells was determined by MTT assay. Neuro2A, HeLa or 3T3 cells were seeded in 96-well tissue culture plates (TPP, Transdingen, Switzerland) at a density of 15000 cells per well, the day before transfection. Cells were transfected with different concentrations of **386**-nlsEGFP in 100 μL growth media (containing 10% FCS) for two hours. After washing with PBS and incubation in fresh media (3 h), MTT solution (10 μL per well, 5.0 mg/mL MTT in phosphate-buffered saline buffer, pH 7.4) was added. The medium was replaced by 100 μL of DMSO after 3 h. The optical absorbance was measured at 590 nm, with a reference wavelength of 630 nm, by a microplate reader (Spectraflour Plus, Tecan Austria GmbH, Austria). The metabolic activity of the transduced cells was expressed as relative cell viability, compared to untreated cells. Relative cell viability was defined as

$$\%[\textit{haemolysis}] = \frac{A_{590}(\textit{treated})}{A_{590}(\textit{untreated})} 100$$

4.7.5 Activity test of modified β -galactosidase

The formation of a fluorescent product (4-methylumbelliferone (4-MU); $\lambda_{\text{excitation}}$ 360 nm, $\lambda_{\text{emission}}$ 440 nm) out from the nonfluorescent 4-methylumbelliferone- β -D-galactopyranoside substrat (MUG) by hydrolysis through β -galactosidase (149) was

used to determine the relative activity of modified β -galactosidase, compared to unmodified enzyme. The assay was performed with minor modification as described elsewhere (150). Briefly: MUG (1 mM, non-limiting surplus) substrate was dissolved in PBS buffer (pH 7.4; 5 mM MgCl_2). The reaction was started by the addition of enzyme (0.5 $\mu\text{g}/\text{ml}$). Enzyme kinetic was monitored, by following the formation of the fluorescent 4-MU product over time, on a Varian Cary Eclipse fluorescence spectrophotometer. As the substrate was used in non-limiting surplus, the enzyme activity is displayed by the slope of the curve.

4.7.6 Erythrocyte leakage assay

This experiment was done quite similar as described elsewhere (62). From fresh, citrate-treated blood mouse erythrocytes were isolated and washed in phosphate buffered saline (PBS) by four centrifugation steps (800 g, 10 min, 4° C). With PBS (pH 7.3) the erythrocytes were diluted to the final cell concentration (5.0×10^7 cells/ml). AzMMMA modified melittin was diluted in PBS buffer (pH 7.3) to give melittin concentrations of 5, 2.5, 1.0, 0.5, 0.25 μM . For comparison the same concentrations of pure melittin were prepared. The same solutions were prepared with PBS buffer (pH 5.0). The acidic samples were preincubated for 3 h at 37° C under constant shaking. Meanwhile erythrocyte suspension (75 μL , 3.75×10^6 cells, per well) was pipetted in a V-bottomed 96-well plate (NUNC, Denmark). After mixing with 75 μL of the different samples and incubation for 60 min at 37°C under constant shaking, the cells were pelletized (800 g, 10 min). The hemoglobin release was analyzed by measuring the absorbance of supernatant (80 μl) at 405 nm using a 96-well microplate reader (Spectrafluor Plus, Tecan Austria GmbH, Grödig, Austria). To get data for 100% lysis, erythrocyte suspension (75 μL) was freeze-thawed three times and centrifuged (800 g, 10 min) and diluted with PBS buffer (75 μL , pH 7.3). Relative haemolysis was defined as:

$$\%[\text{haemolysis}] = \frac{A_{405}(\text{melittin}) - A_{405}(\text{untreated})}{A_{405}(\text{freeze - thawed}) - A_{405}(\text{untreated})} 100$$

5 Results

5.1 nlsEGFP as a model protein

First aim of this work was to establish a cellular test system that enables evaluation of the efficiency of the developed protein transduction technologies. For these studies nlsEGFP (Figure 5.1) was used as one of two model proteins.

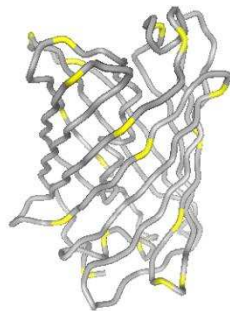


Figure 5.1: 3D structure of EGFP. Calculated with ModWeb and visualized by DeepView version 4.04. Lysine residues are marked yellow.

For multiple reasons nlsEGFP presents a good model for intracellular protein transduction. Most important its fluorescent properties can be used to pursue its cellular uptake, qualitatively with a fluorescent microscope, or in a more quantitative fashion with FACS experiments. Furthermore with a molecular weight of around 31 kDa, it represents a protein of average molecule size. With an isoelectric point around 6.5 it is only slightly charged at physiological pH value of 7.4. An additional feature is, that its fluorescence intensity is pH dependent (Figure 5.2). At pH 5.0 that is found in late endosomes the absorbance is only about 10 percent of the absorbance at pH 7.5. This finding is consistent with the pH dependent fluorescence reported for EGFP (151). High cellular fluorescence is a hint for successful endosomal escape of the transduced nlsEGFP, because protein encapsulated in acidic late endosomes shows only marginal fluorescence. The nuclear localization signal (derived from SV40 large T-antigen) fused to the N-terminus is a second property that is indicating endosomal escape as free cytosolic protein should be translocated into the nucleus (152).

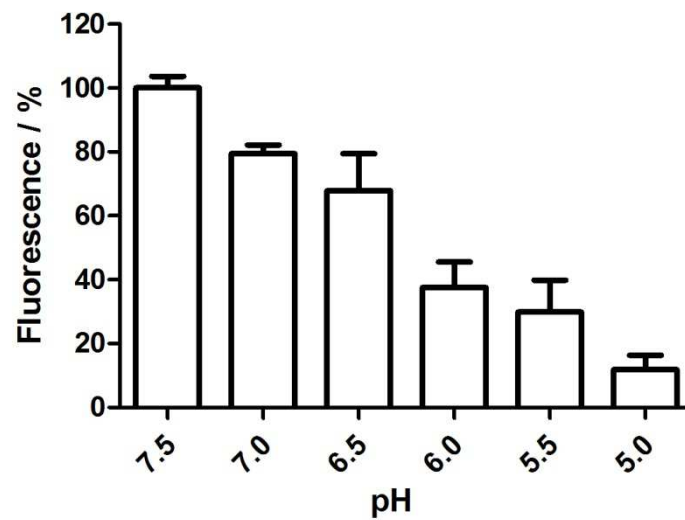


Figure 5.2: Fluorescence of nlsEGFP at different pH values. Fluorescence is normalized to the mean value at pH 7.5.

5.1.1 Cloning, heterolog expression and purification of nlsEGFP and TAT-nlsEGFP

The gene encoding for nlsEGFP was amplified from the vector pc1068-pRHGPCNA and provided with new cloning sites for the insertion into the expression vector pET 23a(+) by PCR reaction. The successful amplification is shown in Figure 5.3.

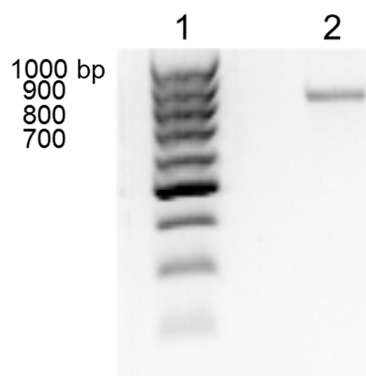


Figure 5.3: PCR amplification of nlsEGFP gene from plasmid pc1068-pRHGPCNA (Scheme 9.1). Lane 1: DNA standard; Lane 2: PCR product.

After cloning and transformation into *E. coli* expression strain BL21DE3, protein expression was induced. Figure 5.4 and Figure 5.5 are documenting the purification of the HIS tagged nlsEGFP and the HIV-TAT bearing counterpart over affinity chromatography. Both proteins were obtained in over 90 percent purity.

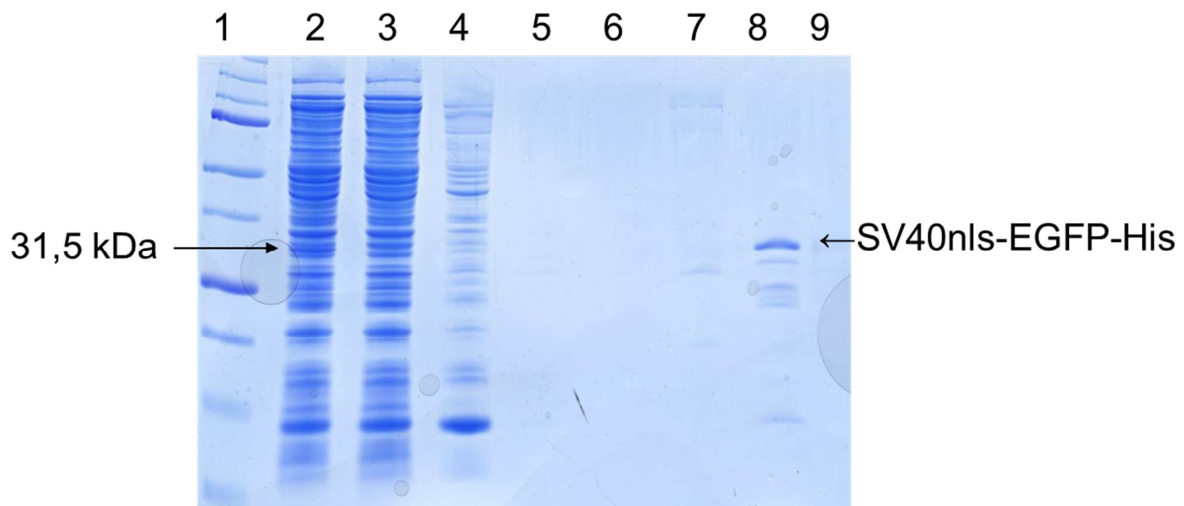


Figure 5.4: Purification of nlsEGFP over affinity chromatography. Lane1: Protein Ladder; Lane2: *E. coli* lysate; Lane 3: flow through; Lane4-6: wash steps; Lane 7-9: elution fractions.

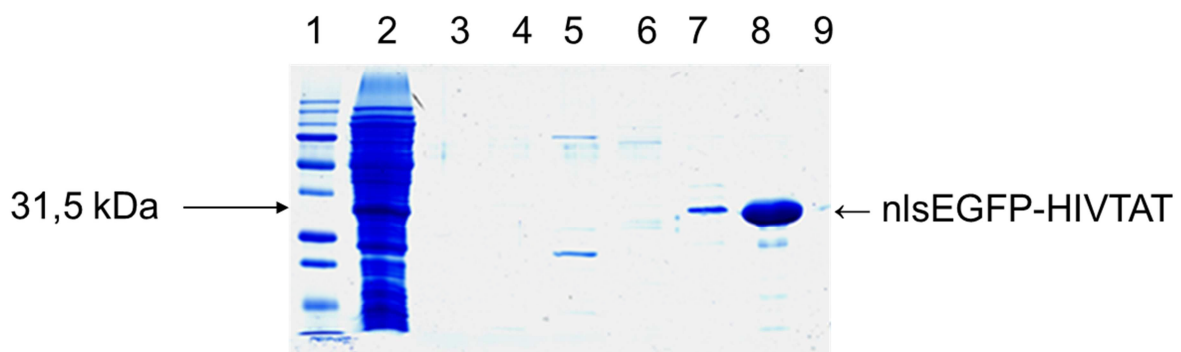


Figure 5.5: Purification of nlsEGFP over affinity chromatography. Lane1: Protein Ladder; Lane2: *E. coli* lysate; Lane 3-6: wash steps; Lane 7-9: elution fractions.

From a four liter overnight *E. coli* culture in TB medium about 50 mg of pure protein were obtained. The fluorescence properties of both proteins were evaluated by measuring absorbance and fluorescence spectra (Figure 5.6). Both proteins exhibited a fluorescence maximum at about 510 nm. Absorption maxima were detected at around 400 nm and 490 nm for both proteins. The extinction coefficient was around 55000 at pH 7.4. All these data is consistent with values found for EGFP in literature.

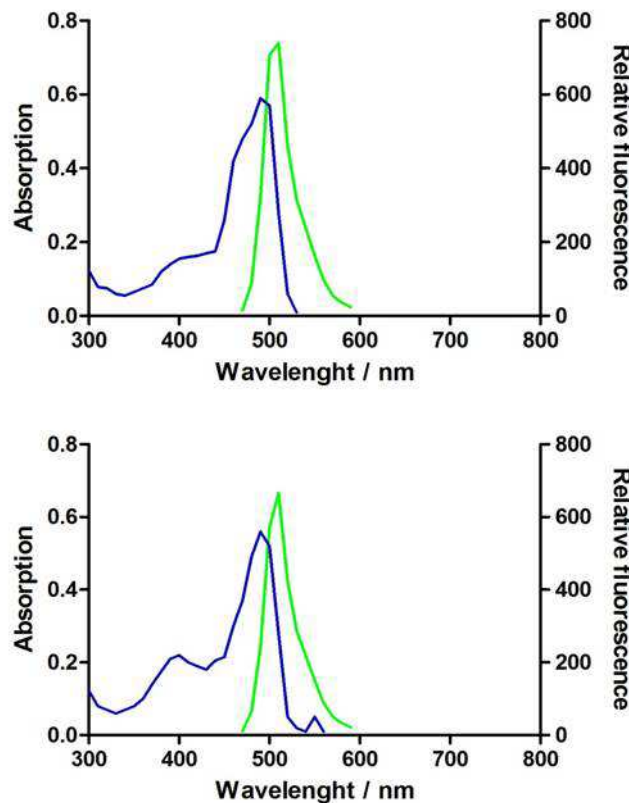


Figure 5.6: Fluorescence and absorption spectra of nlsEGFP and nlsEGFP-TAT. Blue lines present extinction spectra; green lines present emission spectra.

5.1.2 Microinjection of nlsEGFP and TAT-nlsEGFP

As already mentioned above the nuclear localization signal was fused by genetic engineering to the model protein to indicate successful endosomal escape of the transduction shuttles. To evaluate the functionality of the fused nuclear localization signal (derived from SV 40 large T-antigen) nlsEGFP was microinjected into the cytosol of HeLa cells. The fluorescence microscope pictures in Figure 5.7 show that injected nlsEGFP is translocated into the nucleus very fast. Already 30 minutes after microinjection quite a large amount of the protein was transported into the nucleus. The second picture reveals that the amount of subcellular translocated nlsEGFP is further increased after 120 minutes. From this point of time further incubation did not enhance the amount of protein that is transported into the nucleus (Figure 5.7, picture C).

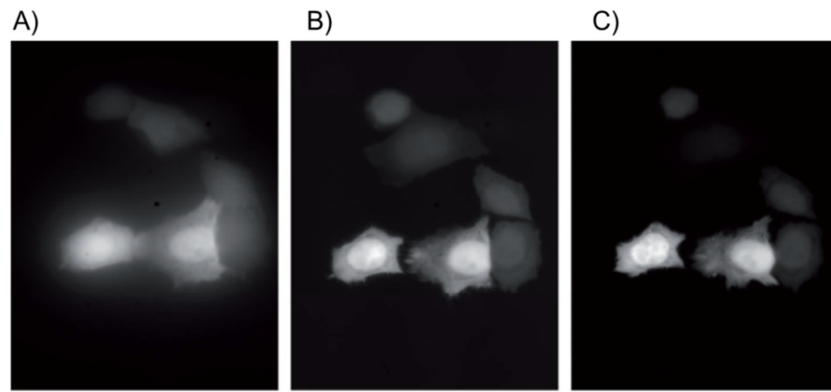


Figure 5.7: Microinjection of SV40nls-EGFP in HELA cells. A) 30 min after microinjection; B) 120 min after injection; C) 180 min after injection.

The nuclear translocation was also investigated for the PTD tagged nlsEGFP. Figure 5.8 exhibits that TAT-nlsEGFP is also transported into the nucleus. The nuclear transport is even faster than the translocation observed for the counterpart without the CPP. Already 15 minutes after injection almost all injected TAT-nlsEGFP is found in the nucleus. Beside faster transport into the nucleus also the percentage of cellular protein translocated into the nucleus is higher. In contrast to nlsEGFP without fused CPP the protein is not distributed homogenously in the nucleus, but rather concentrates in the nucleoli. This finding is consistent with literature that describes the same finding for other HIV-TAT tagged proteins (153, 154).

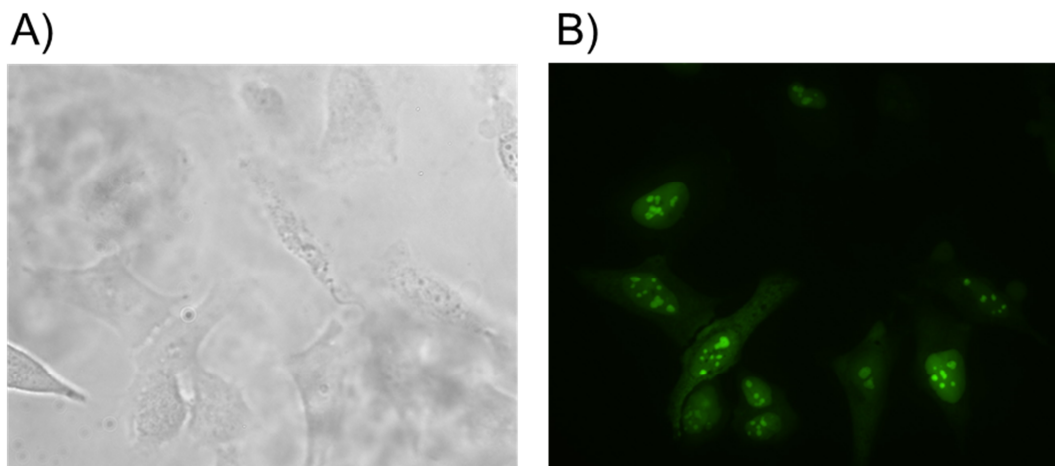


Figure 5.8: Microinjection of TAT-nlsEGFP in HELA cells. A) bright-field picture was taken immediately before microinjection; B) EGFP fluorescence 15 min after injection.

5.2 Protein transduction with TAT-nlsEGFP

The establishing of a standard protein transduction technology with the model protein nlsEGFP was one aim of this thesis. The standard technology should enable the possibility to directly compare the efficiency of new developed protein transduction techniques. For this reason as already mentioned an nlsEGFP protein that is carrying the HIV-TAT protein transduction domain was created. The HIV-TAT cell penetrating peptide is built up from mostly cationic amino acids that effect first binding of the protein to the negative charged cell surface followed by cellular internalization. As the HIV-TAT peptide is one of the mostly used CPPs for protein delivery it should serve as a “gold standard” when comparing other techniques with this standard method. Figure 5.9 shows pictures taken on a fluorescence microscope of cells transfected with a concentration of 2.5 μM TAT-nlsEGFP. The bright field Image reveals that this treatment is well tolerated by the cells. Strong EGFP fluorescence of the transfected cells is observed using this transduction concentration. Furthermore the fluorescence picture reveals that the protein is not equally distributed inside the cell which is a first hint that quite a great amount of protein is entrapped in endosomes. Another indicator for this hypothesis is the fact that only a small amount of protein is found in the nucleus.

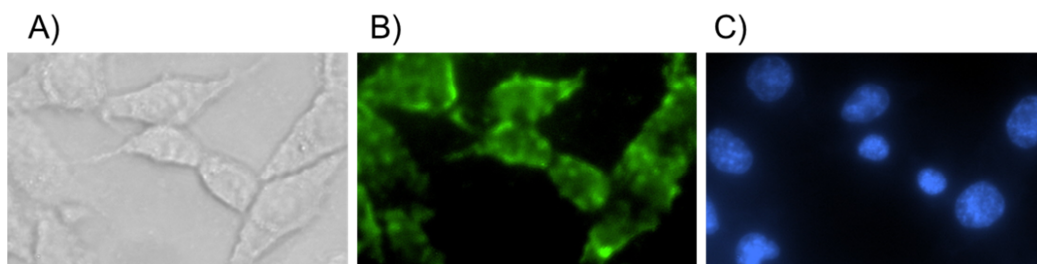


Figure 5.9: Transduction of 3T3 cells. A) Brightfield picture of transduced cells; B) EGFP fluorescence; C) Hoechst 33342 stain of nucleus.

To obtain more quantitative information of the uptake and internalization efficiency FACS measurements of cells transfected with different concentrations of TAT-nlsEGFP were done. The experiment shown in Figure 5.10 displays that cells treated with a transfection concentration of 0.5 μM exhibit stronger fluorescence than untreated cells or cells treated with nlsEGFP without fused TAT protein transduction domain. At a concentration of 1.5 μM nearly 100 percent of the cells are found to be EGFP positive. As expected the fluorescence intensity is increased with raising the

transfection concentration from 0.5 to 1.5 μM . Further increase of the concentration to 5.0 μM does not boost the fluorescence intensity much.

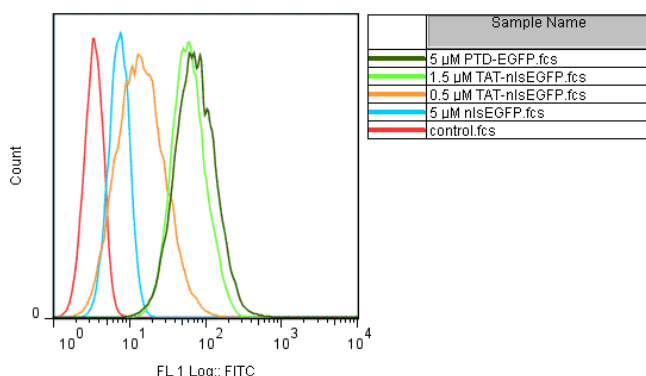


Figure 5.10: Transduction of 3T3 cells with different concentrations of TATnlsEGFP.

Although the brightfield picture in Figure 5.9 which shows nicely shaped cells gave a first hint that TAT-nlsEGFP is well tolerated by the cells, this theory should be confirmed by doing a cell viability assay. The result of such a MTT assay experiment is highlighted in Figure 5.11. Up to a concentration of 1 μM cell viability is not more affected by treatment with TAT-nlsEGFP compared to nlsEGFP. At higher concentrations the toxicity is slightly higher than the one observed for the counterpart without TAT sequence. But even at the highest tested concentration of 5.0 μM around 60 percent of the metabolic activity compared to untreated cells is observed.

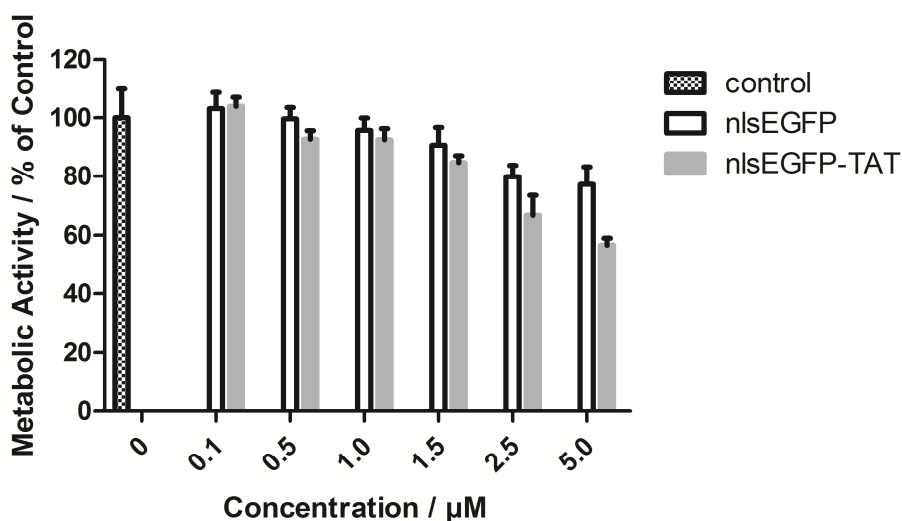


Figure 5.11: Cell viability of 3T3 cells treated with different amounts of nlsEGFP-TAT or nlsEGFP.

5.3 Cationic lipid mediated protein delivery

Most commercial available protein transduction carriers are based on cationic lipids. Also for comparison reasons this technique was tested for its ability to mediate successful transduction of the model protein nlsEGFP. Murine fibroblast cells were transfected with 1 μ M nlsEGFP complexed with the cationic lipid SAINTphd. Under the tested serum containing conditions almost no cellular uptake could be observed (Figure 5.12).

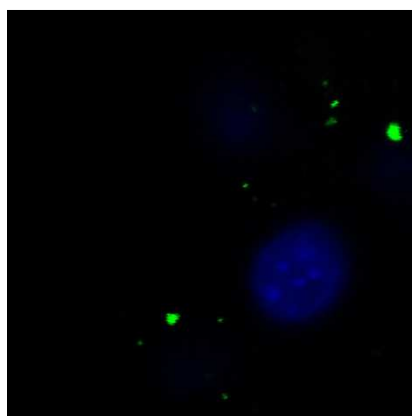


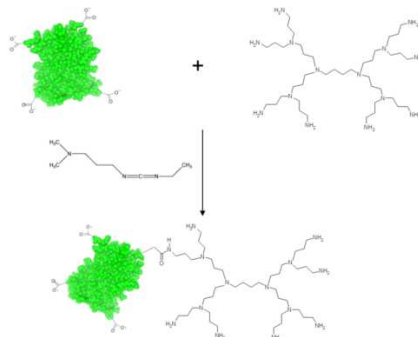
Figure 5.12: 3T3 cells transfected with the cationic lipid SAINTphd. Nucleus was stained with Hoechst 33342 after transduction.

5.4 Dendrimer based protein transduction

5.4.1 Synthesis of G3 PPI-nlsEGFP

Protein delivery mediated by structure defined polycationic carrier molecules was one of the major aims of this thesis. By Russ et al. modified generation 3 polypropylenimine dendrimers were previously used successfully for gene delivery (155). Inspired by these promising results the properties of this carrier molecule for protein transduction should be investigated. For most proteins even those who possess a low isoelectric point the negative charge density in contrast to nucleic acids is not high enough for creating stable complexes mediated just by ionic interactions. Therefore it was decided to covalently couple the dendrimers to the protein surface. For the establishment of the covalent bond the terminal amines of the dendrimer on the one hand and the carboxylic groups of the protein on the other hand were used. As illustrated in Scheme 5.1 the carboxy side chain of aspartate

and glutamate was activated with the zero length crosslinker EDC, resulting in stable amide bonds between the PPI dendrimer and nlsEGFP.



Scheme 5.1: Covalent coupling of G3-PPI dendrimer to nlsEGFP. Because of better clarity only a generation 2 dendrimer is shown.

Successful modification of nlsEGFP with G3 PPI dendrimer was proven by SDS-PAGE. The SDS gel in Figure 5.13 reveals 3 different bands for the reaction product. These bands correspond to nlsEGFP molecules bearing 1 to 3 PPI dendrimers on the surface. Without further purification this mixture of different dendrimer-nlsEGFP conjugates were used for transfection experiments.

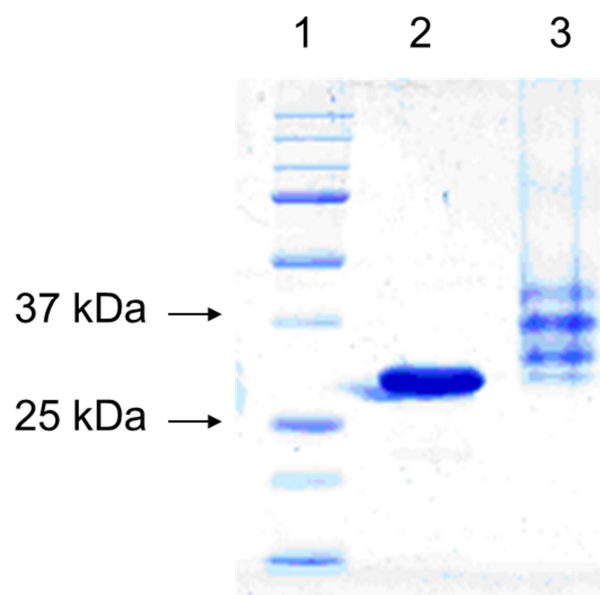


Figure 5.13: Modification of nlsEGFP with G3-PPI dendrimer. Lane 1: protein ladder; Lane 2: unmodified nlsEGFP; Lane 3: G3-PPI modified nlsEGFP.

5.4.2 Protein transduction with G3 PPI-nlsEGFP

Transduction studies with the G3 PPI-nlsEGFP conjugate were done on the murine fibroblast cell line 3T3. FACS experiments (Figure 5.14) reveal that G3 PPI is a highly effective carrier molecule for protein delivery. Already with a transfection concentration of $0.01\mu\text{M}$ nearly 100 percent of 3T3 cells are EGFP positive. To reach the same fluorescence level when doing transfection with PTD bearing nlsEGFP, almost $0.5\mu\text{M}$ protein have to be used. As expected Figure 5.14 shows that higher transfection concentration leads to higher cellular uptake and therefore brighter EGFP fluorescence is observed.

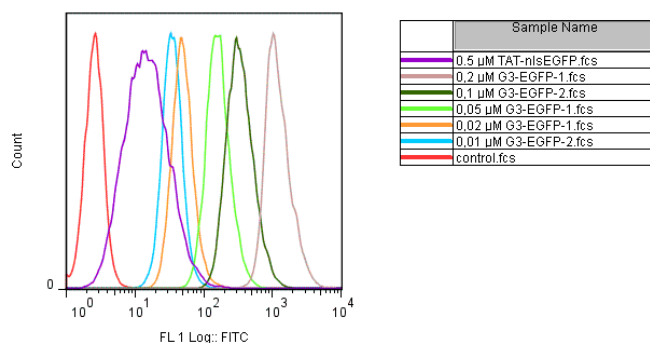


Figure 5.14: Transfection of 3T3 cells with G3 PPI-nlsEGFP. Average cellular EGFP fluorescence intensity of 3T3 murine fibroblasts after transduction with different concentrations of G3 PPI-nlsEGFP.

Aside the necessary transfection concentration, it was evaluated if transfection time has got an influence on cellular internalization. The examination of FACS data shown in Figure 5.15 reveals a quite linear dependency of cellular fluorescence and transfection time for up to three hours when a concentration of $0.1\mu\text{M}$ G3 PPI-nlsEGFP is used. This observation is a hint for endocytosis as uptake mechanism.

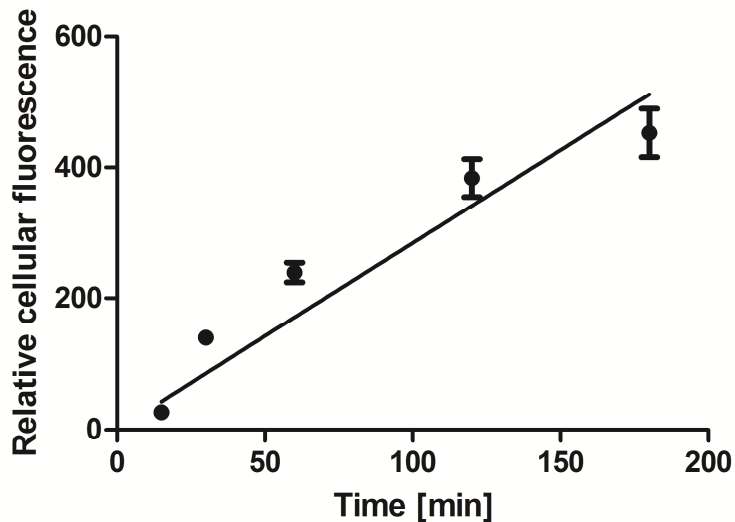


Figure 5.15: Transfection of 3T3 cells with G3 PPI-nlsEGFP. Average cellular EGFP fluorescence intensity of 3T3 murine fibroblasts after different transfection times. Transfection was done with 0.1 μM G3 PPI-nlsEGFP.

To get more information about internalization and especially about endosomal escape, transfected cells were watched on a confocal fluorescence microscope. Figure 5.16 illustrates bright fluorescence of 3T3 cells transfected with 0.5 μg per ml G3 PPI-nlsEGFP in the cell medium. The protein seems to be quite equally distributed in the cytoplasm which is a first hint for successful endosomal escape. Although due to the nuclear localization signal of nlsEGFP, free cytosolic protein should be subcellularly translocated into the nucleus, only small amounts of protein are found in the nucleus. The nlsEGFP protein seems to stick to negative charged cell components like the nuclear membrane and the endoplasmatic reticulum.

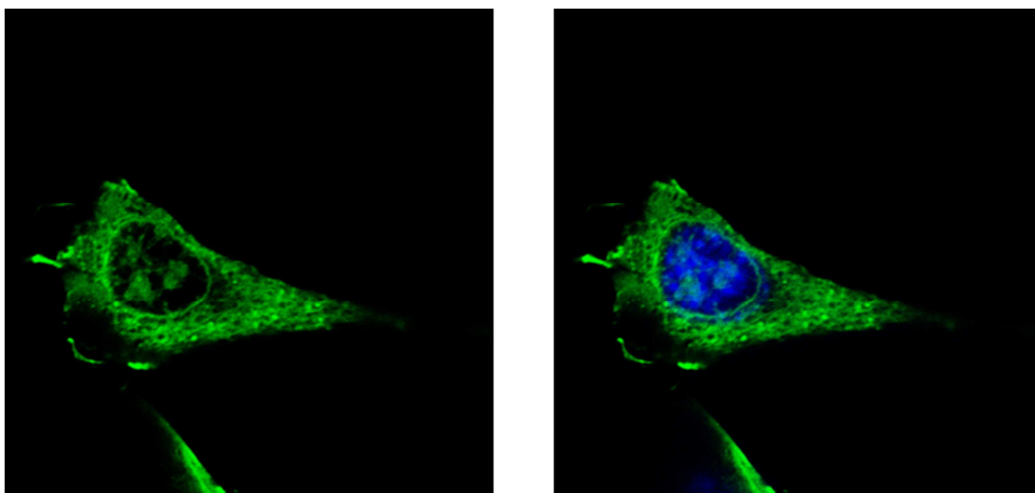


Figure 5.16: Transfection of 3T3 murine fibroblasts with G3PPI-nlsEGFP.

In addition to high transfection efficacy, an appropriate transduction shuttle system should be well tolerated by the cells. To investigate G3 PPI-nlsEGFP under this aspect a cell viability assay, whose examination is displayed in Figure 5.17 was done. The figure approved the apprehension that emerged during FACS measurements and observation of the cells under the microscope. G3 PPI-nlsEGFP is very toxic for cells already in low concentrations. Toxicity occurs already when cells are treated with only 0.05 μM G3 PPI-nlsEGFP. With a transfection concentration of 0.5 μM cells exhibit only 50 percent of the metabolic activity compared to untreated control cells.

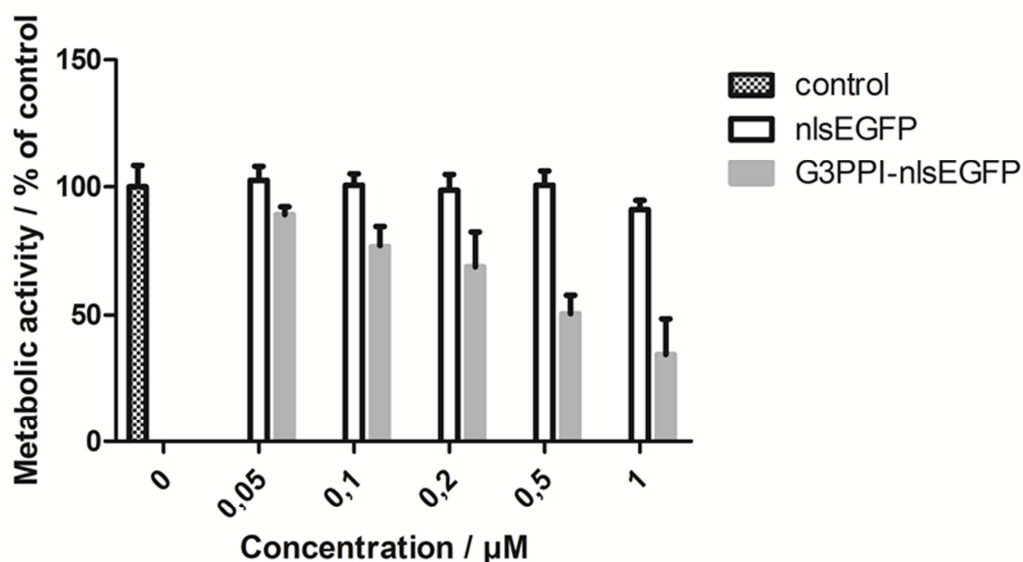


Figure 5.17: Cell viability of 3T3 cells treated with different amounts of nlsEGFP or G3PPI-nlsEGFP.

5.4.3 Microinjection of G3 PPI-nlsEGFP

Although the high cellular toxicity, which aggravates the application of covalently coupled G3 PPI as a protein transduction system, the second diagnosed drawback of this technology, the bad subcellular translocation into the nucleus should be investigated further. Figure 5.7 shows that unmodified nlsEGFP is translocated very fast into the nucleus after microinjection. In contrast only small amounts of G3 PPI-nlsEGFP are found in the nucleus of microinjected HeLa cells after 15 minutes

(Figure 5.18). 90 minutes after injection the situation is almost the same. The nuclear membrane shows bright EGFP fluorescence. The small amount of protein that was transported into the nucleus is concentrated in the nucleoli. This observation is a well-known phenomenon for highly positive charged proteins. Microinjection reinforces the hypothesis that G3 PPI-nlsEGFP is sticking due to its high positive surface charge to negative charged cellular components like the nuclear membrane and therefore nuclear transport is hampered.

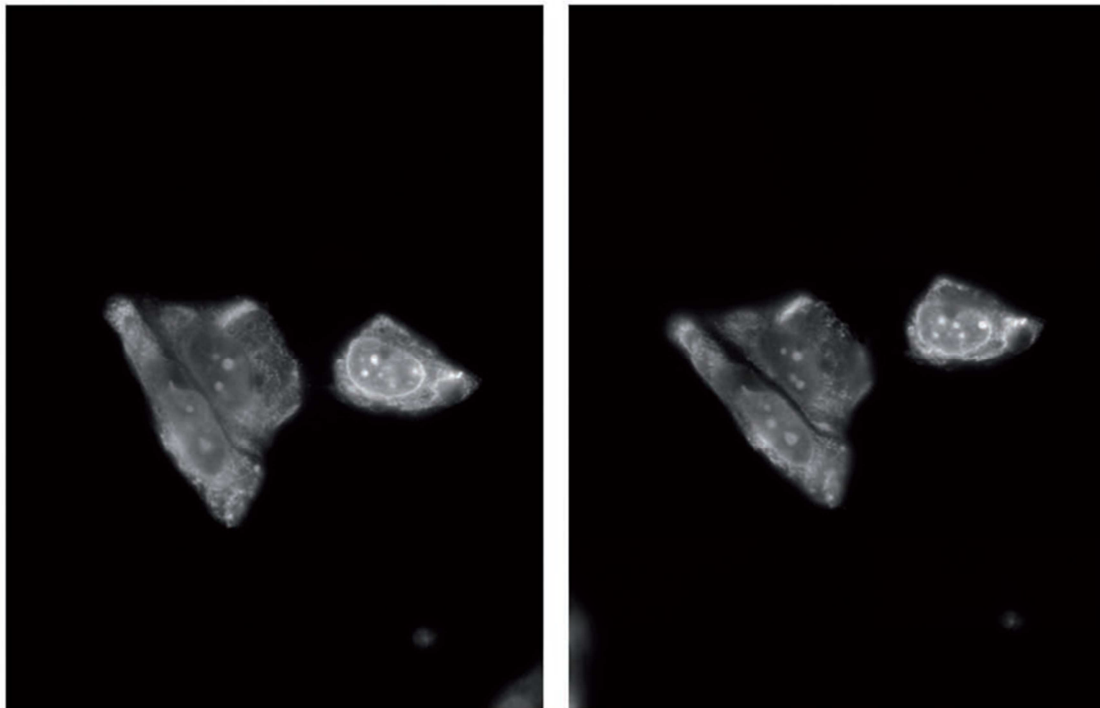


Figure 5.18: Microinjection of G3PPI-nlsEGFP. A) Picture was taken 15 minutes after injection. B) Picture was taken 90 minutes after injection.

5.5 Protein transduction with G3PPI coupled to nlsEGFP over a bioreversible bond

5.5.1 Synthesis of G3PPI-SS-nlsEGFP

To overcome the problem of the unnatural subcellular behavior of G3 PPI-nlsEGFP in comparison to unmodified nlsEGFP, the dendrimer should be coupled reversible to the protein. The bond between carrier and protein should be cleaved after cellular uptake resulting in cytosolic nlsEGFP without dendrimer modification. For introducing such a cleavable bond the protein as well as the dendrimer was modified with the

crosslinker SPDP. The G3PPI was reduced with DTT resulting in a thiol bearing dendrimer. This dendrimer could be simply reacted with SPDP modified nlsEGFP.

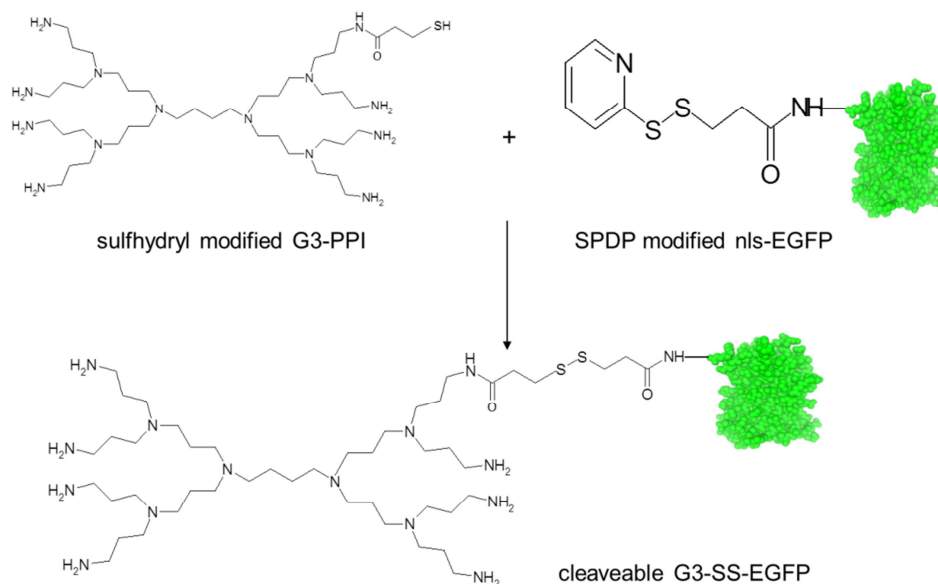


Figure 5.19: Synthesis of biological reversible G3PPI-SS-nlsEGFP. G3-PPI was modified with SPDP and subsequently reduced. nlsEGFP was modified with SPDP crosslinker.

Figure 5.20 shows the successful modification of the protein with the dendrimer. Furthermore it reveals that the binding between carrier and protein is cleaved in presence of reducing agents resulting in nlsEGFP without covalent dendrimer modification.

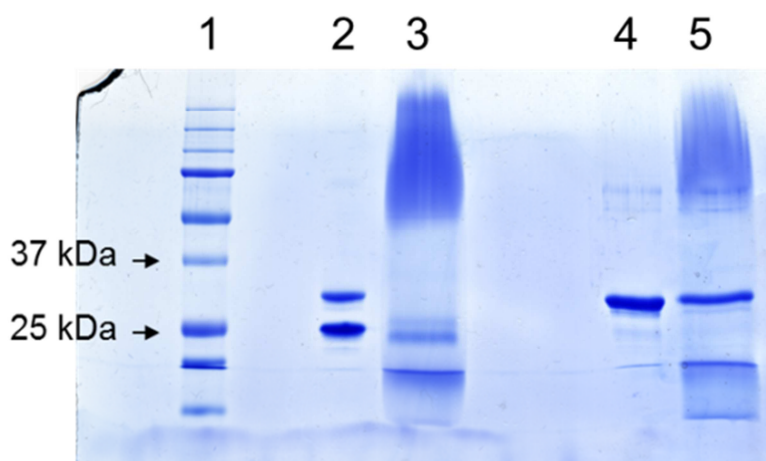


Figure 5.20: SDS-PAGE showing successful modification of nlsEGFP with G3PPI over reducible disulfide bond. Lane1: protein ladder; Lane2: native nlsEGFP; Lane 3: G3PPI-SS-nlsEGFP; Lane 4: reduced nlsEGFP; Lane 5: reduced G3PPI-SS-nlsEGFP

5.5.2 Protein transduction using G3PPI-SS-nlsEGFP

Again as with the noncleavable counterpart transfection studies were done on 3T3 murine fibroblasts. The fluorescent pictures in Figure 5.21 show that nuclear import of nlsEGFP after internalization is improved by introducing a biological cleaveable bond between the carrier and the protein. The brightfield pictures of cells transfected with G3 PPI-SS-nlsEGFP (data not shown) are indicating that toxicity is not significant reduced in comparison to the stable construct.

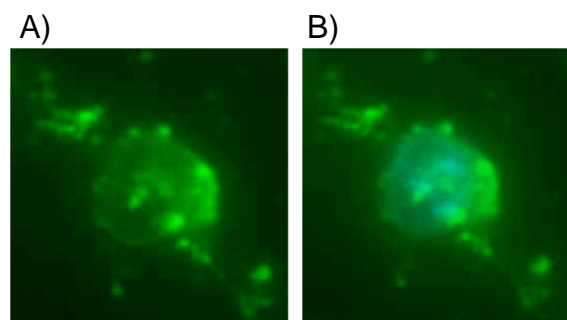


Figure 5.21: Transfection of 3T3 murine fibroblasts with G3PPI-nlsEGFP. A) EGFP fluorescence; B) Merged LM-micrograph: EGFP fluorescence and Hoechst fluorescence of the nucleus.

FACS experiments of cells transfected with G3 PPI-SS-nlsEGFP reveal that transfection efficiency is not decreased by the implementation of a reducible bond between the dendrimer and the nlsEGFP protein. Already a concentration of 0.01 μM of G3 PPI-SS-nlsEGFP leads to detectable EGFP fluorescence of the cells (Figure 5.22). The cellular fluorescence observed for 0.05 and 0.2 μM is also comparable to the fluorescence intensity of cells transfected with the same concentration of the non-cleavable construct (Figure 5.14).

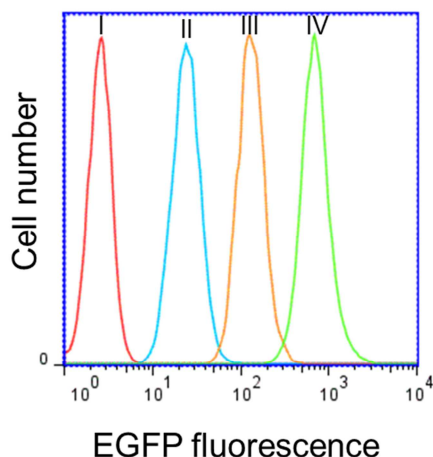


Figure 5.22: Fluorescence assisted cell sorting of 3T3 murine fibroblasts after transduction with varying concentrations of G3PPI-SS-nlsEGFP. I) Untreated cells; II) Transduction with 0.01 μM G3PPI-SS-nlsEGFP; III) Transduction with 0.05 μM G3PPI-SS-nlsEGFP; IV) Transduction with 0.2 μM G3PPI-SS-nlsEGFP.

Cell viability assays confirm the assumption that toxicity could not be reduced by the insertion of a cleavable bond between carrier and cargo. Figure 5.23 is showing rather even higher cellular toxicity compared to the corresponding values obtained for the non-cleavable construct (Figure 5.17). Already a treatment of cells with 0.1 μM reduces the metabolic activity by a third in comparison to untreated control cells.

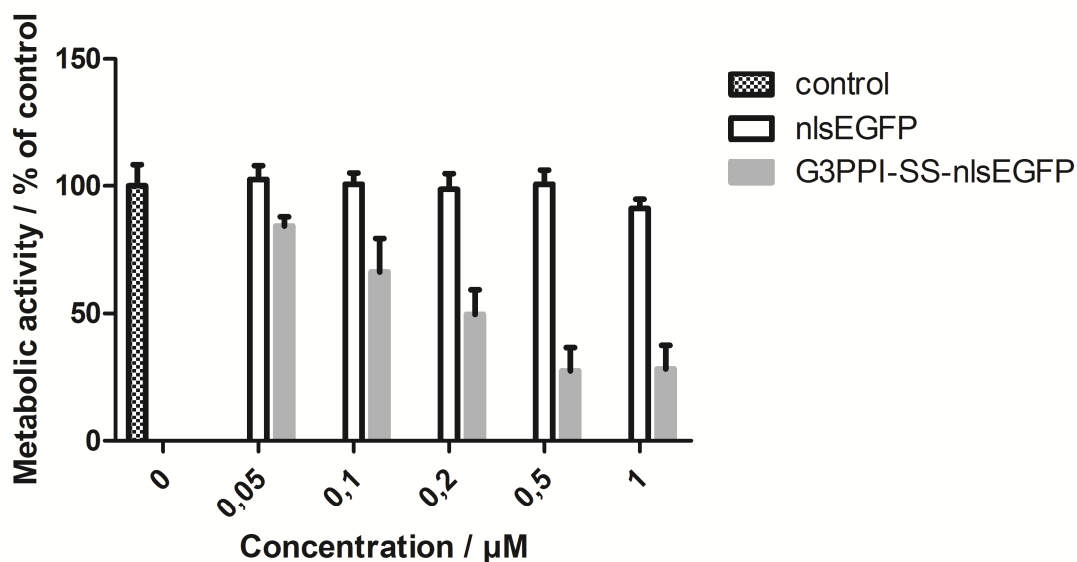
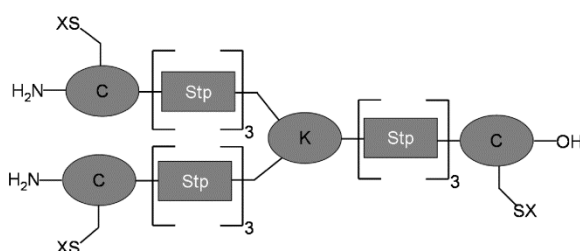


Figure 5.23: Cell viability of 3T3 cells treated with different amounts of nlsEGFP or G3 PPI-SS-nlsEGFP.

5.6 Protein transduction using the structure defined oligomer **386**

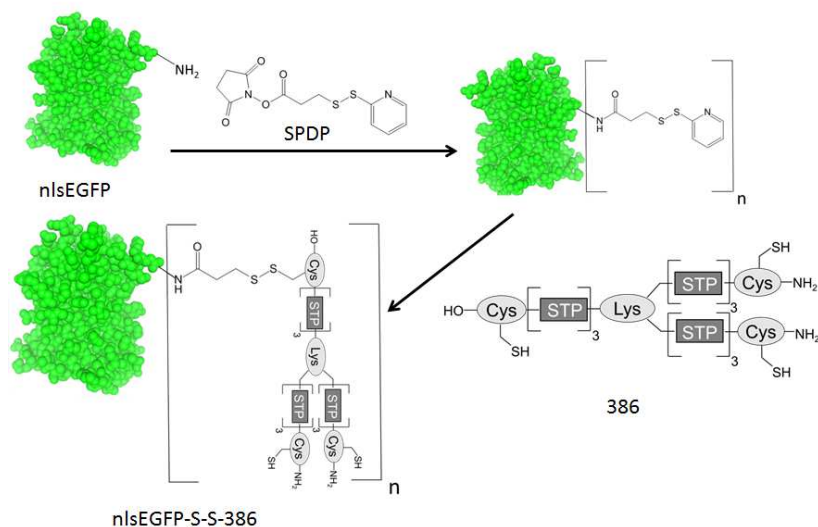
Above results show that the G3 PPI dendrimer is an effective carrier for protein delivery but its inherent cellular toxicity limits its application. For this reason another structure defined carrier with high efficiency and low cytotoxicity should be found. The 3 arm structure **386** was previously developed as a carrier for the delivery of DNA and siRNA. In case of nucleic acid delivery it combines high efficiency with low cytotoxicity (59, 156). The transduction oligomer **386** is a structure defined cationic oligomer which is built up from natural and artificial amino acids. The main components are succinoyl tetraethylene pentamine units which are supposed to be important for endosomolytic activity and three cysteine residues on the end of each arm. These cysteine residues should enable coupling to cargo molecules as well as lateral stabilization through the formation of disulfide bonds.



Scheme 5.2: Structure of 386. x=H; Stp, succinoyl tetraethylene pentamine; C, cysteine; K, α,ϵ -modified branching lysine.

5.6.1 Synthesis of reducible 386 modified nlsEGFP

The three cysteine residues on the terminus of the oligomer arms should be used for reversible covalent coupling to the nlsEGFP protein. The coupling strategy is illustrated in Scheme 5.3.



Scheme 5.3: Synthesis of 386-SS-nlsEGFP. Step 1: modification of nlsEGFP with SPDP. Step 2: coupling of **386** to SPDP-nlsEGFP.

To enable an effective coupling of the carrier nlsEGFP was modified with the commercial available heterobifunctional crosslinker SPDP. After modification with the linker under the used conditions (4.4.1.1), nlsEGFP is exposing around five activated thiol groups on the surface that enable fast formation of covalent disulfide bonds with the transduction oligomer **386**. Successful modification of nlsEGFP with the transduction oligomer **386** as well as reversibility of the binding in presence of reducing agents is evidenced in Figure 5.24. Dynamic light scattering reveals particle sizes of 26.8 +/- 3.6 nm and a zeta potential of 12.4 +/- 0.6 mV.

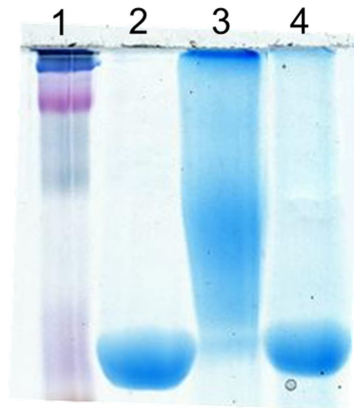


Figure 5.24: SDS PAGE documenting successful modification of nlsEGFP with transduction oligomer 386 and reversibility of the bond. Lane 1: Protein ladder; Lane 2: Unmodified nlsEGFP; Lane 3: **386-SS-nlsEGFP**; Lane4: reduced **386-nlsEGFP**.

5.6.2 Protein transduction with 386-SS-nlsEGFP

Protein transduction ability of the **386** oligomer was evaluated on two different cell lines. In a first experiment for direct comparison to G3 PPI dendrimer and PTD-nlsEGFP 3T3 murine fibroblast cells were transfected and efficiency was evaluated by FACS studies. Although the transfection efficiency is lower than the one of covalently coupled G3 PPI it is far higher in comparison to TAT-nlsEGFP (Figure 5.25).

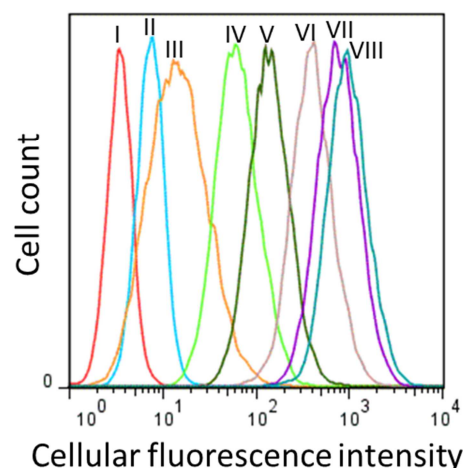


Figure 5.25: Fluorescence assisted cell sorting of 3T3 murine fibroblasts after transduction with varying concentrations of 386-SS-nlsEGFP. I) Untreated cells; II) Transduction with unmodified nlsEGFP 5 μ M; III) Transduction with 0.5 μ M TAT-nlsEGFP; IV) Transduction with 1.5 μ M TAT-nlsEGFP; V) Transduction with 0.25 μ M 386-SS-nlsEGFP; VI) Transduction with 0.5 μ M 386-SS-nlsEGFP; VII) Transduction with 0.75 μ M.; VIII) Transduction with 1.0 μ M.

The mean cellular fluorescence intensity of **386**-SS-nlsEGFP treated cells is about twenty times higher than the mean fluorescence of TAT-nlsEGFP treated ones. Controls which were treated with a high concentration (5 μ M) of unmodified nlsEGFP showed only negligible raise in fluorescence. The same experiment was done with Neuro2A cells. Transfection efficiency on Neuro2A cells was slightly lower, compared to 3T3 cells transfected with the same amount of modified Protein. Fluorescent intensity of Neuro2A cells compared to 3T3 cells was around 55 % lower for cells transfected with 0.25 μ M, at higher concentrations the mean fluorescence intensity was around 20 percent lower (Figure 5.26). We had expected that uptake efficiency is concentration dependent, this was already reported for CPP assisted transfection studies (102). Nevertheless the nearly perfect linear relationship between transfection concentration and fluorescence intensity, for both cell types, in the tested concentration area was a little bit surprising. Linear dependency of concentration and uptake was already reported for internalization mediated by the protein transduction domain Antp (Antennapedia-homeodomain) (100).

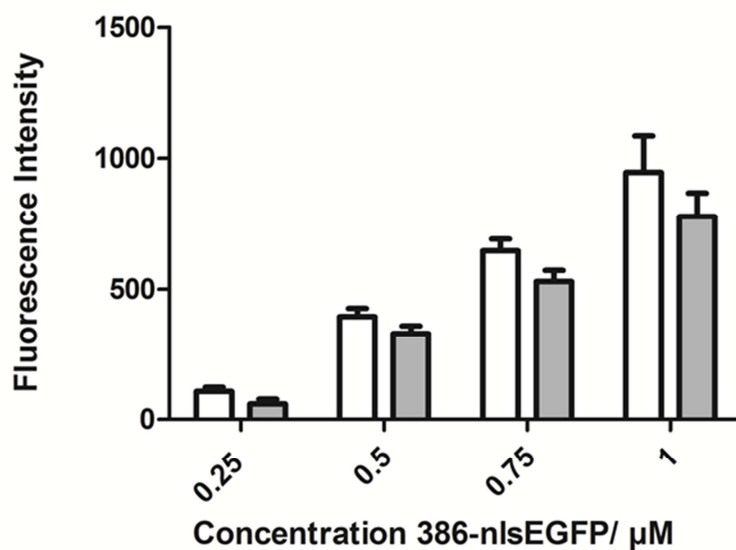


Figure 5.26: Concentration dependent cellular uptake of 386-SS-nlsEGFP. Cells were transfected with different amounts of 386-SS-nlsEGFP. White bars: 3T3 cells. Grey bars: Neuro2A cells.

In a following experiment we found that uptake of **386**-SS-nlsEGFP and therefore observed fluorescence intensity is increasing with incubation time (Figure 5.27). After an incubation time of 15 min around 45 percent and after 30 min incubation already over 90 percent of the cells were EGFP positive, when transfection was done with 0.5 μ M **386**-SS-nlsEGFP. Again, like in the concentration dependent uptake experiment

we could find approximately a linear relationship between fluorescence intensity and time. Such a continuous uptake is supposed to be a strong hint for endocytosis mediated uptake (100).

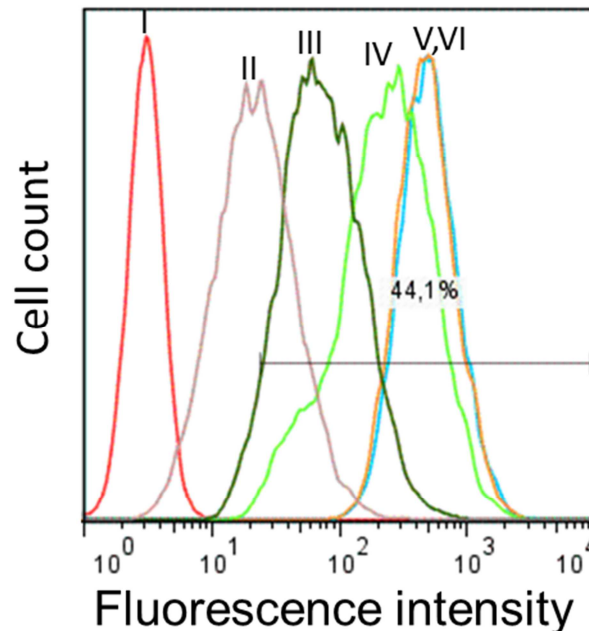


Figure 5.27: Time dependency of protein transduction with 0.5 μM 386-SS-nlsEGFP on 3T3 cells. I) Untreated cells; II) Cells transfected with 386-SS-nlsEGFP for 15 minutes. III) 30 min incubation; IV) 60 min incubation; V) 120 min incubation VI) 180 min incubation.

To investigate the ability of these transduction shuttles to penetrate cells, promote endosomal release and following subcellular transport. Uptake and subcellular distribution were also pursued on a fluorescence microscope. Figure 5.28 is demonstrating nicely that all cells were transfected successfully after an incubation time of two hours, using a 0.5 μM concentration of **386-SS-nlsEGFP**. The cells show homogenous cytoplasmic fluorescence. This suggests endosomal escape of the **386-SS-nlsEGFP**. Moreover, the protein is concentrated in the nucleus of the cells, which gives again a strong hint for successful escape of the transduction shuttles out of the endosomes. Cells treated with unmodified nlsEGFP, as a control, do not show any fluorescence.

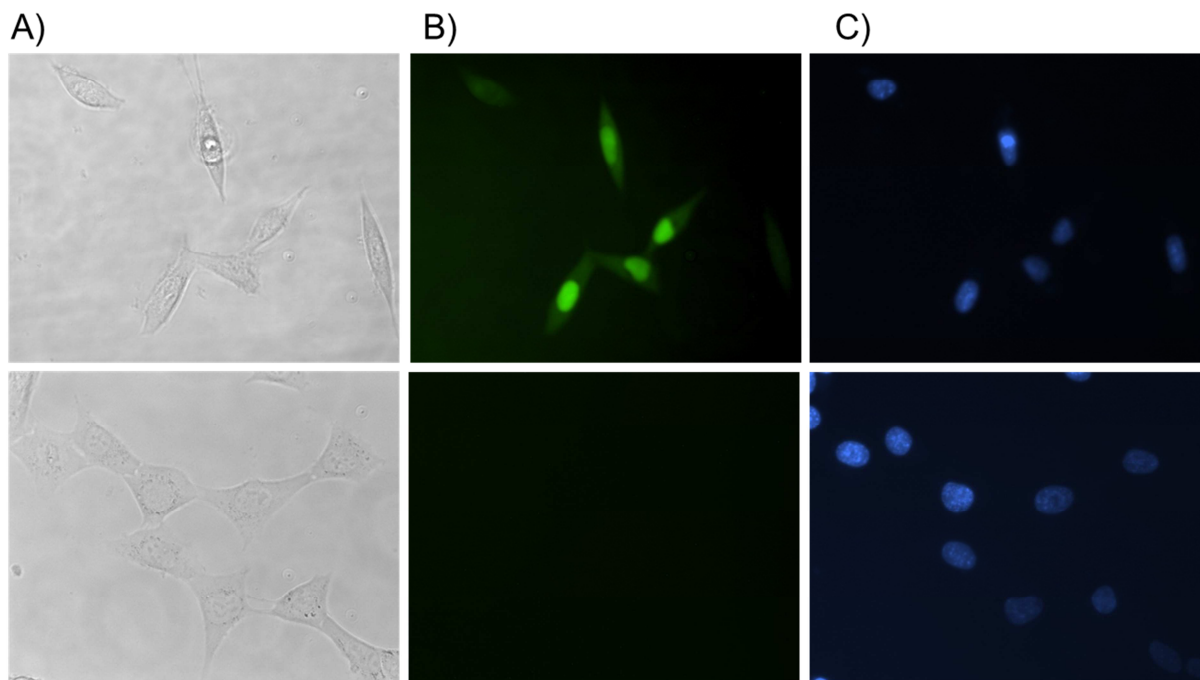


Figure 5.28: . Transduction of 3T3 cells with **386-SS-nlsEGFP**. TOP: Transduction with **386-SS-nlsEGFP**. Bottom: Transduction with unmodified nlsEGFP. A) bright-field picture of the transfected cells, B) EGFP fluorescence of the transfected cells, C) Hoechst 33342 DNA stain of the cell nucleus.

Transduction oligomer **386** has been shown to exhibit low cytotoxicity when used as a carrier for siRNA or DNA (59, 156). Because of its internal amide bonds it is supposed to be degraded intracellularly by proteases. To verify the nontoxic properties for siRNA delivery also in case of being covalently bound to a protein, a cell viability test was performed that confirmed this assumption. Figure 5.29 shows the low toxicity of the transduction shuttle, even at high transduction concentrations. It exhibited only marginal higher toxicity than the cells treated with unmodified nlsEGFP protein. With the standard concentration used for the transfections above ($0.5 \mu\text{M}$) a decline in metabolic activity of only 10 percent in comparison to untreated cells was observed. Even after transfection with $2.5 \mu\text{M}$ **386-SS-nlsEGFP** cell viability decreased by only 25%.

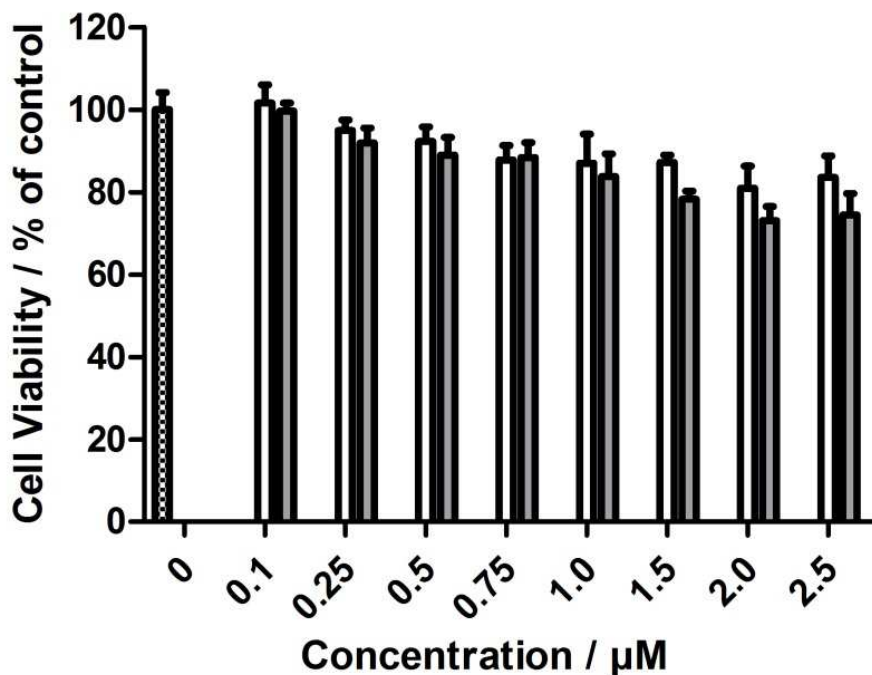


Figure 5.29: Cell viability of 3T3 cells treated with different amounts of nlsEGFP or 386-SS-nlsEGFP. White bars: cells transfected with unmodified nlsEGFP. Grey bars: cells transfected with 386-SS-nlsEGFP

Flow cytometry experiments using 0.5 μM 386-SS-nlsEGFP also demonstrate that internalized nlsEGFP is disappearing after a few days (Figure 5.30). This finding was expected, as due to cell proliferation the intracellular nlsEGFP concentration is dying out and of course the principal reason is proteosomal degradation. 24 hours after transfection cells lost approximately one third of their original mean fluorescence. Within 48 hours after transfection the fluorescence decreased to a fourth and after 72 hours to below 10 percent of the primordial value.

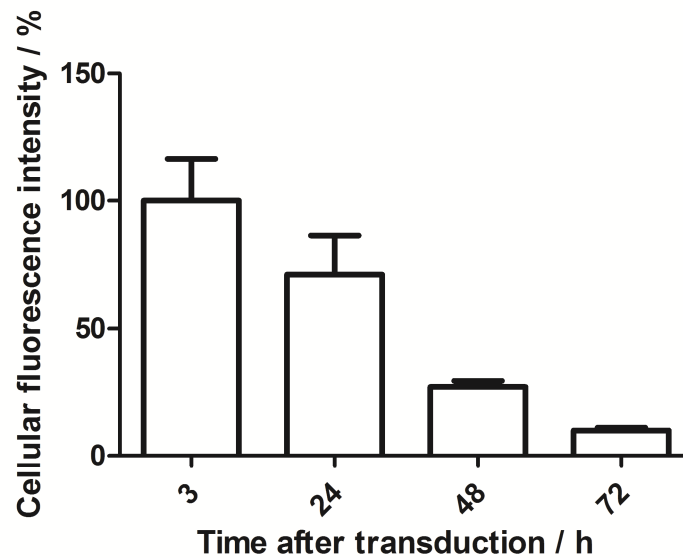


Figure 5.30: Cellular fluorescence intensity of cells after treatment with 386-SS-nlsEGFP at different times.

As already mentioned in the section above the linear relationship of transfection time and uptake efficiency gave a first hint for an endocytotic uptake mechanism. To confirm this hypothesis, further experiments were done. Transfection at 4°C lowers internalization of the modified protein (Figure 5.31) in 3T3 cells dramatically. Cells transfected at 4°C exhibited only 25 percent of the fluorescence compared to control cells transfected at 37°C. This observation is indicating that internalization of **386** modified nlsEGFP is an energy dependent process and is consistent with most CPPs (102, 148, 157). To further analyze the endocytotic pathway in 3T3 cells, transfection experiments in presence of chlorpromazine (inhibits clathrin mediated endocytosis), amiloride (inhibits macropinocytosis) and β -cyclodextrin (inhibits caveolae mediated endocytosis) were done. All this endocytosis inhibitors reduce transduction efficiency at least a little bit, suggesting that all three endocytosis pathways participate in internalization. Clathrin mediated endocytosis is the predominantly internalization route, as chlorpromazine reduces cellular fluorescence to 55 percent compared to control cells, transfected under standard conditions. Caveolae mediated endocytosis and macropinocytosis seem to contribute respectively to around 15-20 percent of the uptake. The finding that clathrin mediated endocytosis may be the major internalization route is in accordance with the measured particle size, as particles smaller than 200 nm are supposed to be taken up mainly through this pathway (158). Aoyama and coworkers found that receptor-mediated endocytosis is strongly size-

dependent with an optimum of around 25 nm (159-161). That correlates exactly with the measured size of the transduction shuttles and the observed uptake pathway.

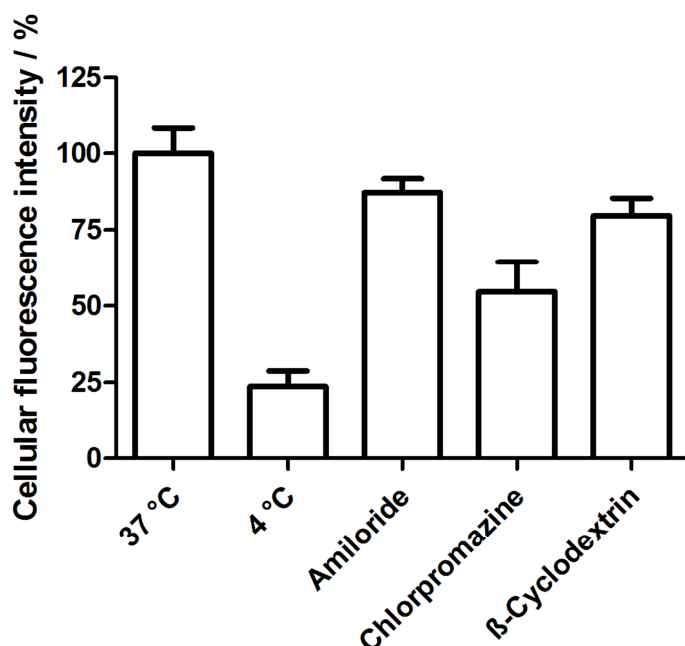


Figure 5.31: Average cellular fluorescence intensity of 3T3 cells after transduction with 386-nlsEGFP at 4°C and in presence of three different endocytosis inhibitors: Amiloride, chlorpromazine and β-cyclodextrin. Fluorescence intensity is normalized to cells transduced at 37 °C.

5.6.3 Transduction of 386-SS-βgalactosidase

Aside the development of a carrier system for protein delivery, one of the major aims of this thesis is the establishing of a test system for protein delivery. nlsEGFP is a good model to observe uptake and internalization, but a potential therapeutic applicable protein transduction system has to demonstrate that enzyme activity is maintained during the delivery process inside the target cell. For this reasons β-galactosidase from E.coli was modified with the cationic transduction oligomer **386**, to demonstrate on the one hand the ability of the carrier to transduce also big molecules (464-kDa homo-tetramer), but in the first instance this model should show that enzyme activity is maintained inside the target cell.

5.6.3.1 Synthesis of 386-SS- β galactosidase

Coupling was done again over the SPDP linker (as described under the material and methods part), resulting in a biological reversible bond of the transduction oligomer to β -galactosidase. Each β -gal molecule was modified with an average of 8 linker molecules. Through covalent coupling of the transduction oligomer **386** to linker modified β -galactosidase, particles of 48.3 +/- 2.4 nm with a surface charge of 9.5 +/- 0.2 mV arise.

5.6.3.2 Activity of modified β -galactosidase

To determine the relative activity of modified β -galactosidase, compared to unmodified enzyme, the formation of a fluorescent product (4-methylumbelliferone (4-MU); $\lambda_{\text{excitation}}$ 360 nm, $\lambda_{\text{emission}}$ 440 nm) out from the nonfluorescent 4-methylumbelliferone- β -D-galactopyranoside substrat (MUG) by hydrolysis through β -galactosidase (149) was quantified. Figure 5.32 displays that β -galactosidase is losing nearly 85 percent of its enzyme activity during the modification process.

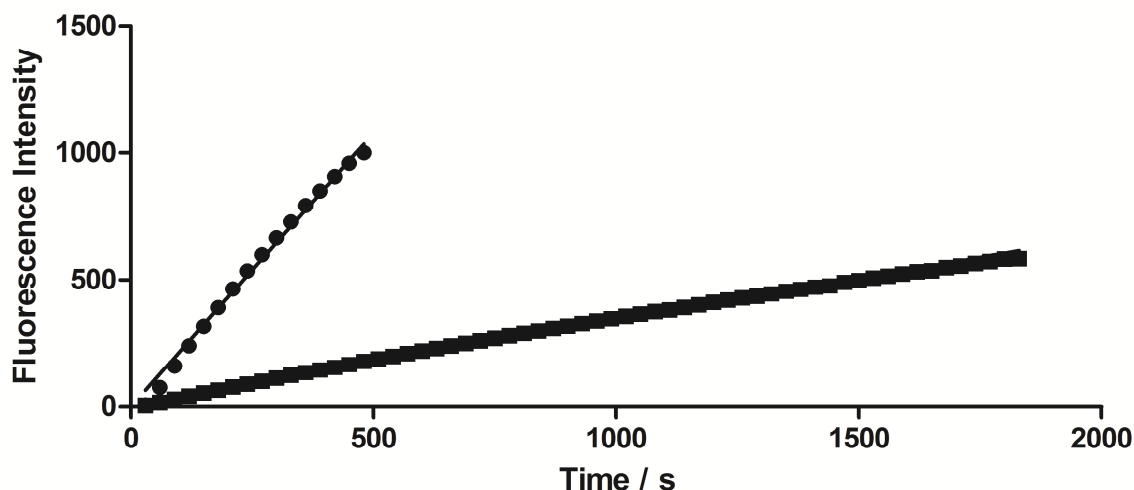


Figure 5.32: Enzyme activity of 386-SS- β Gal in comparison to unmodified β -galactosidase. Dots activity of unmodified β -galactosidase. Squares activity of 386-SS- β galactosidase.

5.6.3.3 Transfection experiments with β -galactosidase

Although enzyme activity is hampered by the modification, transfection experiments with the carrier modified enzyme were done. **386**-SS- β gal was transduced into Neuro2A cells, as described under materials and methods. First a qualitative experiment should show if any enzyme activity at all could be verified, or if activity was lost completely during modification, transfection, internalization or possible intracellular degradation. Transduced β -gal is able to hydrolyse X-Gal (5-bromo-4-chloro-3-indoxyl- β -D-galactopyranosid) substrate into β -galactose and its colored product 5-bromo-4-chloro-3-hydroxyindole (162) (Figure 5.33). Only cells that were transduced with **386**-SS- β gal are blue tinted. Control cells which were treated with unmodified β -gal, before incubation with X-Gal substrate, do not show any staining. Therefore we can conclude that transduction of β -galactosidase was successful and a certain enzyme activity is maintained.

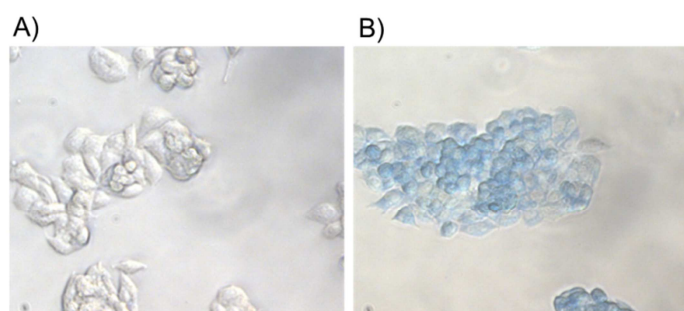


Figure 5.33: Transduction of Neuro2A cell with β -galactosidase. Comparison of Neuro2A cells after treatment with **386**- β -galactosidase (right) washing and following incubation with X-Gal (5-bromo-4-chloro-indolyl- β -D-galactopyranoside) substrate. Left: Transduction with unmodified, natural β -galactosidase.

For a more quantitative analysis we used C12-FDG substrate, which led to FITC fluorescence after cleavage. Fluorescence was quantified by flow cytometry. We observed considerable fluorescence of the **386**-SS- β gal transduced cells but not for cells transduced with unmodified β -gal (Figure 5.34). Therefore we could conclude that transduction oligomer **386** is able to transport remarkable amounts of active β -gal enzyme into cells, even at the low transduction concentration of $1\mu\text{M}$.

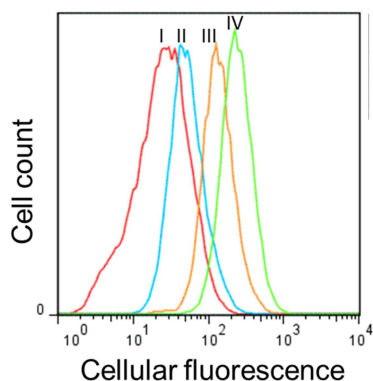


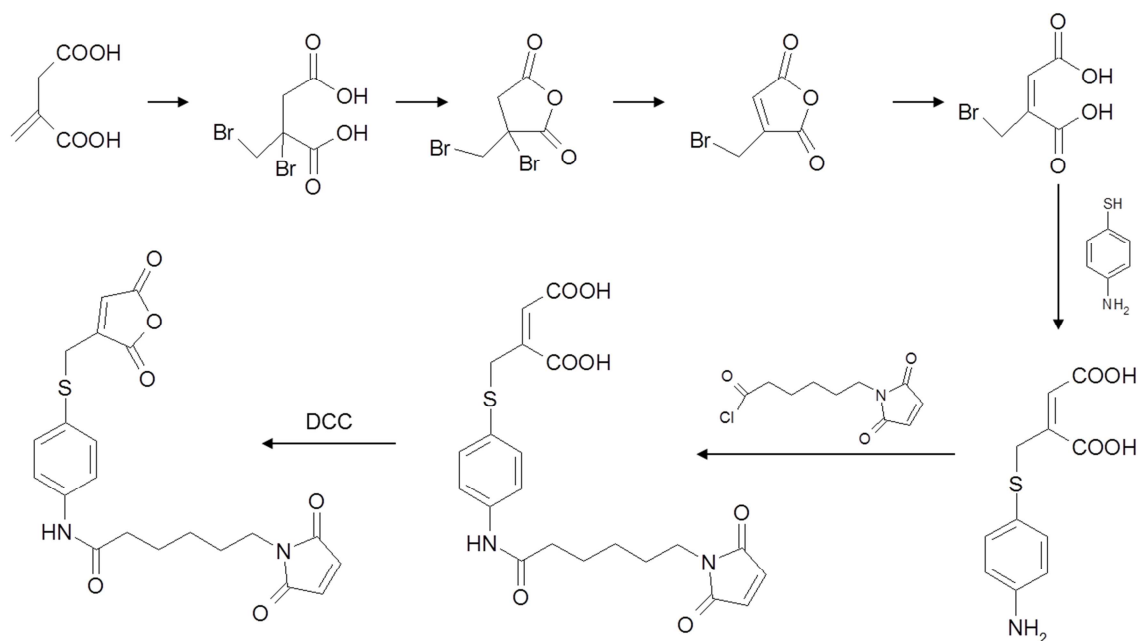
Figure 5.34: Fluorescence assisted cell sorting of Neuro2A cells following transduction with different concentrations of 386-SS- β galactosidase washing and incubation with C12-FDG substrate. I) control, untreated cells; II) Cells transfected with 2.5 μ M unmodified β -galactosidase; III) Cells transfected with 1.0 μ M 386-SS- β galactosidase; IV) Cells treated with 2.5 μ M 386-SS- β galactosidase.

5.7 Development of acid labile, traceless heterobifunctional click linkers for protein delivery

The third main aim of this thesis was the development of a linker for protein delivery. This linker should allow easy and highly effective covalent coupling of the carrier molecule to the cargo protein without many side reactions. It was desired that the whole surface of the protein could be modified and therefore the cargo protein could be completely encaged by the transduction oligomer. Furthermore the linker should enable cleavage between the internalized protein and the transduction carrier under mild biological conditions. The cleavage should be triggered by the tiny chemical changes, occurring during internalization and further intracellular processing. Last but not least it would be in favor, if the linker is cleaved off traceless and therefore releases the cargo in its natural unmodified state.

5.7.1 Synthesis of MAM linker

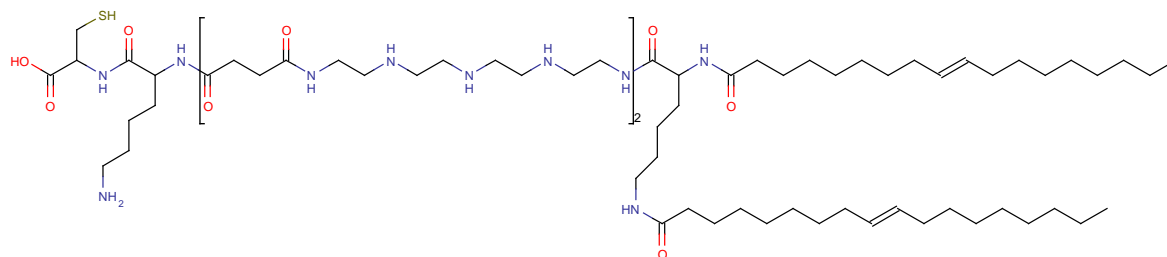
Blättler and Coworkers (134) presented in 1985 a linker based on maleic anhydride. It is the only linker described in literature so far, which may fulfill (except of bioorthogonality) all of the desired requirements. The linker was synthesized as described by Blättler et al. and illustrated in Scheme 5.4 with acceptable yield.



Scheme 5.4: Synthesis of MAM linker.

5.7.2 Acid lability of MAM linker

The MAM linker was evaluated, if it is applicable for protein delivery. Therefore nlsEGFP was modified with the MAM linker and subsequently the transduction oligomer **71** (Scheme 5.5) was covalently coupled. Transduction oligomer **71** was designed and synthesized by Christina Troiber (AK Wagner, LMU) as part of her phd work.



Scheme 5.5: Structure of polymer 71. Drawn by Christina Troiber (AK Wagner, LMU)

Figure 5.35 is showing the result of such a modification procedure. The band in lane 3 reveals that modification was successful. Due to the hydrophobicity of the carrier the modified protein is running deeper into the SDS-PAGE, although it is of higher molecular weight than the unmodified protein (lane 2). Lane 4 and 5 were charged with modified protein after acidic incubation. The modification seems to be partly

reversible but only at very low pH values. Because of the insufficient release and the low required pH for cleavage, the linker is not really useful for protein delivery.

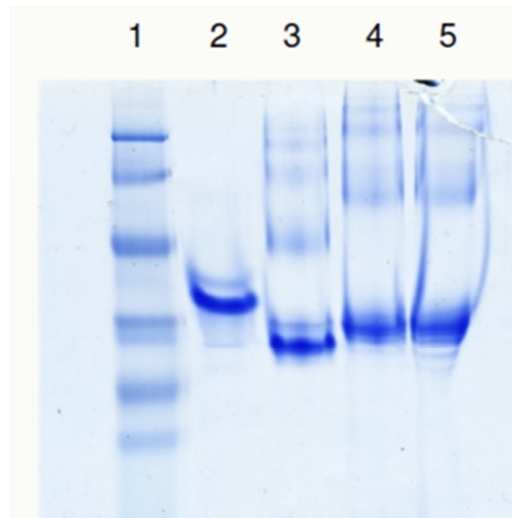


Figure 5.35: Modification of nlsEGFP with MAM linker and transduction oligomer 71. Lane 1: Protein ladder; Lane 2: unmodified nlsEGFP; Lane 3: nlsEGFP-MAM-**71** pH 8.5; Lane 4: nlsEGFP-MAM-**71** after incubation at pH 5.0; Lane 5: nlsEGFP-MAM-**71** after incubation at pH 3;

Although the experiment above showed insufficient release of the carrier from the protein under biological relevant conditions, transduction experiments with polymer **71** coupled via the MAM linker to nlsEGFP were done.

The pictures taken on the fluorescent microscope and shown in Figure 5.36 reveal that polymer **71** is able to deliver covalently bound nlsEGFP into 3T3 cells. But the pictures also indicate that quite a great amount of the protein seems to be encapsulated in endosomes and therefore only small amounts of nlsEGFP are translocated into the nucleus of the cells.

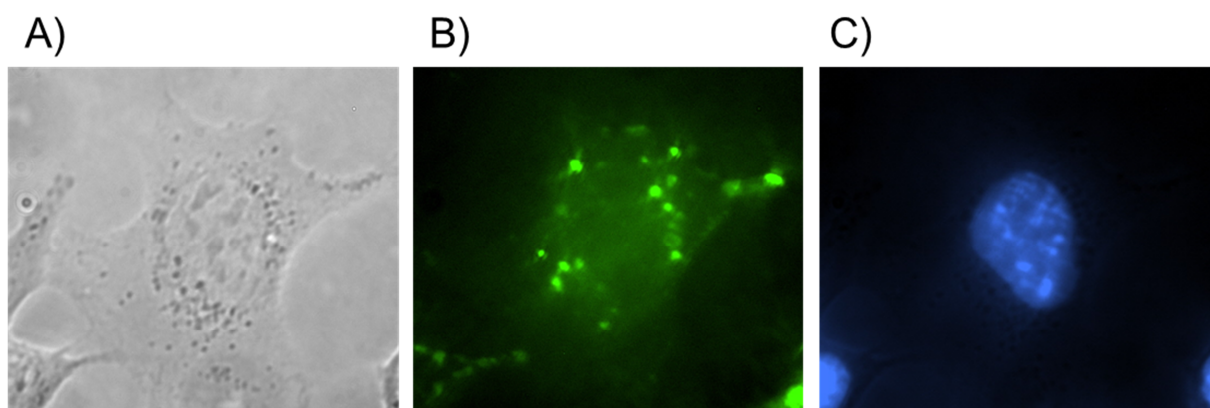
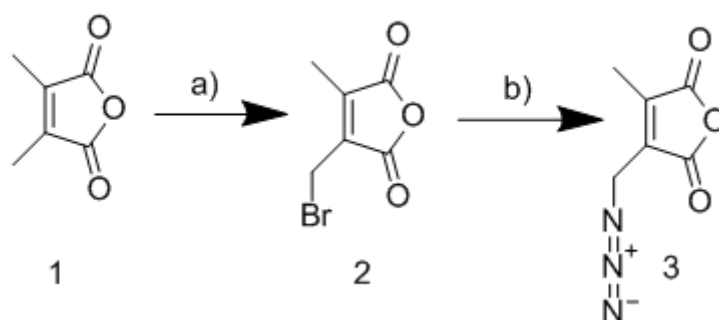


Figure 5.36: Transduction of 3T3 cells with 71-MAM-nlsEGFP. A) bright-field picture of the transfected cells, B) EGFP fluorescence of the transfected cells, C) Hoechst 33342 DNA stain of the cell nucleus.

5.7.3 Synthesis of AzMMMan linker

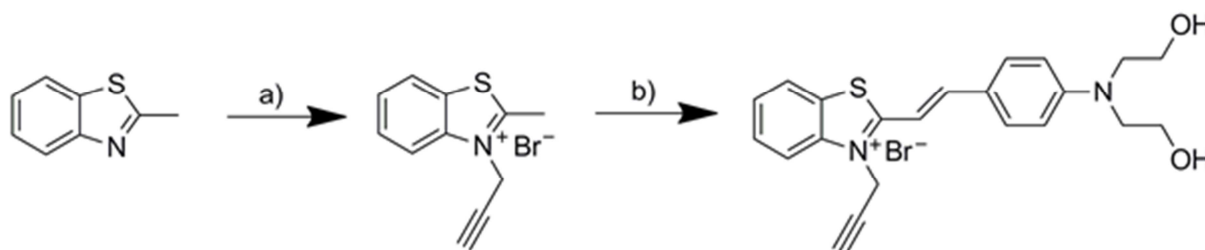
As already mentioned so far no linker, which fulfills all requirements for protein delivery was described in literature so far. In recent years click chemistry reactions, especially the copper catalyzed 1,3-dipolar cycloaddition (CuAAC) and the Staudinger ligation, became useful tools for conjugating biomolecules (49, 135-137). Both reactions have great advantages compared to other linking strategies, like high efficiency and bioorthogonality. Nevertheless, as already mentioned above, for the application in protein delivery, a completely bioreversible bond would be favorable. Dimethylmaleic anhydride is known to form amide bonds with amines that are cleaved under very mild acidic conditions (62, 125, 163-166). The new linker based on substituted dimethylmaleic anhydride should combine the advantages of click chemistry with the implementation of a pH sensitive bond between conjugated biomolecules. This linker should be labile under mild acidic conditions, which are typical for early endosomes (133). Moreover this linker should be cleaved off traceless, resulting in an unmodified molecule of interest. Scheme 5.6 is showing the structure and the synthesis strategy for the new AzMMMan linker. The azidomethyl-methylmaleic anhydride linker (compound 3, Scheme 5.6) (AzMMMan) was synthesized from dimethylmaleic anhydride by two simple reaction steps (radical substitution with N-bromosuccinimide resulting in bromomethyl methylmaleic anhydride (compound 2, Scheme 5.6), followed by a type of Finkelstein reaction with sodium azide). The overall synthesis yield is 49 percent.



Scheme 5.6: Synthesis of AzMMMan linker. a) N-bromosuccinimide, benzoyl peroxide, 56% b) sodium azide, 88%.

5.7.4 Synthesis of water soluble alkyne hemicyanine dye

The water soluble alkyne dye was used on the one hand to determine the degree of protein modification with the new linker and on the other hand to investigate cleavage kinetics under acidic conditions. Scheme 5.7 is illustrating the synthesis strategy for the new alkyne dye. In the first step methylbenzothiazole was reacted with propargylbromide. The reaction yield is 21 percent of the theoretical value. In the following condensation reaction the reaction product was transformed with 4-N,N-bishydroxyethyl aminobenzaldehyde (78 % yield).



Scheme 5.7: Synthesis of hemicyanine dye. a) propargyl bromide, acetonitrile, 21%; b) 4-N,N-bishydroxyethyl aminobenzaldehyde, ethanol, 78%.

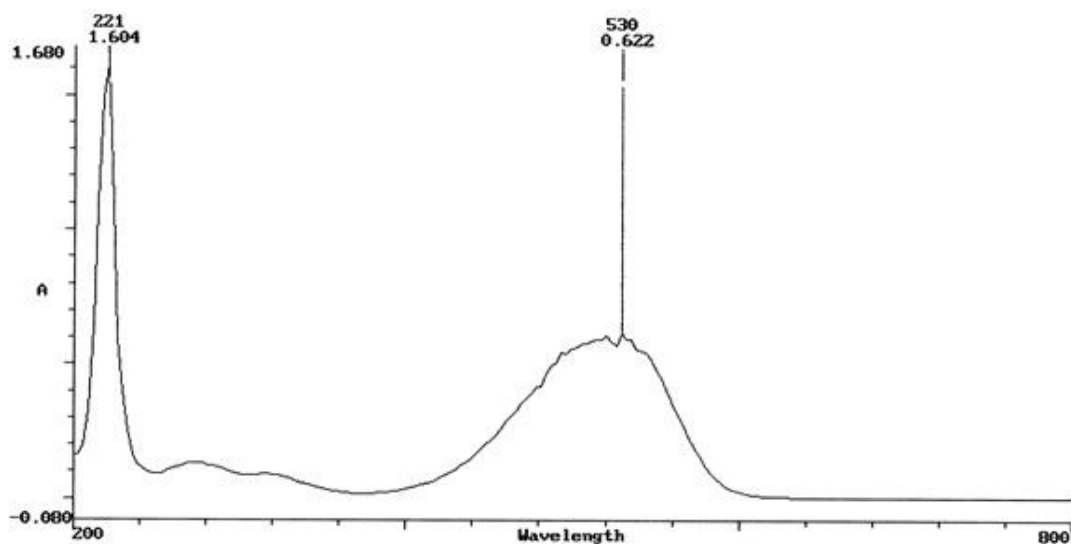


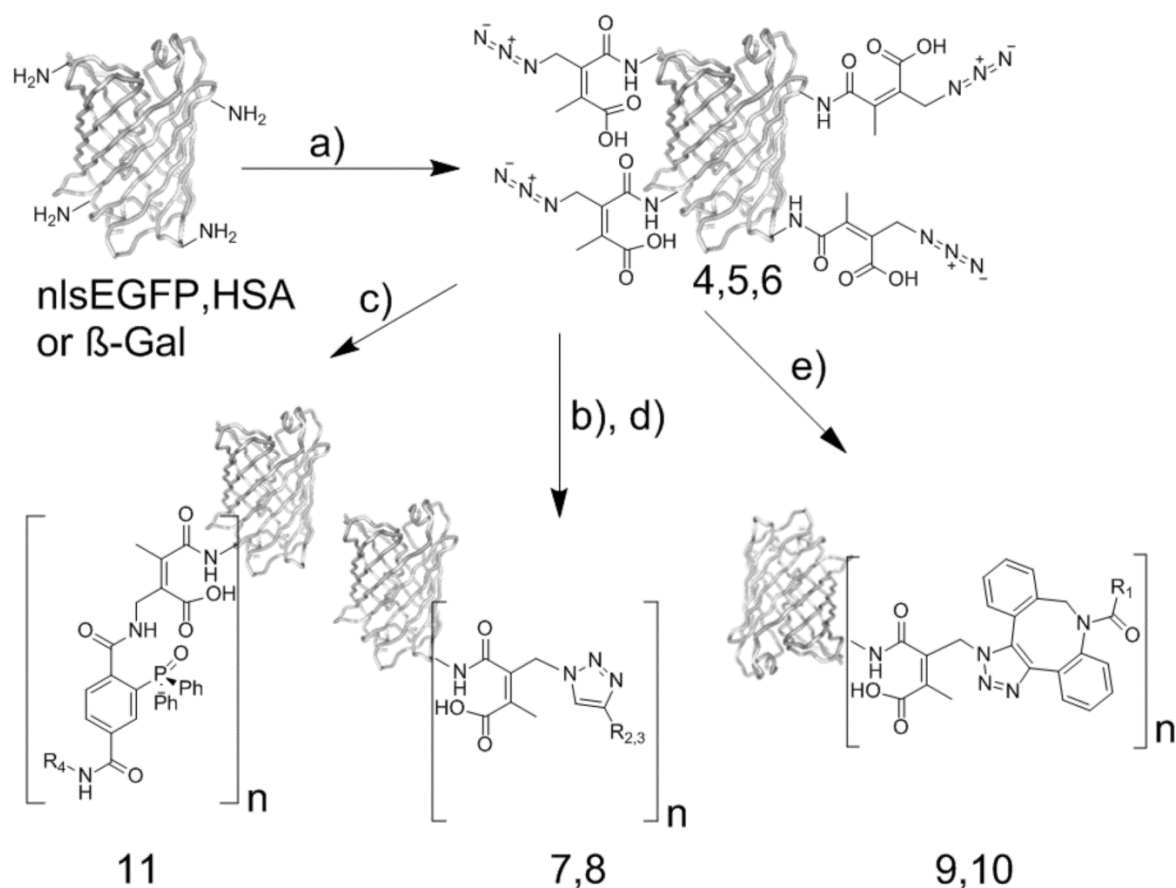
Figure 5.37: Absorption spectrum of alkyne hemicyanine dye.

After purification the characteristics of the dye were investigated. It is well soluble in water and has got an absorption maximum at a wavelength of 530 nm. For this reason it is easy to determine dye coupled to HSA, as HSA does exhibit nearly no

absorption at this wavelength. The molar extinction coefficient is $35000 \text{ M}^{-1}\text{cm}^{-1}$ in PBS buffer (pH 8.5).

5.7.5 Modification of proteins with AzMMMan

The heterobifunctional linker was used to introduce acid labile azido groups into human serum albumin (HSA), EGFP, or β -galactosidase (β -Gal) (Scheme 5.8 step a) by reaction of the maleic anhydride moiety with amino groups of the proteins. In subsequent reactions (Scheme 5.8 step b-e) the linker modified proteins were reacted with dye (to determine the amount of coupled linker, acid lability) or transduction oligomer for protein delivery investigations.



Scheme 5.8: pH-reversible modification of proteins with AzMMMan and following click modifications with dyes, PEG, or transduction oligomer. a) Modification of nlsEGFP, HSA, or β -Gal with AzMMMan linker 3. CuAAC conjugation of AzMMMan-HSA 4 with b) alkyne-hemicyanin dye 12 or d) alkyne-PEG, resulting in conjugates 7 or 8, respectively. c) Staudinger ligation of Dylight 488 (R_4) to AzMMMan-HSA resulting in conjugate 11. e) Conjugation of AzMMMan-nlsEGFP 5 or AzMMMan- β -Gal 6 with carrier polymer 386 (R_1) via copper free cycloaddition resulting in conjugate 9 or 10, respectively.

5.7.5.1 Determination of AzMMMan modification degree of HSA

HSA was reacted with different linker concentrations. After purification of the reaction batches, the reaction products were reacted with a surplus of alkyne dye. The degree of linker modification could be determined by measuring the absorbance of the coupled dye in conjugate **7** (Scheme 5.8). As expected, the number of azides introduced in HSA was nearly linear to the initial concentration of AzMMMan (Figure 5.38).

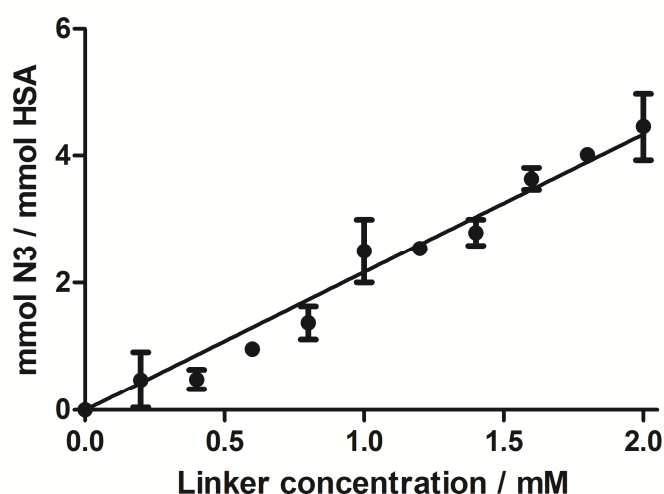


Figure 5.38: Reaction of HSA with different concentrations of AzMMMan. The number of azido groups incorporated into HSA was determined by reaction of compound **4** (Scheme 5.8) with alkyne dye.

5.7.5.2 Acid lability and serum stability of AzMMMan-HSA-Alkyne dye

Figure 5.39 displays the kinetics of pH-dependent cleavage of dye-conjugate **7** (Scheme 5.8). Dye labeled HSA **7** (Scheme 5.8) was incubated in buffers of different pH. The cleavage of alkyne dye from the protein was determined at various times by measuring residual dye absorbance of purified protein fractions. At basic pH of 8.5 the conjugate was quite stable, with only about 25 percent cleavage after 24 hours. In contrast, at pH 6 the same amount was released already after 30 minutes. Half-life at pH 5 is about half an hour, whereas at pH 4 already 90 percent of the linker was cleaved in that time. The cleavage of the linker appears to follow a pseudo first order kinetic.

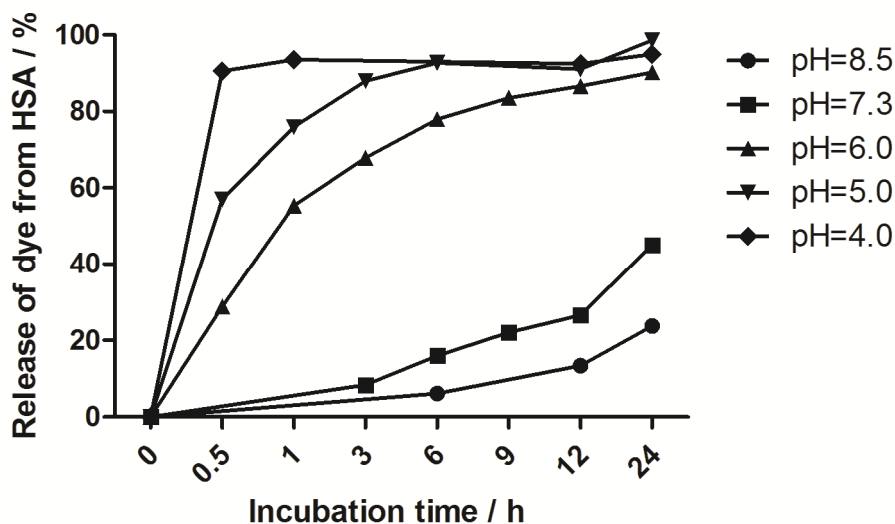


Figure 5.39: Acid catalyzed release of alkyne dye from conjugate 4 (Scheme 5.8) at 37° C. Samples of 4 (Scheme 5.8) were incubated in buffers of different pH. At each time point, the fraction (%) of dye remaining conjugated with HSA was determined after protein purification. Percentage of released dye is calculated as (100- % HSA conjugated dye).

Figure 5.40 reveals that conjugate 7 (Scheme 5.8) is quite stable under physiological serum conditions at 37 °C. After 2 hours incubation in buffer containing 30% FCS still 94 % of the dye remained coupled to HSA. Even after an incubation time of 12 hours 60 % of the bonds still are intact. The cleavage rate does not differ much from incubation in pure PBS buffer at physiological pH (Figure 5.39).

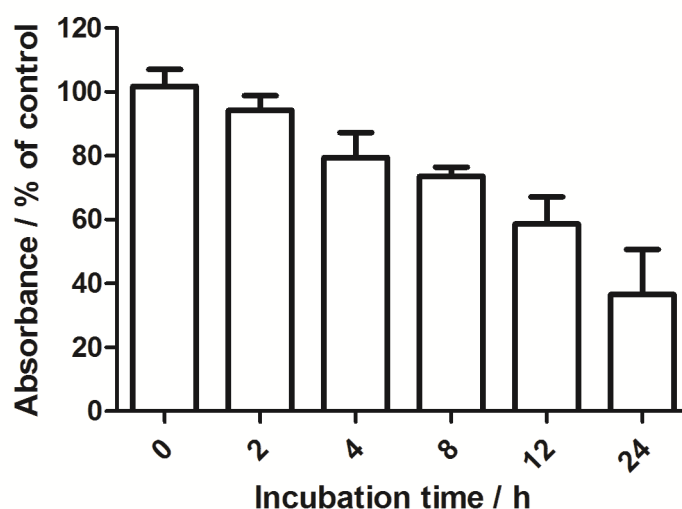
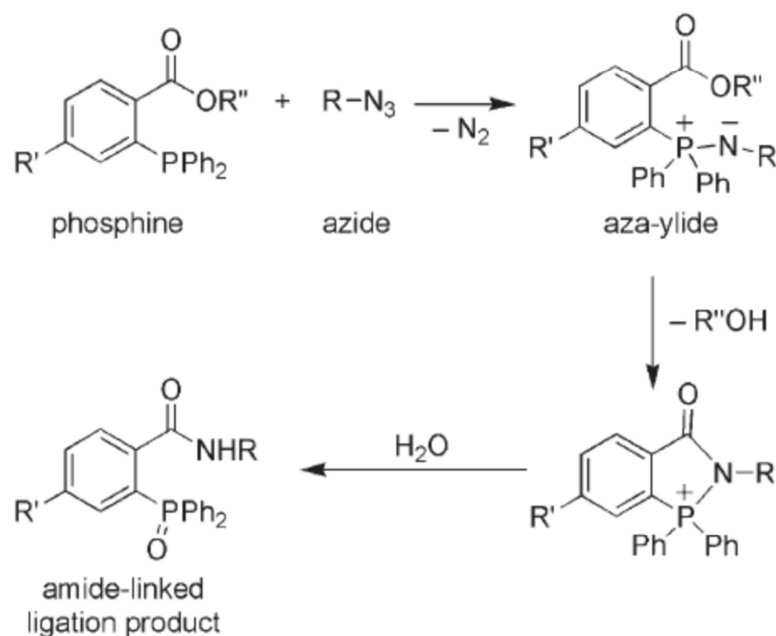


Figure 5.40: Serum stability of conjugate 7 (Scheme 5.8) at 37° C. Samples of 7 were incubated in PBS buffer pH 7.4 containing 30 % FCS. Dye remaining conjugated with the protein was determined by measuring the absorbance of the conjugate after purification from released dye.

Aside the copper catalyzed cycloaddition reaction shown in the section above also the so called Staudinger ligation can be performed with the azido-proteins (Scheme 5.9) (137).



Scheme 5.9: Staudinger Ligation. Reaction mechanism of phosphines with azides.

A phosphine containing dye was coupled to AzMMMan-HSA **4** (Scheme 5.8, step c), resulting in conjugate **11** (Scheme 5.8). Figure 5.41 shows similar pH-dependent cleavage of the two HSA conjugates independent of dye was coupled by Staudinger ligation (compound **11**, Scheme 5.8) or by CuAAC (compound **7**, Scheme 5.8).

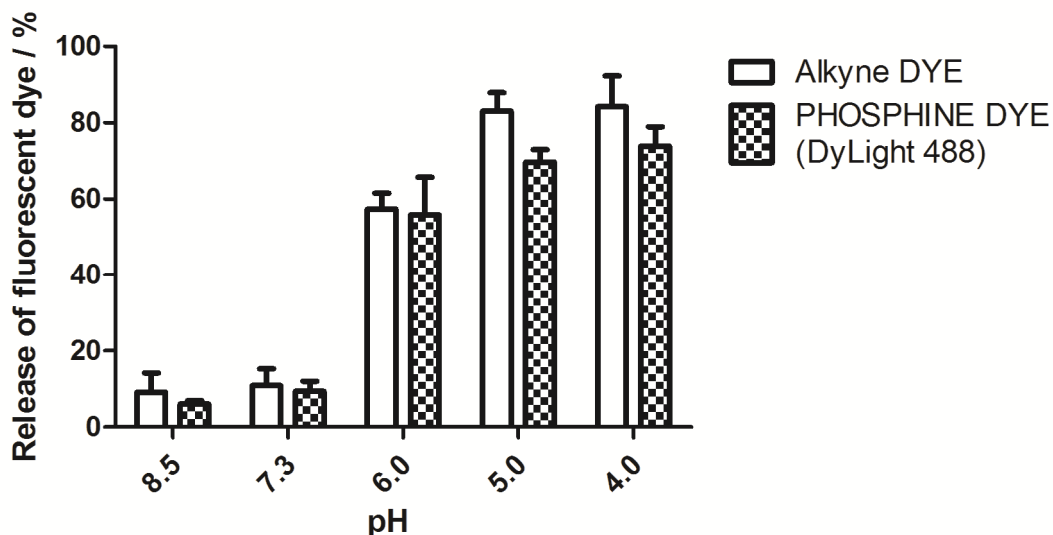


Figure 5.41: Comparative release of dye coupled over Staudinger Ligation and CuAAC. White bars: HSA-dye conjugate 7 (Scheme 5.8), generated with alkyne dye via CuAAC. Patterned bars: HSA dye conjugate 11 (Scheme 5.8), generated with phosphine dye via Staudinger ligation.

5.7.5.3 Modification of melittin with AzMMMan

Modification of melittin, the active lytic peptide from bee venom (26 amino acids) demonstrates, what great influence blocking of amino groups can have on functionality of molecules. Figure 5.42 illustrates, that melittin is losing its lytic activity towards erythrocytes when the amino groups are reacted with the AzMMMan crosslinker. The lytic activity is retrieved back under mild acidic conditions. This experiment shows that for some applications it might be necessary that not only the binding between crosslinked molecules is divided, but rather the linker molecule itself is cleaved off traceless to release the molecule of interest in its natural unmodified condition.

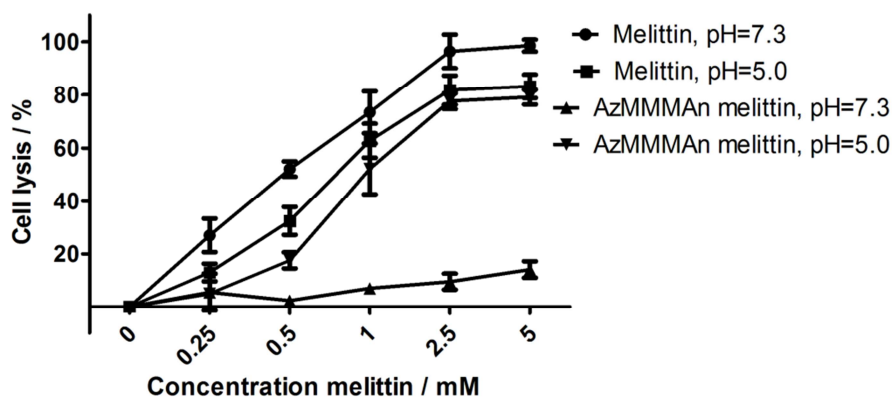


Figure 5.42: Acid lability of melittin modification. Hämoglobin release assay from erythrocytes incubated with unmodified melittin at pH 7.3 and 5.0 in comparison to AzMMMAAn modified melittin at pH 7.3 and pH 5.

5.7.5.4 Click modification of AzMMMAAn-HSA with PEG

Another application of the AzMMMAAn linker is reversible PEGylation of proteins (Scheme 5.8, step d). Figure 5.43 gives evidence that HSA can be effectively coupled with alkyne bearing PEG (lane 3). The PEG conjugate 8 (Scheme 5.8) shows extended stability at physiological pH (lane 4) but is cleaved under very mild acidic conditions of pH 6 (lane 5). At pH 5 or 4 almost all PEG is released (lanes 6 and 7).

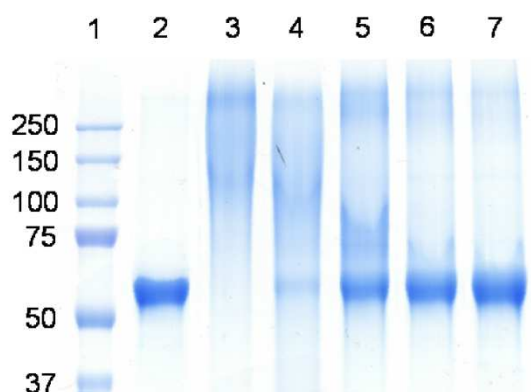


Figure 5.43: Acid catalyzed release of PEG from HSA conjugate 8. SDS-polyacrylamide gel electrophoresis after 16 h incubation. Lane 1 marker, lane 2 unmodified HSA, lane 3 pH 8.5, lane 4 pH 7.3, lane 5 pH 6, lane 6 pH 5, lane 7 pH 4.

A more detailed cleavage kinetic of PEG-AzMMMAAn-HSA at the endosomal pH of 5 is displayed in Figure 5.44. For this purpose PEG was distally end-labeled with tetramethylrhodamine (TMR) dye. The release of TMR-PEG from HSA conjugate was

determined at various times by measuring absorbance of TMR dye remaining incorporated in purified PEGylated protein conjugate. In contrast to the type of coupling reaction which has a minor influence on cleavage kinetics (Figure 5.41) the coupled molecule has more impact on acidic bond cleavage. PEG release from the protein was considerably slower compared with dye release from conjugate 7 (Scheme 5.8) (Figure 5.39).

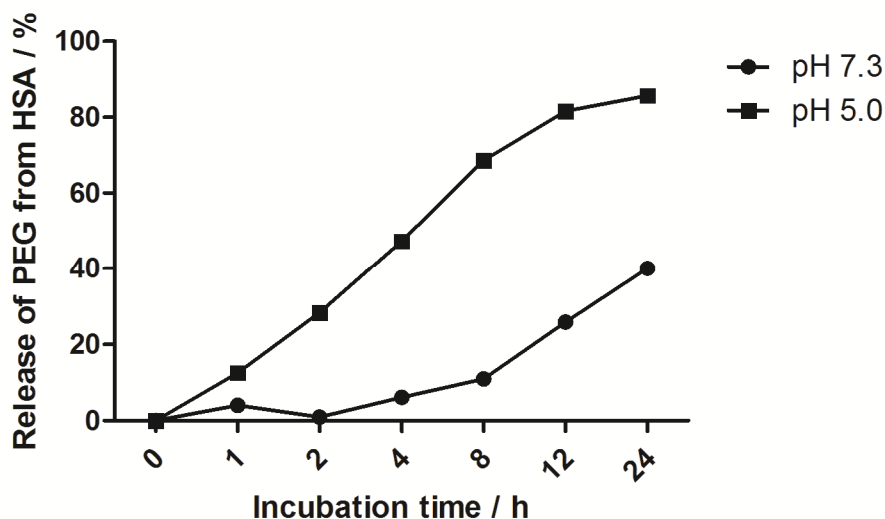


Figure 5.44: Kinetics of PEG release from HSA conjugate at endosomal relevant pH of 5 and stability of the conjugate at physiological pH of 7.3. TMR-labeled PEG released from HSA protein was determined by comparing the absorbance of the intact PEG-HSA conjugate before and after incubation.

5.7.5.5 Protein transduction using acid labile AzMMMan click linker and 386

Protein transduction, i.e. the intracellular delivery of proteins, can take advantage of the endosomal acidification process (108, 167, 168). nlsEGFP bearing a nuclear localization sequence (which mediates natural active nuclear import once a protein resides in the cytosol) was bound to the three-arm cationic oligo(aminoethane) amide **386** (Scheme 5.8, step e) resulting in conjugate **9**. Cationic carriers like **386** containing diaminoethane motifs bind cells and act as proton sponges which upon endosomal acidification become increasingly positively charged, triggering endosome disruption and release of its content (110, 169). For intracellular delivery of nlsEGFP protein, two different linking strategies, conventional irreversible conjugation and pH-reversible conjugation, were compared. For the synthesis of an irreversible conjugate, the commercial linker SMCC was used, resulting in thioether linkage. In

the new strategy, oligomer **386** was coupled with AzMMMan-nlsEGFP by copper-free cycloaddition via dibenzylcyclooctyne (Scheme 5.8, step e). Thus conjugate **9** contains an acid-labile bond between carrier **386** and nlsEGFP, which is expected to be reversible in the endosomal microenvironment before transfer into the cytosol. Successful modification of the nlsEGFP protein with transduction oligomer **386** and acidic lability of the resulting conjugate **9** (Scheme 5.8) is shown in Figure 5.45.

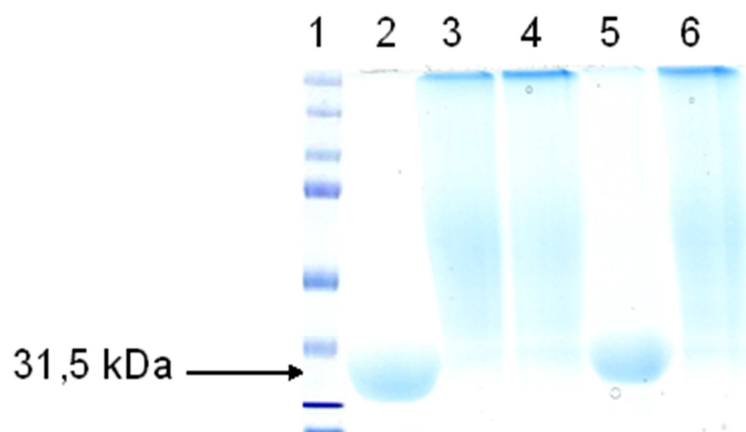


Figure 5.45: SDS-PAGE gel is showing the successful modification of nlsEGFP with oligomer 386 and acid lability of the AzMMMan construct. Lane 1: protein standard ladder; lane 2: unmodified nlsEGFP; lane 3: conjugate **9** (nlsEGFP conjugate with **386** via AzMMMan linkage); lane 4: nlsEGFP conjugate with **386** via irreversible SMCC modification; lane 5: conjugate **9** (Scheme 5.8) after acidic incubation at pH 5; lane 6: nlsEGFP-**386** conjugate via SMCC modification, after acidic incubation at pH 5.

The cleavage kinetics was determined in more detail (Figure 5.46) by labeling the **386** carrier with TMR dye and further processing analogously as described for the investigation of PEG release from HSA (Figure 5.44). As already observed for the PEG-HSA conjugate, coupling of carrier **386** to nlsEGFP is retarding the cleavage kinetics. Nevertheless, after 1 hour incubation at endosomal pH 5.0, >20% and after 2 hours almost 50% of the transduction oligomer was released from the nlsEGFP protein.

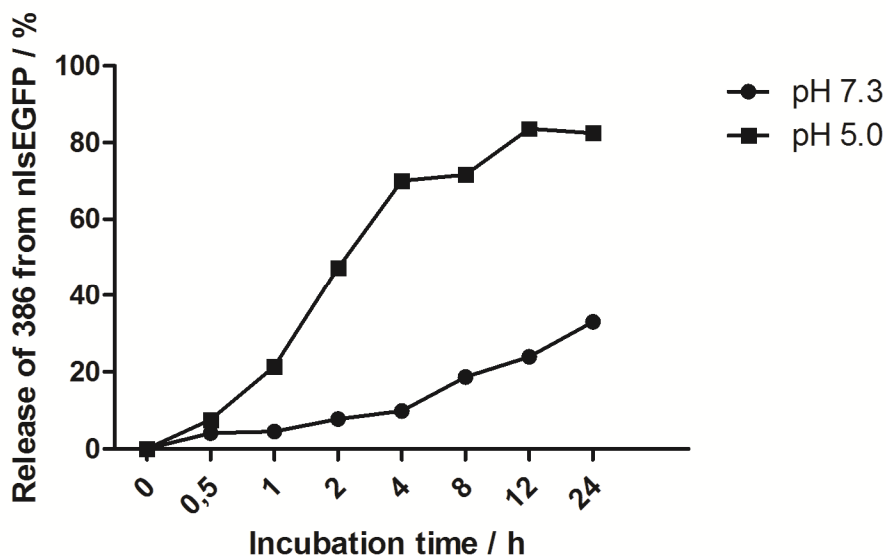


Figure 5.46: Acid catalyzed release of TMR-386 from conjugate 9 (Scheme 5.8) at 37° C. Samples of TMR-labeled 9 were incubated in PBS buffers of pH 7.3 and pH 5.0. Dye labeled 386 released from the protein was determined indirectly by measuring the absorbance of the conjugate after purification.

The cell culture experiment shown in Figure 5.47 demonstrates how important intracellular cleavage can be for protein delivery in the case of covalent binding to a carrier molecule using the novel AzMMMan linker. Both constructs, based on the pH-reversible conjugation or on conventional irreversible conjugation by SMCC thioether linkage, were able to deliver nlsEGFP into the cytosol of HeLa cells (Figure 5.47, row 1 and row 2). Flow cytometry experiments suggest that the stable thioether construct seems to be slightly more efficient (data not shown). Cells in row 3 were transfected with unmodified nlsEGFP as a control. The fluorescence image shows that no protein was internalized. However, only nlsEGFP which had been coupled to the carrier by acid labile bonds was further translocated into the nucleus to a large extent (Figure 5.47, row 1). Transfection of cells with conjugate 9 (Scheme 5.8) at 4° C in the presence of three different endocytosis inhibitors (amiloride (inhibitor for macropinocytosis), chlorpromazine (inhibitor for clathrin-mediated endocytosis), β -cyclodextrin (inhibitor for caveolae-mediated endocytosis)) almost completely eliminates internalization (Figure 5.47, row 4). This observation suggests an active, energy dependent internalization mechanism. The experiment shown in Figure 5.47, row 5 evidences that acidification in the endosome is a critical requirement for intracellular release of the carrier. Cells were preincubated and transfected in the presence of chloroquine and ammonium chloride. Both substances prevent acidification of the cellular endosomes. Transfections under these conditions result in

a similar observation that was made for the noncleavable construct. The conjugate is taken up by the cell and the balanced distribution suggests at least some endosomal escape, but only minor translocation of the protein into the nucleus was observed.

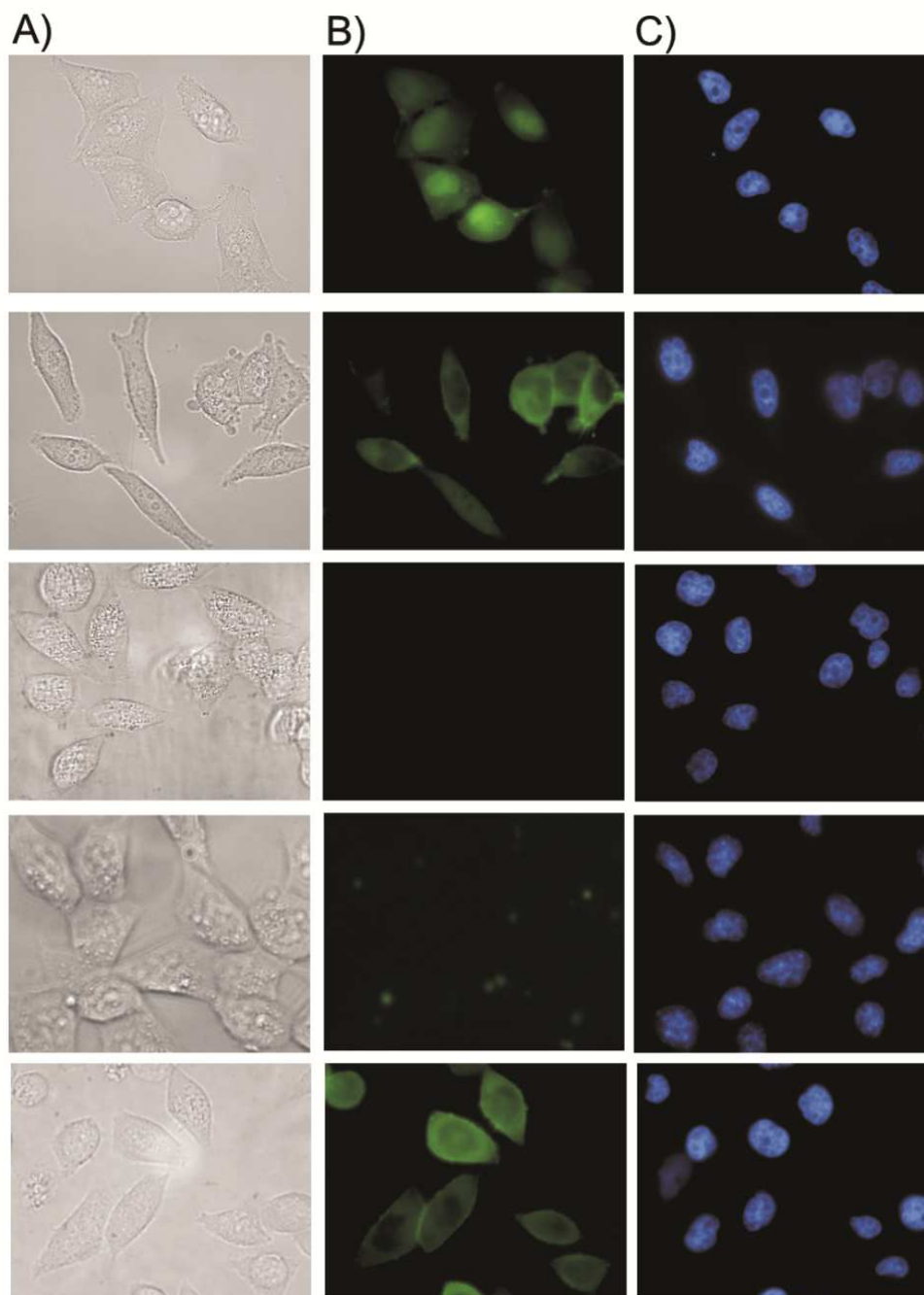


Figure 5.47: Transduction of HeLa cells with 386 modified nlsEGFP. Row 1: carrier **386** was coupled with nlsEGFP via the cleavable AzMMMan linker (compound **9**, Scheme 5.8). Row 2: carrier **386** was coupled by irreversible SMCC thioether linkage. Row 3: transfection was done with unmodified nlsEGFP. Row 4: transfection with conjugate **9** (Scheme 5.8) at 4°C in presence of endocytosis inhibitors. Row 5: transfection with conjugate **9** in presence of endosome acidification inhibitors. A) Brightfield picture of the transfected cells, B) EGFP fluorescence of the transfected cells, C) Hoechst 33342 DNA stain of the cell nucleus.

Transduction oligomer **386** has been shown to exhibit low cytotoxicity when used as a carrier for siRNA or DNA (59, 156). To verify the nontoxic properties also in case of being covalently bound to a protein over an acid labile bond, a cell viability test was performed that confirms this assumption. Figure 5.48 shows the low toxicity of the transduction shuttle, even at high transduction concentrations. It exhibits only marginal higher toxicity than the unmodified nlsEGFP protein. With the standard concentration used for the transfections above (10 $\mu\text{g/ml}$) a decline in metabolic activity of only 10 percent in comparison to untreated cells is observed. Even after transfection with the highest tested concentration of 80 $\mu\text{g/ml}$ **386** nlsEGFP conjugate cell viability decreased by only 33%. The toxicity profile of stable and reversible bound carrier does not differ much. However at the highest tested concentration the irreversible SMCC construct seems to be slightly more toxic.

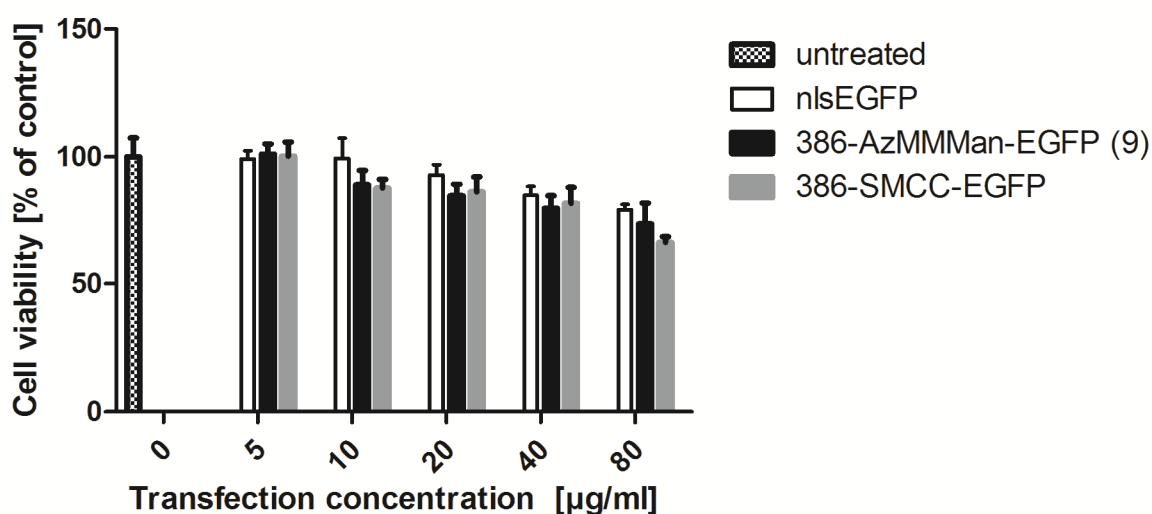


Figure 5.48: Cell viability assay of HeLa cells transfected with different concentrations of 386-nlsEGFP conjugates. Unmodified nlsEGFP was used for comparison.

To investigate if the protein conformation is irreversibly changed through the modification with the AzMMMan linker and the transduction oligomer **386** a CD spectroscopy experiment was performed. We compared unmodified nlsEGFP with with AzMMMan linker and **386** modified nlsEGFP after acidic incubation and purification. Figure 5.49 shows that the cd spectra of unmodified nlsEGFP and conjugate **9** (Scheme 5.8) after acidic incubation and purification do not differ much. This indicates that the natural conformation of the nlsEGFP protein is not disturbed by the reversible modification.

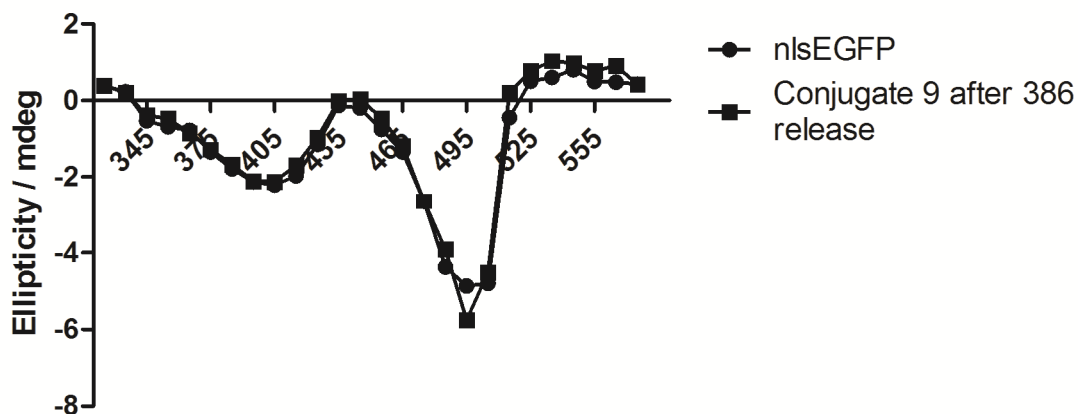


Figure 5.49: CD spectra of unmodified nlsEGFP and of conjugate **9** (386-AzMMMan-nlsEGFP, Scheme 5.8) after acidic incubation and purification.

Fluorescence properties and also CD spectra of construct **9** (Scheme 5.8) are indicating that the protein conformation is not significantly affected by the modification with the linker and the transduction oligomer. Therefore we examined whether the activity of an enzyme would be maintained and survive the modification, delivery, and intracellular release steps. As a model enzyme we have chosen β -galactosidase (β -Gal). It is of rather big size (119 kDa), and the activity of the enzyme in the cytosol can easily be investigated by the use of the fluorescent substrates. Carrier **386** was covalently bound to the β -Gal protein over the AzMMMan linker (Scheme 5.8, step e), resulting in conjugate **10** (Scheme 5.8). This construct was able to transport biological active β -galactosidase into the cytosol of HeLa cells. β -Gal activity was detected by using the fluorescent substrate C12-FDG (C12-fluorescein-di-beta-D-galactopyranoside), which exhibits FITC fluorescence after cleavage. This fluorescence was determined by flow cytometric analysis. Already with a transfection concentration of 1 μ M a significant raise in fluorescence was observed. Transfection with 2.5 μ M β -Gal further raised fluorescent properties. In contrast, cells treated with 2.5 μ M unmodified β -Gal (without shuttle) did not show a significant shift in fluorescence. This experiment evidences that the transduction shuttle is able to transduce biological active proteins into the cytosol of cells.

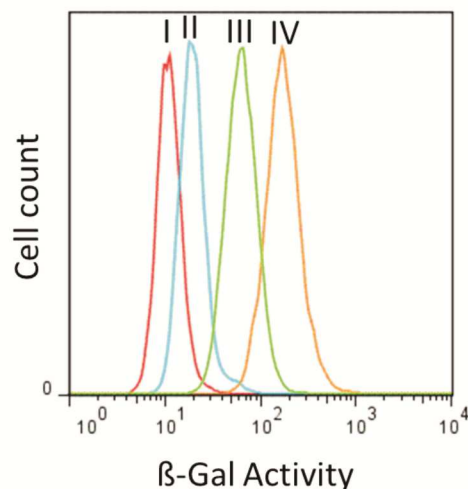
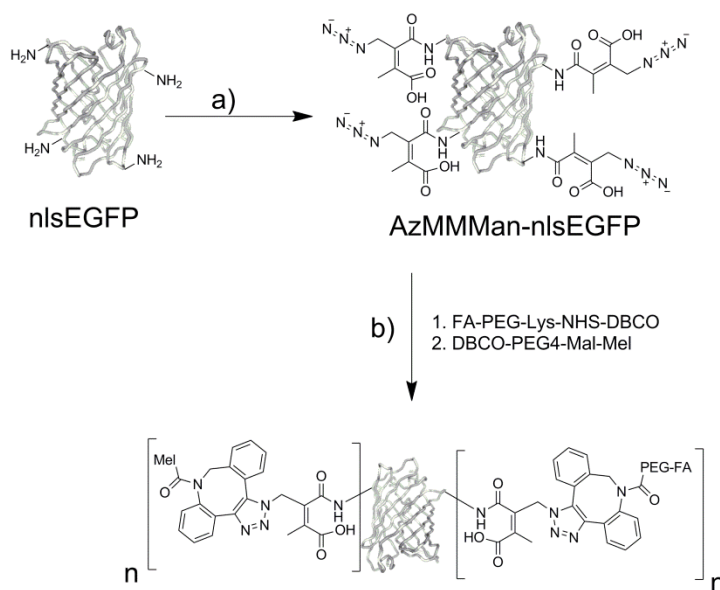


Figure 5.50: HeLa cells were transfected with conjugate 10 (386-AzMMMan-βGal), washed and incubated with C12-FDG substrate and evaluated by flow cytometry. I: untreated cells. II: cells transfected with 2.5 μM unmodified β-Gal. III: cells transfected with 1 μM conjugate 10. IV: cells treated with 2.5 μM of conjugate 10.

5.7.5.6 Polycation free protein transduction using a folic acid-PEG conjugate and melittin peptide

As already shown in Figure 5.32 modification of enzymes with the polycation **386** can have an influence on enzymatic activity. For this reasons a new polycation free transduction shuttle was designed (Scheme 4.2).



Scheme 4.2: Synthesis of a polycation-free protein transduction shuttle.

A folic acid- PEG conjugate (synthesized by Christian Dohmen, AK Wagner as part of his phd work) that was recently developed for the delivery of siRNA (49, 63) should effect internalization. To enable endosomal escape, additionally the endosomolytic peptide mellitin was covalently bound to folic acid-PEG modified nlsEGFP. Successful transfection of KB cells with the polycation free transduction shuttle (at a concentration of 25 μg per ml) is demonstrated in Figure 5.51 (transduction experiment performed by Daniel Edinger, AK Wagner, LMU). Quite a great amount of transduction shuttle is internalized and the even distribution of the protein inside the cytosol indicates endosomal escape. In addition, the protein is translocated into the nuclei of the cells, confirming successful escape of the transduction shuttles out of the endosomes and subsequent active nuclear import facilitated by the NLS sequence.

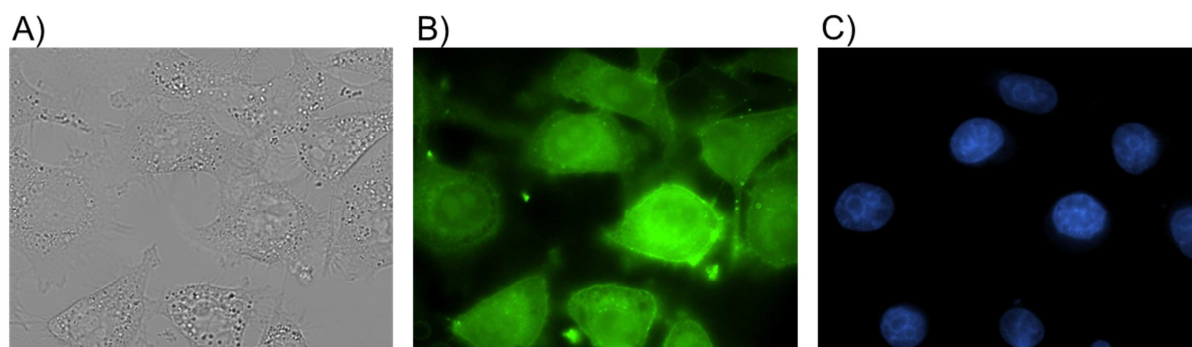
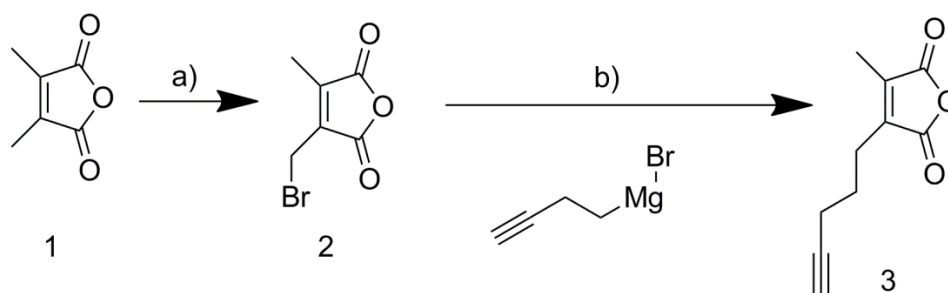


Figure 5.51: Transfection of KB cells with FAPEGxMel-nlsEGFP. A) bright-field picture of the transfected cells, B) EGFP fluorescence of the transfected cells, C) Hoechst 33342 DNA stain of the cell nucleus. This transduction experiment was performed by Daniel Edinger (AK Wagner, LMU).

5.7.6 Synthesis of PentyneMMan crosslinker

For some applications it may be of advantage to modify the protein instead of the azide with the alkyne. Therefore the alkyne bearing counterpart to the AzMMMan linker was synthesized. The pentyne-methylmaleic anhydride linker (PentyneMMan) was synthesized from dimethylmaleic anhydride by two simple reaction steps (radical substitution with NBS resulting in bromomethyl methylmaleic anhydride, followed by a carbon-carbon coupling step (Grignard reaction with 4-bromo-1-butyne). The yield for the second reaction step was 31 percent.



Scheme 5.10: Synthesis of PentyneMMan linker. a) N-bromosuccinimide, benzoyl peroxide, 56% b) diethyl ether, 31%.

5.7.7 Acid lability of PentyneMMan linker

To investigate if the PentyneMMan linker shows the same acidic reversibility than the AzMMMan linker, HSA was modified with the linker and subsequently an azide containing dye was coupled. Dye labeled HSA was incubated in buffers of different pH. The cleavage of azide dye from the protein was determined at various times by measuring residual dye absorbance of purified protein fractions (Figure 5.52). At basic pH of 8.5 the conjugate was quite stable, with only about 30 percent cleavage after 24 hours. At pH 6 nearly 40 % was released already after 30 minutes. Half-life at pH 5 is about a quarter hour. At pH 4 over 90 percent of the linker was cleaved in 30 minutes. The cleavage of the PentyneMMan linker as well as for the AzMMMan linker follows a pseudo first order kinetic. In summary the bond formed by the PentyneMMan linker seems to be a little bit more acid labile than the bond formed by the AzMMMan linker.

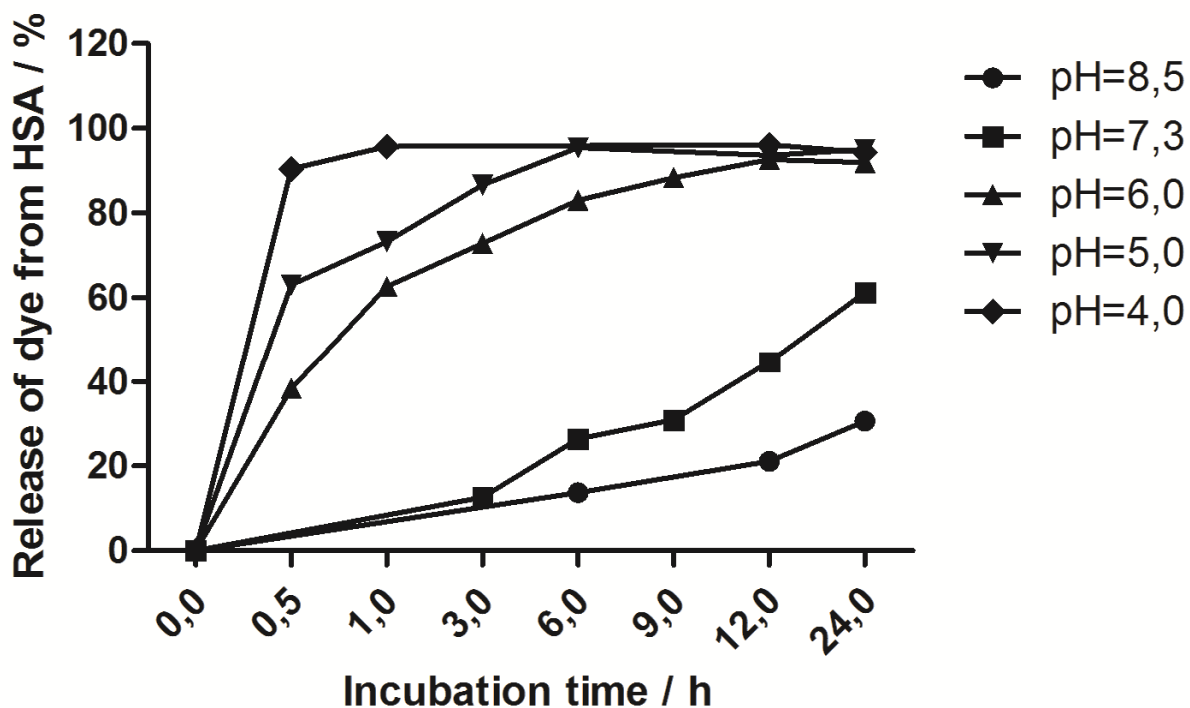


Figure 5.52: Acid catalyzed release of azide dye coupled over PentyneMMan to HSA at 37° C. Samples of azide dye modified PentyneMMan-HSA were incubated in buffers of different pH. At each time point, the fraction (%) of dye remaining conjugated with HSA was determined after protein purification. Percentage of released dye is calculated as (100%-HSA conjugated dye).

6 Discussion

6.1 Establishing of a cellular test system for protein delivery

Protein delivery into the cytosol of living target cells is a very complex process. Many different hurdles have to be overcome on the way into the cytoplasm. The delivery process may be subdivided into 5 main uptake steps. First the transduction shuttle must stay stable at physiological conditions in presence of serum. The second point is effective binding of the carrier system to the surface of the target cell. This binding may be mediated either by electrostatic interaction or via specific target cell interactions. Once bound to the surface the protein complex has to be internalized by the cell. The most common uptake pathway in protein delivery is endocytosis. Endocytosis leads to an entrapment of the internalized particle in cellular compartments surrounded by a phospholipid bilayer membrane, called endosomes. In most cases these endosomes are maturing to acidic lysosomes, leading to degradation of the internalized protein by proteases. For this reason the escape out of this endosomal compartment is indispensable for successful protein delivery into the cytosol of cells. But even after the carrier-cargo complex has reached the cytosol the delivery process is not finished. Now ideally in the fifth and last delivery step, the carrier has to be cleaved off from the cargo to assure natural behavior of the internalized protein. During all these critical five delivery steps the natural conformation of the protein has to be maintained to warrant activity of an internalized enzyme for example. A perfect test system for protein delivery should highlight every single step of this internalization process isolated. This should enable appropriate adjustment of the carrier system in case of one of these critical hurdles is not overcome by the transduction shuttle. Moreover a perfect test system should allow easy and fast qualitative determination of cellular uptake and further processing. To enable the comparison of different protein delivery techniques with regard to efficiency the test system should allow aside qualitative uptake the quantitative determination of the internalized protein amount and the percentage of successfully transfected cells. Of course it will never be completely avoidable that the carrier system has to be a little bit adjusted and modified according to the special demand of

a certain cargo. Nevertheless the test system should provide a platform that is transferable to as much other proteins as possible. Therefore the test proteins should be of average protein size and surface charge. Last but not least the test proteins have to be available in great quantities. So they have to be either cheaply commercially available or have to be easy to express and purify. The protein delivery test system developed in this thesis is addressing all requirements mentioned above. The nlsEGFP protein is easily heterologously expressible in *E. coli* and β -galactosidase is cheaply commercially available. As the test proteins nlsEGFP and β -galactosidase are of average protein size and charge, their transfection results should be transferable to a great amount of other proteins. Cellular binding and uptake, because of the inherent fluorescent properties of nlsEGFP, can be easily determined as well qualitatively on a fluorescent microscope as well as quantitatively via FACS analysis. Endosomal escape is indicated by even distribution of the nlsEGFP protein inside the cytosol of the transfected cell and more exactly by successful subcellular transport. This subcellular transport of nlsEGFP into the nucleus, mediated by the tagged nuclear localization signal, is only possible after endosomal release. Moreover the results in Figure 5.47 reveal that cleavage between carrier and cargo is advertised by the test system. The β -galactosidase enzyme was used as a second test protein which should evidence that the conformation of the proteins is not irreversibly disturbed by modification and the subsequent delivery processes. β -galactosidase allows also qualitative (Figure 5.33) and quantitative (Figure 5.34) conclusion of the transfection efficiency by the use of fluorescence substrates. In literature as well nlsEGFP (170) as also β -galactosidase (147) were already used as test proteins for protein delivery. However, only the combination of results obtained by transfection experiments with these two test proteins, gives a good hint for a broad applicability of the investigated transduction technology.

6.2 Development of a sequence defined carrier system for protein delivery

Protein transduction into living cells holds enormous potential in biological as well as in medical applications. With few exceptions native proteins, because of their size and charge, are unable to penetrate into the cytosol of living cells. Hence, an all-

purpose intracellular protein delivery technology is highly desirable as it would open the door for reams of different therapeutic uses. As already mentioned in the section above, the requirements on such a carrier platform are enormous. The carrier has to protect the protein cargo from proteolysis and aggregation in the extracellular space of the target cell. Afterwards the carrier has to promote cellular binding and further uptake of the complex by the target cell. Once inside the cell the retrograde transport out of the endosome mediated by the carrier system is indispensable for successful protein delivery. Moreover the carrier system has to combine high transduction efficiency with low cytotoxicity. Up to date many different carriers have been investigated in regard to exhibit these required properties. Cationic polymers as polyethylenimines belong to one of the most effective drug carrier classes and have been widely used as well for nucleic acid (126) as for protein delivery (107). Polyethylenimine lacks of defined structure and more important exhibits due to the big molecule size quite high cellular toxicity (171). For this reasons a generation three polypropylenimine dendrimer as carrier was used as a first protein transduction carrier molecule. G3 PPI is of rather low molecular weight and furthermore a structure defined molecule. Covalent coupling of the G3 PPI dendrimer over the zero length crosslinker EDC to nlsEGFP leads to high efficient protein transduction into living cells (Figure 5.14). Although the fluorescent pictures show good internalization and even distribution of the nls-EGFP protein is indicating endosomal escape, only small amounts of the internalized protein is translocated into the nucleus of the transfected cells. Also microinjection experiments reveal that G3 PPI modified nlsEGFP (Figure 5.18) in contrast to unmodified nlsEGFP (Figure 5.7) is subcellularly not transported into the nucleus. The lacking nuclear import of G3 PPI modified nlsEGFP is consistent with a direct (by chemical modification of the nls residues) or indirect (by sterical shielding) inactivation of the nuclear localization signal. Alternatively, active nuclear transport may be hampered by unspecific cytosolic retention of the polycationic transduction shuttle. The microinjection pictures of G3PPI-nlsEGFP are indicating that the last point may be one of the major reasons as quite a great amount of the protein is sticking to negative charged cell components for example the nuclear membrane shows high EGFP fluorescence. To achieve aside high efficient internalization natural subcellular behavior a cleavable bond between the G3PPI carrier and the nlsEGFP cargo was introduced. Transduction studies with this G3PPI-SS-nlsEGFP showed a little bit better nuclear translocation

compared to the non-cleavable counterpart (Figure 5.21). The shape of cells transfected with the reducible construct indicated high cytotoxicity that was further evidenced by a performed cell viability assay (Figure 5.23). High toxicity of G3PPI was already observed for the noncleavable G3PPI-nlsEGFP construct but the significant higher toxicity of the cleavable G3PPI-nlsEGFP was not expected in that extent. The higher toxicity of the cleavable transduction shuttle may be explained with the fact that free cytosolic G3PPI dendrimer can interact more with cellular components, for example mRNAs, DNA, membranes etc., than protein bound dendrimer which is at least partly shielded by the irreversible covalently bound nlsEGFP protein. High toxicity is known to be another possible reason for unnatural behavior of internalized proteins. This could explain the rather low nuclear transport of nlsEGFP, when it is transduced with G3PPI as a carrier molecule, even in cases when the bond between carrier and cargo is biological cleavable. To overcome the problem of high toxicity other carrier molecules were tested for their applicability in protein delivery. Like G3PPI dendrimer, polymer **71** is a structure defined cationic oligomer. In contrast to the G3PPI dendrimer that is based on polypropylenimine units, polymer **71** is built up from amino acids and fatty acid subunits. The carrier was previously designed in the Wagner laboratory for the transfection of DNA and siRNA. In these studies it exhibited high transduction efficiency combined with low cytotoxicity. Covalent coupling to the nlsEGFP protein over the MAM linker molecule was quite difficult. Only low amounts of polymer can be coupled to the protein, because otherwise the modified protein is building non soluble aggregates. The formation of these aggregates is consistent with the following explanation. Transduction oligomer **71** contains oleic acid residues that should enable membrane destabilization and therefore endosomal escape. After covalent coupling to the protein these fatty acids change the naturally hydrophilic surface of the nlsEGFP protein and makes it more hydrophobic. Now van der Waals forces are leading to the observed protein aggregation. The weak nuclear transport of nlsEGFP transduced with oligomer **71** can be explained in following manner. Because only a small modification degree is possible, the amount of carrier covalently bound to the protein is not sufficient to promote endosomal escape (Figure 5.36). Another cause for the lack of nuclear translocation may be found in insufficient cleavage of the used MAM linker and therefore again interaction of the carrier with cellular components hampers nuclear transport. For this reasons **386** another structure defined carrier that showed

similar good properties for nucleic acid delivery as transduction oligomer **71** was used. In contrast to **71**, the structure of **386** does not contain fatty acid residues. This fact enables a high modification degree of the nlsEGFP without leading to protein aggregation and the formation of insoluble particles. The stp subunits, because of their high positive charge density effect good cellular binding of **386** modified nlsEGFP to the cell surface and therefore internalization of the conjugate. Moreover the membrane destabilizing properties of **386** enable good endosomal escape. If **386** is coupled over a biological cleavable bond to the protein natural behavior of cytosolic nlsEGFP is indicated by fast nuclear translocation of free cytosolic nlsEGFP (Figure 5.28). Although **386** is showing lower transfection efficiency than G3PPI (Figure 5.26), the fact of the low cytotoxicity makes it much more applicable for protein delivery. The linear dependency of concentration and uptake that was found for **386** modified nlsEGFP was already reported for internalization mediated by the protein transduction domain Antp (Antennapedia homeodomain) (100). Furthermore an approximately linear relationship between fluorescence intensity and time was found. Such a continuous uptake is supposed to be a strong hint for endocytosis mediated uptake (100). This hypothesis was further evidenced by uptake inhibition experiments. The uptake inhibition experiments did not allow the identification of a certain endocytosis pathway, but rather suggest that different mechanisms are involved in the internalization process (Figure 5.31). Although it cannot be excluded completely that in some cases the observation of reduced uptake may also be explained by the toxicity of the inhibitor which leads to lower cellular metabolism. The bright fluorescence of **386**-SS-nlsEGFP and **386**-AzMMMan-nlsEGFP is indicating that the conformation of the nlsEGFP is not affected much by the modification. This was further evidenced by CD spectroscopy experiments which reveal a natural conformation of nlsEGFP after splitting off the carrier (Figure 5.49). Aside the rather low sized nlsEGFP, **386** was able to deliver β -galactosidase with high molecular weight into the cytosol of different cell lines. Moreover the enzyme is found to be enzymatically active inside the cytosol of the transduced cells. Although enzyme activity was found in transduced cells an experiment investigating the kinetics of substrate conversion revealed that **386** modified β -galactosidase exhibits only 10 percent of the activity compared to untreated enzyme. This finding may be explained by the charge inversion of the protein, as unmodified β -gal is a protein with a negative isoelectric point (theoretical pI 5.8), whereas on the modified protein the

positive charges overbalances the negative ones by far. Another possible reason for the loss in activity may be the rather rough chemical conditions during the modification process. To resolve this problem another carrier system was tested for its protein delivery properties. PEG modified folic acid as a targeting ligand and the endosomolytic peptide mellittin were covalently coupled to the nlsEGFP. This transduction shuttle is completely free of polycations. Ideally, this protein transduction shuttle comprises functionalities for all essential steps during the delivery process: shielding of the protein during circulation (to prevent immunogenic side effects as well as degradation), a targeting moiety (for receptor specific delivery and uptake by the target cells) and finally an endosomolytic moiety (for effective release of the payload from the endosomal compartment). First transduction studies show promising results for the transfection of nlsEGFP (Figure 5.51).

6.3 Design of a traceless-cleavable linker for protein delivery

For protein delivery in contrast to nucleic acid delivery in most cases a covalent bond between the carrier and the cargo is necessary. Nucleic acids exhibit a high density of negative charges resulting in a strong electrostatic interaction between the polycationic carrier and the nucleic acid. The formed polyplexes are very stable even under serum containing conditions. Although the polar and charged side chains of the amino acids are mostly exposed on the surface of the protein whereas the hydrophobic residues assemble in the core the charge density is far lower compared to nucleic acids. Moreover the surface of most proteins does not only contain negative charged moieties resulting from the glutamic acid or asparagine side chains but usually also the positive charged side chains of lysine, histidine and arginine amino acids are exposed. For example the used nlsEGFP protein is built up of 281 amino acids, whereof 36 residues are negative charged (aspartate and glutamate) and 33 are positive charged (arginine and lysine). This is resulting in a negative charge density of one negative charge per 10511 Da. In comparison an average double stranded DNA molecule of the same molecular weight exhibits a charge density of one negative charge per 312 Da. Regarding this great difference in the charge density it becomes clear why proteins do not form stable complexes with

polycations, in contrast to nucleic acids. To overcome this problem, different strategies were developed. For example each positive charge occurring from a lysine residue can be transformed in two negative charges by modification with citraconic anhydride. With this strategy the charge density of cytochrome c could be enhanced to one negative charge per 320 Da (75). Another strategy for forming stable polyplexes is the exploitation of hexa-histidine tag fused to the cargo protein. A carrier that contains a chelat forming nitrile triacetic acid complex is binding strongly to this histidine tag (27). The major disadvantage of this system is that no complete encapsulation of the cargo protein with the carrier is possible as these hexa-histidine tags in most cases are either fused to the amino- or to the carboxy-end of the protein. In contrast, the covalent coupling of the carrier to lysine residues of the cargo protein, over linker molecules, allows complete encapsulation. Up to date many different linker molecules for covalent modification of proteins have been developed. Covalent modification of proteins can have great influence on their properties. For example the bee venom peptide mellittin can lose its lytic activity after covalent modification (Figure 5.42). For this reasons most of them are limited applicable for protein delivery as they form stable non-cleavable bonds between the carrier and the cargo (e.g. amide bonds, thioether and others). Among the biological cleavable linkers the used SPDP crosslinker is one of the most famous. The disulfide bonds between the carrier and the cargo protein are cleaved by the reducing conditions endemism in the cytosol. For protein delivery also acid labile linkers are applicable, due to the acidification process occurring in endosomes after internalization of the transduction shuttle. Such acid labile linkers have already been described in literature (172-174). Major disadvantage of these linkers is the fact that after cleavage of the acid labile bond a small linker fragment is retarded on the cargo molecule. The acid labile linkers used and developed in this thesis are based on maleic anhydride which forms an acid labile amide bond with amines of the cargo molecule. Under acidic conditions, this labile amide bond is cleaved traceless, resulting in an unmodified cargo molecule. Blatter and coworkers (134) developed a heterobifunctional MAM linker based on maleic anhydride. Figure 5.35 and Figure 5.36 show that its applicability for protein delivery is limited due to insufficient cleavage of the acid labile bond under physiological relevant pH conditions. It is well known that amide bond formed by dimethyl maleic anhydride are due to the Thorpe-Ingold effect much more acid labile than those formed with maleic anhydride (62). This is also the explanation

why the AzMMMan and PentyneMMMan linkers, developed in this thesis, are cleaved at higher pH values (Figure 5.39, Figure 5.52). How important the cleavage under mild physiological relevant conditions is becomes clear when comparing the results of nlsEGFP coupled to the carrier molecule over AzMMMan and MAM. nlsEGFP coupled to the carrier with AzMMMan shows natural cytosolic behavior and is subcellularly transported into the nucleus, whereas nlsEGFP coupled over the MAM linker lacks of this translocation due to insufficient cleavage. The experiment in which endosomal acidification is prevented with chloroquine is evidencing that cleavage of the carrier is indispensable for natural subcellular behavior of nlsEGFP (Figure 5.47). Aside the higher acid lability, the developed AzMMMan and PentyneMMMan linkers have got a second advantage compared to the MAM linker. In recent years click chemistry reactions, especially the copper catalyzed 1,3-dipolar cycloaddition (CuAAC) and the Staudinger ligation, became useful tools for conjugating biomolecules.(49, 135-137) Both reactions have great advantages compared to other linking strategies, like high efficiency and bioorthogonality. In contrast the second functional group of the MAM linker is a maleimide. This maleimido group is not bioorthogonal, as it can react with thiol groups from cysteine residues as well as with amine groups from lysine residues for example. Figure 5.41 reveals that the coupling type (Staudinger Ligation or CuAAC) has got only a minor influence on the acid lability of the construct, whereas the coupled molecule has more impact on acidic bond cleavage. PEG release from the protein (Figure 5.44) was considerably slower compared with dye release (Figure 5.39). This may be explained by better sterical shielding of the maleimido group by PEG. Although the PentyneMMMan linker seems to be a little more acid labile than the AzMMMan linker they do not differ much in this property. The better solubility of the AzMMMan linker tipped the balance why it was preferred for use in the protein delivery experiments.

7 Summary

Intracellular protein delivery is offering numerous possibilities in research and in therapy. Aside gene therapy, protein delivery into living cells is one of the most promising tools for the treatment of various so far intractable diseases including cancer. To develop a practicable protein delivery platform, a test system which allows easy control of successful intracellular delivery is needed. Therefore a test system based on two model proteins was established. A nuclear localization signal tagged EGFP molecule is enabling fast control of cellular uptake and endosomal release. The second model protein β -galactosidase is evidencing that protein conformation is not irreversibly disturbed by modification with the carrier molecules. Protein transduction technology is opening the door for a promising alternative to gene therapy, as it is lacking of the potential malignant side effects of gene therapy. The most limiting step in the development of a therapeutic drug remains the delivery process. In the last decade, many techniques to deliver proteins into living cells were developed. Although great efforts were made, so far no all-purpose technique is available that addresses all critical steps, like efficient uptake, endo-lysosomal escape, low toxicity, while maintaining enzymatic activity. Each method has got its limitation, for example cell type dependence. Among the so far used carriers, the most effective ones are cationic polymers like polyethylenimine. These carriers are lacking of precise structure and often show high toxicity, dependent on the molecular weight of the used polymer. In this thesis the properties of the three arm cationic oligomer **386**, which was previously designed for siRNA delivery was investigated in regard of being applicable as a transduction carrier for protein delivery. This carrier molecule, in contrast to other cationic polymers used for protein delivery, is of precise structure, of low molecular weight and potentially degradable by proteases. The transduction oligomer was covalently bound to the protein by a bioreversible bond. Our results reveal that covalent coupling of the structure defined cationic oligomer **386** to a protein leads to a high efficient, serum insensitive and low toxic alternative to established protein transduction technologies. For a general all-purpose delivery system covalent coupling of the carrier to the cargo protein is indispensable. Protein delivery requires special properties to the linker molecule. Therefore in this work a new pH sensitive linker was developed which combines the advantages of click reactions with the implementation of a traceless cleavable bond between two

conjugated molecules. Three different click chemistries were performed which all are compatible with the acid labile properties. A traceless cleavage may be a particularly important feature in protein transduction strategies, to maintain full bioactivity of enzymes and other proteins. The current example of **386** carrier-mediated cytosolic delivery and subsequent nuclear import of released nls-EGFP demonstrates the advantage of the traceless linker. To demonstrate that the modification does not irreversibly affect structure and biological activity of proteins, **386**-AzMMMan- β -galactosidase was delivered as a model enzyme. It exhibited cytosolic activity in the transduced cells far higher than without shuttle. Aside from these encouraging options for protein delivery and modification, the linker might have broader use in the design of novel programmed, acid labile and biodegradable drug delivery systems. Targeted therapeutics could, after delivery into acidic tumor areas or upon cellular uptake into endosomes, be dismantled from their outer shell including targeting ligands. Besides drug delivery, the linker may also be of interest for other applications, such as reversible labeling of various biological and also chemical molecules. The developed linking strategy and the presented concepts for transduction shuttles may help to get a step closer in the design of an all-purpose protein delivery platform, applicable on bench as on bedside.

8 Abbreviations

μM	Micromolar
μmol	Micromole
AA	Amino acid
ACN	Acetonitrile
Antp	Antennapedia homeodomain
ATCC	American type culture collection
AzMMMan	Azidomethyl methyl maleic anhydride
B6	Peptide sequence with affinity for the transferrin receptor
C12-FDG	5-dodecanoylamino fluorescein di- β -D-galactopyranoside
Calcd	Calculated
CD	circular dichroism
CHCL3	Chloroform
C-NMR	Carbon Nuclear magnetic resonance spectroscopy
CPP	Cell penetrating peptide
CuAAc	Copper catalyzed alkyne azide cycloaddition
CuBr	Copper bromide
CuI	Copper iodide
Da	Dalton
DBCO	Dibenzylcyclooctyne
DCC	Dicyclocarbodiimide
DCM	Dichloromethane
DCU	Dicyclourea

DCVC	Dry column vacuum chromatography
DIC	Differential interference contrast
DLS	Dynamic light scattering
DMF	N,N-Dimethylformamide
DMSO	Dimethyl sulfoxide
DNA	Deoxyribonucleic acid
DTT	DL-Dithiothreitol
e.g.	Exempli gratia, for example
EDC	N-(3-Dimethylaminopropyl)-N'-ethylcarbodiimide hydrochloride
EDTA	Ethylenediaminetetraacetic acid
EGF-R	Epidermal growth factor receptor
EGFP	Enhanced green fluorescent protein
Et ₂ O	Diethyl ether
etc.	Et cetera
EtOH	Ethanol
FA	Folic acid
FACS	Fluorescent analyzed cell sorting
FCC	Flash column chromatography
FCS	Fetal calve serum
FDA	Food and Drug Administration
FITC	Fluorescein isothiocyanate
G3	Generation three
GE 11	Peptide binding to the EGF-receptor

GFP	Green fluorescent protein
GTP	Guanosine 5'-triphosphate
HCl	Hydrochloric acid
Hepes	N-(2-hydroxyethyl) piperazine-N'-(2-ethansulfonic acid)
Hepps	N-2-Hydroxyethylpiperazin-N'-3-propansulfonsäure
HIV	Human immunodeficiency virus
HMPA	Hexamethylphosphoramide
H-NMR	Proton Nuclear magnetic resonance spectroscopy
HSA	Human serum albumine
IR	Infrared
IU	International Units
kDa	kilo Dalton
Mal	Maleimide
MAM	Maleic anhydride maleimide
Mel	Melittin
MetOH	Methanol
mg	Milligramm
MHz	Megahertz
mL	Milliliter
mM	Millimolar
mmol	Millimole
mRNA	Messenger RNA
MSN	Mesoporous silica nanoparticle

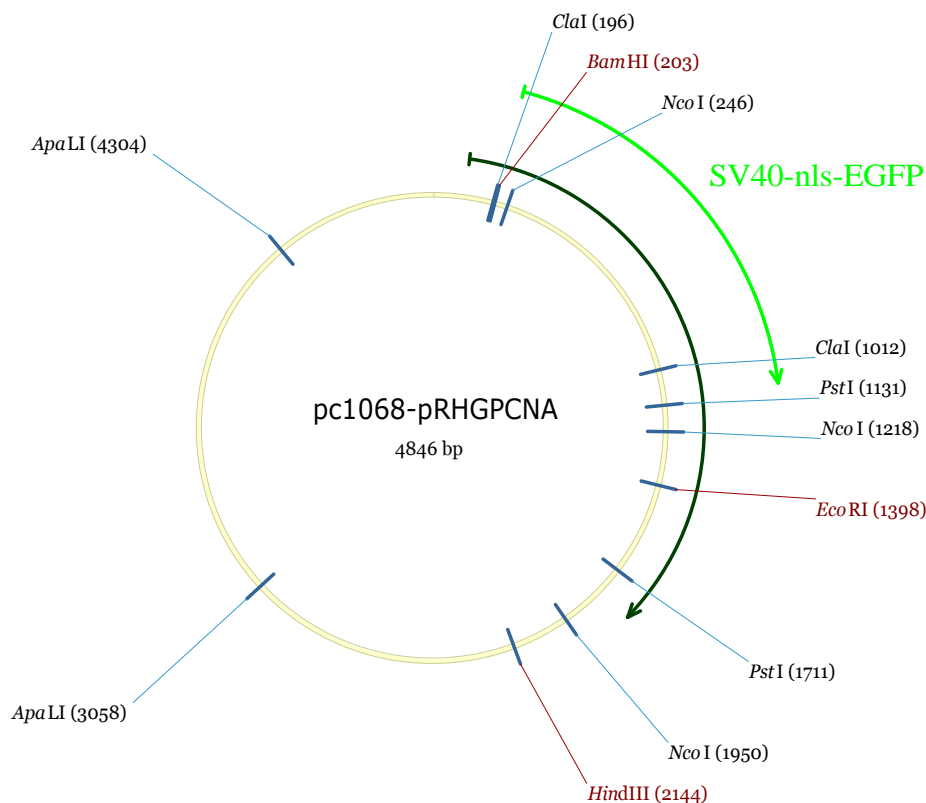
MTBE	Methyl tertiary butyl ether
MTT	1-(4,5-Dimethylthiazol-2-yl)-3,5-diphenylformazan
MUG	4-Methylumbelliferyl β -D-galactopyranoside
MWCO	Molecular Weight Cut Off
NBS	N-Bromosuccinimide
NHS	N-Hydroxysuccinimide
NLS	Nuclear localization signal
nlsEGFP	Nuclear localization signal tagged EGFP
nm	Nanometer
NTA	Nitrilotriacetic acid
PBS	Phosphate buffered saline
PCR	Polymerase chain reaction
PEG	Polyethylene glycol
PEI	Polyethylenimine
PentyneMMan	Pentyne methyl maleic anhydride
pH	Potentia Hydrogenii
PPI	Polypropylenimine
PTD	Protein transduction domain
RGD	Peptide sequence (arginine, glycine, aspartic acid)
RNA	Ribonucleic acid
RNAi	RNA interference
SDS	Sodium dodecyl sulfate
PAGE	Poly Acrylamide Gel Electrophoresis

SEC	Size exclusion chromatography
siRNA	Small interfering RNA
SMCC	N-Succinimidyl 4-(maleimidomethyl)cyclohexanecarboxylate
SPDP	N-Succinimidyl 3-(2-pyridyldithio)propionate
β -Gal	Beta galactosidase
Stp	Succinoyl-tetraethylenpentamine
SWNTs	Single walled carbon nanotubes
TAT	Trans-Activator of Transcription
TB	Terrefic Broth
TBTA	Tris[(1-benzyl-1H-1,2,3-triazol-4-yl)methyl]amin)
tertButOH	Tertiary butanol
THF	Tetrahydrofuran
TLC	Thin layer chromatography
TMR	Tetramethylrhodamine
Tris	Tris(hydroxymethyl)aminomethane
UV	Ultraviolet
Vis	Visible
VLPs	Virus like particles
X-Gal	5-Brom-4-chlor-3-indoxyl- β -D-galactopyranosid

9 Appendix

9.1 Plasmid maps and base sequences

9.1.1 pc1068-pRHGPCNA



Scheme 9.1: Plasmid pc1068-pRHGPCNA

Base Sequence:

```
GATCTCGATCCCGCGAAATTAATACGACTCACTATAGGGAGACCACAACGGTTT
CCCTCTAGAAATAATTTTGTTTAACTTTAAGAAGGAGATATACATATGCGGGGTT
CTCATCATCATCATCATCATGGTATGGCTAGCATGACTGGTGGACAGCAAATGG
GTCGGGATCTGTACGACGATGACGATAAGGATCGATGGGGATCCCCGAAGAAG
AAGCGCAAAGTACTGGTACCGGTCGCCACCATGGTGAGCAAGGGCGAGGAGCT
GTTACCGGGGTGGTGCCCATCCTGGTTCGAGCTGGACGGCGACGTAAACGGC
CACAAGTTCAGCGTGTCCGGCGAGGGCGAGGGCGATGCCACCTACGGCAAGC
TGACCCTGAAGTTCATCTGCACCACCGGCAAGCTGCCCGTGCCCTGGCCCACC
CTCGTGACCACCCTGACCTACGGCGTGCAAGTGCCTTCAGCCGCTACCCCGACCA
CATGAAGCAGCAGCACTTCTTCAAGTCCGCCATGCCCGAAGGCTACGTCCAGG
AGCGCACCATCTTCTTCAAGGACGACGGCAACTACAAGACCCGCGCCGAGGTG
```

AAGTTCGAGGGGCGACACCCTGGTGAACCGCATCGAGCTGAAGGGCATCGACTT
CAAGGAGGACGGCAACATCCTGGGGCACAAGCTGGAGTACAACACTACAACAGCC
ACAACGTCTATATCATGGCCGACAAGCAGAAGAACGGCATCAAGGCCAACTTCA
AGATCCGCCACAACATCGAGGACGGCAGCGTGCAGCTCGCCGACCACTACCAG
CAGAACACCCCCATCGGCGACGGCCCCGTGCTGCTGCCCGACAACCACTACCT
GAGCACCCAGTCCGCCCTGAGCAAAGACCCCAACGAGAAGCGCGATCACATGG
TCCTGCTGGAGTTCGTGACCGCCGCCGGGATCACTCTCGGCATGGACGAGCTG
TACAAGGGCGAAGGGCAAGGGCAAGGGCAAGGGCCGGGCCGCGGCTACGCG
TATCGATCCATGTTTCGAGGCGCGCCTGGTCCAGGGCTCCATCCTCAAGAAGGT
GTTGGAGGCACTCAAGGACCTCATCAACGAGGCCTGCTGGGATATTAGCTCCA
GCGGTGTAAACCTGCAGAGCATGGACTCGTCCCACGTCTCTTTGGTGCAGCTC
ACCCTGCGGTCTGAGGGCTTCGACACCTACCGCTGCGACCGCAACCTGGCCAT
GGGCGTGAACCTCACCAGTATGTCCAAAATACTAAAATGCGCCGGCAATGAAGA
TATCATTACACTAAGGGCCGAAGATAACGCGGATACCTTGGCGCTAGTATTTGA
AGCACCAAACCAGGAGAAAGTTTCAGACTATGAAATGAAGTTGATGGATTTAGAT
GTTGAACAACCTTGAATTCCAGAACAGGAGTACAGCTGTGTAGTAAAGATGCCT
TCTGGTGAATTTGCACGTATATGCCGAGATCTCAGCCATATTGGAGATGCTGTT
GTAATTTCTGTGCAAAGACGGAGTGAAATTTTCTGCAAGTGGAGAACTTGGAA
AATGGAAACATTAAATTGTCACAGACAAGTAATGTGGATAAAGAGGAGGAAGCT
GTTACCATAGAGATGAATGAACCAGTTCAACTAACTTTTGCCTGAGGTACCTGA
ACTTCTTTACAAAAGCCACTCCACTCTCTTCAACGGTGACACTCAGTATGTCTGC
AGATGTACCCCTTGTTGTAGAGTATAAAATTGCGGATATGGGACACTTAAAATAC
TACTTGGCTCCCAAGATCGAGGATGAAGAAGGATCTTAGTCTAGAGTCGAGATC
CTGAGAACTTCAGGGTGAGTTTGGGGACCCTTGATTGTTCTTTCTTTTTCGCTAT
TGTAATAATTCATGTTATATGGAGGGGGCAAAGTTTTTCAGGGTGTTGTTTAGAATG
GGAAGATGTCCCTTGTATCACCATGGACCCTCATGATAATTTTGTCTTTCACT
TTCTACTCTGTTGACAACCATTGTCTCCTCTTATTTTCTTTTCATTTTCTGTAACCT
TTTTCGTTAACTTTAGCTTGCATTTGTAACGAATTTTTAAATTCATTTTGTATT
TGTCAGATTGTAAGTACTTTCTCTAATCACTTTTTTTTCAATTCGAAGCTTGATCC
GGCTGCTAACAAAGCCCGAAAGGAAGCTGAGTTGGCTGCTGCCACCGCTGAGC
AATAACTAGCATAACCCCTTGGGGCCTCTAAACGGGTCTTGAGGGGTTTTTTGC
TGAAAGGAGGAACTATATCCGGATCTGGCGTAATAGCGAAGAGGCCCGCACCG
ATCGCCCTTCCCAACAGTTGCGCAGCCTGAATGGCGAATGGGACGCGCCCTGT
AGCGGCGCATTAAAGCGCGGGCGGGTGTGGTGGTTACGCGCAGCGTGACCGCTA

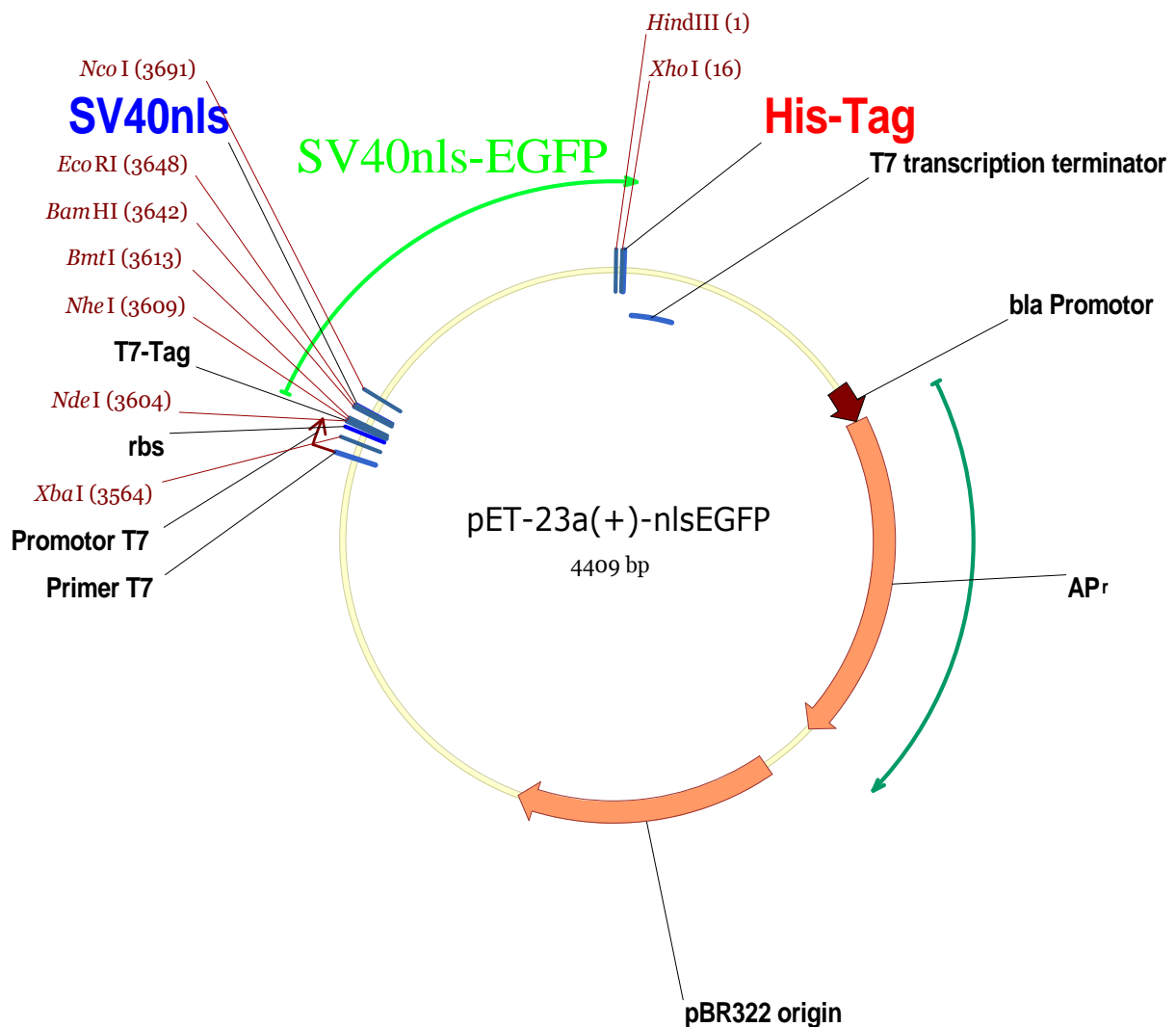
CACTTGCCAGCGCCCTAGCGCCCGCTCCTTTTCGCTTTCTTCCCTTCCTTTCTCG
CCACGTTTCGCCGGCTTTCCCGTCAAGCTCTAAATCGGGGGCTCCCTTTAGGG
TTCCGATTTAGTGCTTTACGGCACCTCGACCCCAAAAACTTGATTAGGGTGAT
GGTTCACGTAGTGGGCCATCGCCCTGATAGACGGTTTTTCGCCCTTTGACGTTG
GAGTCCACGTTCTTTAATAGTGGACTCTTGTTCCAACTGGAACAACACTCAACC
CTATCTCGGTCTATTCTTTTGATTTATAAGGGATTTTGCCGATTTTCGGCCTATTG
GTTAAAAAATGAGCTGATTTAACAAAAATTTAACGCGAATTTTAACAAAATATTAA
CGCTTACAATTTAGGTGGCACTTTTCGGGGAAATGTGCGCGGAACCCCTATTTG
TTTATTTTTCTAAATACATTCAAATATGTATCCGCTCATGAGACAATAACCCTGAT
AAATGCTTCAATAATATTGAAAAAGGAAGAGTATGAGTATTCAACATTTCCGTGT
CGCCCTTATTCCCTTTTTTGCGGCATTTTGCTTCCTGTTTTTGCTCACCCAGAA
ACGCTGGTGAAAGTAAAAGATGCTGAAGATCAGTTGGGTGCACGAGTGGGTTA
CATCGAACTGGATCTCAACAGCGGTAAGATCCTTGAGAGTTTTCGCCCCGAAGA
ACGTTTTCCAATGATGAGCACTTTTAAAGTTCTGCTATGTGGCGCGGTATTATCC
CGTATTGACGCCGGCAAGAGCAACTCGGTGCGCCGCATACACTATTCTCAGAAT
GACTTGGTTGAGTACTCACCAGTCACAGAAAAGCATCTTACGGATGGCATGACA
GTAAGAGAATTATGCAGTGCTGCCATAACCATGAGTGATAAACTGCGGCCAAC
TTACTTCTGACAACGATCGGAGGACCGAAGGAGCTAACCGCTTTTTTGACAAC
ATGGGGGATCATGTAACCTCGCCTTGATCGTTGGGAACCGGAGCTGAATGAAGC
CATACCAAACGACGAGCGTGACACCACGATGCCTGTAGCAATGGCAACAACGTT
GCGCAAACATTAACCTGGCGAACTACTTACTCTAGCTTCCCGGCAACAATTAATA
GACTGGATGGAGGCGGATAAAGTTGCAGGACCACTTCTGCGCTCGGCCCTTCC
GGCTGGCTGGTTTATTGCTGATAAATCTGGAGCCGGTGAGCGTGGGTCTCGCG
GTATCATTGCAGCACTGGGGCCAGATGGTAAGCCCTCCCGTATCGTAGTTATCT
ACACGACGGGGAGTCAGGCAACTATGGATGAACGAAATAGACAGATCGCTGAG
ATAGGTGCCTCACTGATTAAGCATTGGTAACCTGTCAGACCAAGTTTACTCATATA
TACTTTAGATTGATTTAAAACCTTCATTTTTAATTTAAAAGGATCTAGGTGAAGATC
CTTTTTGATAATCTCATGACCAAATCCCTTAACGTGAGTTTTTCGTTCCACTGAG
CGTCAGACCCCGTAGAAAAGATCAAAGGATCTTCTTGAGATCCTTTTTTTCTGCG
CGTAATCTGCTGCTTGCAAACAAAAAACCACCGCTACCAGCGGTGGTTTGT
GCCGGATCAAGAGCTACCAACTCTTTTTCCGAAGGTAACCTGGCTTCAGCAGAGC
GCAGATACCAAATACTGTTCTTCTAGTGTAGCCGTAGTTAGGCCACCACTTCAA
GAACTCTGTAGCACCGCCTACATACCTCGCTCTGCTAATCCTGTTACCAGTGGC
TGCTGCCAGTGGCGATAAGTCGTGTCTTACCGGGTTGGACTCAAGACGATAGTT

ACCGGATAAGGCGCAGCGGTCTGGGCTGAACGGGGGGTTCGTGCACACAGCCC
AGCTTGGAGCGAACGACCTACACCGAACTGAGATACCTACAGCGTGAGCTATG
AGAAAGCGCCACGCTTCCCGAAGGGAGAAAGGCGGACAGGTATCCGGTAAGC
GGCAGGGTTCGGAACAGGAGAGCGCACGAGGGAGCTTCCAGGGGGAAACGCCT
GGTATCTTTATAGTCCTGTCTGGGTTTCGCCACCTCTGACTTGAGCGTCGATTTTT
GTGATGCTCGTCAGGGGGGCGGAGCCTATGGAAAACGCCAGCAACGCGGCC
TTTTTACGGTTCCTGGCCTTTTGCTGGCCTTTTGCTCACATGTTCTTTCCTGCGT
TATCCCCTGATTCTGTGGATAACCGTATTACCGCCTTTGAGTGAGCTGATACCG
CTCGCCGCAGCCGAACGACCGAGCGCAGCGAGTCAGTGAGCGAGGAAGCGGA
AGAGCGCCCAATACGCAAACCGCCTCTCCCCGCGCGTTGGCCGATTCATTAAT
GCAGAAGGCAATCAGGGTATATTATATTGTA CTTCAGCACAGTTTTAGAGAAC

ACGTCTGCGACCTGAGCAACAACATGAATGGTCTTCGGTTTTCCGTGTTTCGTAA
AGTCTGGAAACGCGGAAGTCAGCGCCCTGCACCATTATGTTCCGGATCTGCATC
GCAGGATGCTGCTGGCTACCCTGTGGAACACCTACATCTGTATTAACGAAGCGC
TGGCATTGACCCTGAGTGATTTTTCTCTGGTCCC GCCGCATCCATACCGCCAGT
TGTTTACCCTCACAACGTTCCAGTAACCGGGCATGTTTCATCATCAGTAACCCGTA
TCGTGAGCATCCTCTCTCGTTTTCATCGGTATCATTACCCCATGAACAGAAATCC
CCCTTACACGGAGGCATCAGTGACCAAACAGGAAAAAACCGCCCTTAACATGGC
CCGCTTTATCAGAAGCCAGACATTAACGCTTCTGGAGAACTCAACGAGCTGGA
CGCGGATGAACAGGCAGACATCTGTGAATCGCTTCACGACCACGCTGATGAGC
TTTACCGCAGCTGCCTCGCGCGTTTTCGGTGATGACGGTGAAAACCTCTGACACA
TGCAGCTCCCGGAGACGGTCACAGCTTGTCTGTAAGCGGATGCCGGGAGCAGA
CAAGCCCGTCAGGGCGCGTCAGCGGGTGTGGCGGGTGTGGGGGCGCAGCCA
TGACCCAGTCACGTAGCGATAGCGGAGTGTATACTGGCTTAACTATGCGGCATC
AGAGCAGATTGTA CTGAGAGTGCACCATATATGCGGTGTGAAATACCGCACAGA
TGCGTAAGGAGAAAATACCGCATCAGGCGCTCTTCCGCTTCCTCGCTCACTGAC
TCGCTGCGCTCGGTCTCGGCTGCGGCGAGCGGTATCAGCTCACTCAAAGGC
GGTAATACGGTTATCCACAGAATCAGGGGATAACGCAGGAAAGAACATGTGAGC
AAAAGGCCAGCAAAGGCCAGGAACCGTAAAAGGCCGCGTTGCTGGCGTTTT
TCCATAGGCTCCGCCCCCTGACGAGCATCACAAAATCGACGCTCAAGTCAGA
GGTGGCGAAACCCGACAGGACTATAAAGATAACCAGGCGTTTCCCCCTGGAAGC
TCCCTCGTGCGCTCTCCTGTTCCGACCCTGCCGCTTACCGGATACCTGTCCGC
CTTTCTCCCTTCGGGAAGCGTGGCGCTTTCTCATAGCTCACGCTGTAGGTATCT
CAGTTCGGTGTAGGTCTGTTCCGCTCCAAGCTGGGCTGTGTGCACGAACCCCCCG
TTCAGCCCGACCGCTGCGCCTTATCCGGTAACTATCGTCTTGAGTCCAACCCGG
TAAGACACGACTTATCGCCACTGGCAGCAGCCACTGGTAACAGGATTAGCAGA
GCGAGGTATGTAGGCGGTGCTACAGAGTTCTTGAAGTGGTGGCCTAACTACGG
CTACACTAGAAGGACAGTATTTGGTATCTGCGCTCTGCTGAAGCCAGTTACCTT
CGGAAAAAGAGTTGGTAGCTCTTGATCCGGCAAACAAACCACCGCTGGTAGCG
GTGGTTTTTTTTGTTTGCAAGCAGCAGATTACGCGCAGAAAAAAGGATCTCAAG
AAGATCCTTTGATCTTTTCTACGGGGTCTGACGCTCAGTGAACGAAAACCTCAC
GTTAAGGGATTTTGGTCATGAGATTATCAAAAAGGATCTTACCTAGATCCTTTT
AAATTA AAAATGAAGTTTTAAATCAATCTAAAGTATATATGAGTAACTTGGTCTG
ACAGTTACCAATGCTTAATCAGTGAGGCACCTATCTCAGCGATCTGTCTATTTTCG
TTCATCCATAGTTGCCTGACTCCCCGTCGTGTAGATAACTACGATACGGGAGGG

CTTACCATCTGGCCCCAGTGCTGCAATGATACCGCGAGACCCACGCTCACCGG
CTCCAGATTTATCAGCAATAAACCAGCCAGCCGGAAGGGCCGAGCGCAGAAGT
GGTCCTGCAACTTTATCCGCCTCCATCCAGTCTATTAATTGTTGCCGGGAAGCT
AGAGTAAGTAGTTCGCCAGTTAATAGTTTGCGCAACGTTGTTGCCATTGCTGCA
GGCATCGTGGTGTACGCTCGTCGTTTGGTATGGCTTCATTGAGCTCCGGTTCC
CAACGATCAAGGCGAGTTACATGATCCCCATGTTGTGCAAAAAGCGGTTAGC
TCCTTCGGTCCTCCGATCGTTGTCAGAAGTAAGTTGGCCGCAGTGTTATCACTC
ATGGTTATGGCAGCACTGCATAATTCTCTTACTGTCATGCCATCCGTAAGATGCT
TTTCTGTGACTGGTGAGTACTCAACCAAGTCATTCTGAGAATAGTGTATGCGGC
GACCGAGTTGCTCTTGCCCGGCGTCAATACGGGATAATACCGCGCCACATAGC
AGAACTTTAAAAGTGCTCATCATTGGAAAACGTTCTTCGGGGCGAAAACCTCAA
GGATCTTACCGCTGTTGAGATCCAGTTCGATGTAACCCACTCGTGCACCCAAC
GATCTTCAGCATCTTTTACTTTCACCAGCGTTTCTGGGTGAGCAAAAACAGGAAG
GCAAAATGCCGCAAAAAGGGAATAAGGGCGACACGGAAATGTTGAATACTCAT
ACTCTTCCTTTTTCAATATTATTGAAGCATTATCAGGGTTATTGTCTCATGAGCG
GATACATATTTGAATGTATTTAGAAAAATAAACAAATAGGGGTTCCGCGCACATT
TCCCCGAAAAGTGCCACCTGAAATTGTAAACGTTAATATTTTGTAAAATTCGCG
TTAAATTTTTGTAAATCAGCTCATTTTTTAACCAATAGGCCGAAATCGGCAAAAT
CCCTTATAAATCAAAGAATAGACCGAGATAGGGTTGAGTGTTGTTCCAGTTTGG
AACAAGAGTCCACTATTAAGAACGTGGACTCCAACGTCAAAGGGCGAAAACC
GTCTATCAGGGCGATGGCCCACTACGTGAACCATCACCTAATCAAGTTTTTTG
GGTTCGAGGTGCCGTAAAGCACTAAATCGGAACCCTAAAGGGAGCCCCGATT
TAGAGCTTGACGGGGAAAGCCGGCGAACGTGGCGAGAAAGGAAGGAAGAAA
GCGAAAGGAGCGGGCGCTAGGGCGCTGGCAAGTGTAGCGGTCACGCTGCGCG
TAACCACCACACCCGCCGCGCTTAATGCGCCGCTACAGGGCGCGTCCCATTCC
CCA

9.1.3 pET 23a(+)-SV40nls-EGFP



Scheme 9.3: Plasmid pET-23a(+)-SV40nls-EGFP

Base Sequence:

```

AGCTTGCGGCCGCACTCGAGCACCACCACCACCACCAGATCCGGCTGCT
AACAAAGCCCGAAAGGAAGCTGAGTTGGCTGCTGCCACCGCTGAGCAATAACT
AGCATAACCCCTTGGGGCCTCTAAACGGGTCTTGAGGGGTTTTTTGCTGAAAGG
AGGAACTATATCCGGATTGGCGAATGGGACGCGCCCTGTAGCGGCGCATTAAAG
CGCGGCGGGTGTGGTGGTTACGCGCAGCGTGACCGCTACACTTGCCAGCGCC
CTAGCGCCCGCTCCTTTCGCTTTCTTCCCTTCTTTCTCGCCACGTTCCGCCGGC
TTTCCCGTCAAGCTCTAAATCGGGGGCTCCCTTTAGGGTTCGATTTAGTGCT
TTACGGCACCTCGACCCCAAAAACTTGATTAGGGTGATGGTTCACGTAGTGGG
CCATCGCCCTGATAGACGGTTTTTTCGCCCTTGACGTTGGAGTCCACGTTCTTT
AATAGTGGACTCTTGTTCCAAACTGGAACAACACTCAACCCTATCTCGGTCTATT

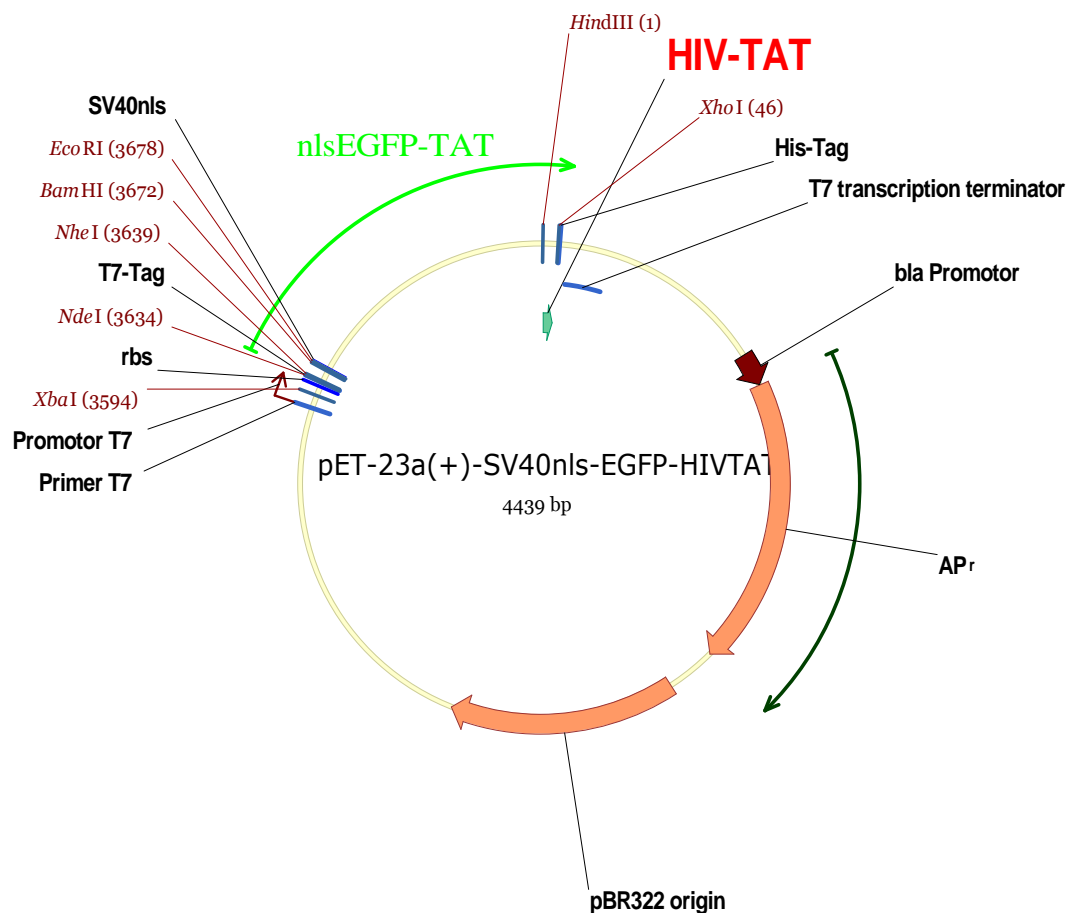
```

CTTTTGATTTATAAGGGATTTTGCCGATTTTCGGCCTATTGGTTAAAAAATGAGCT
GATTTAACAAAAATTTAACGCGAATTTTAACAAAATATTAACGTTTACAATTTTCAG
GTGGCACTTTTCGGGGAAATGTGCGCGGAACCCCTATTTGTTTATTTTTCTAAAT
ACATTCAAATATGTATCCGCTCATGAGACAATAACCCTGATAAATGCTTCAATAAT
ATTGAAAAAGGAAGAGTATGAGTATTCAACATTTCCGTGTCGCCCTTATTCCCTT
TTTTGCGGCATTTTGCCTTCTGTTTTTGTCTACCCAGAAACGCTGGTGAAAGTA
AAAGATGCTGAAGATCAGTTGGGTGCACGAGTGGGTACATCGAACTGGATCTC
AACAGCGGTAAGATCCTTGAGAGTTTTTCGCCCGAAGAACGTTTTCCAATGATG
AGCACTTTTAAAGTTCTGCTATGTGGCGCGGTATTATCCCGTATTGACGCCGGG
CAAGAGCAACTCGGTCGCCGCATACACTATTCTCAGAATGACTTGGTTGAGTAC
TCACCAGTCACAGAAAAGCATCTTACGGATGGCATGACAGTAAGAGAATTATGC
AGTGCTGCCATAACCATGAGTGATAAACTGCGGCCAACTTACTTCTGACAACG
ATCGGAGGACCGAAGGAGCTAACCGCTTTTTTGCACAACATGGGGGATCATGTA
ACTCGCCTTGATCGTTGGGAACCGGAGCTGAATGAAGCCATACCAAACGACGA
GCGTGACACCACGATGCCTGCAGCAATGGCAACAACGTTGCGCAAACATTAAC
TGCGGAACTACTTACTCTAGCTTCCCGGCAACAATTAATAGACTGGATGGAGGC
GGATAAAGTTGCAGGACCACTTCTGCGCTCGGCCCTTCCGGCTGGCTGGTTTAT
TGCTGATAAATCTGGAGCCGGTGAGCGTGGGTCTCGCGGTATCATTGCAGCAC
TGGGGCCAGATGGTAAGCCCTCCCGTATCGTAGTTATCTACACGACGGGGAGT
CAGGCAACTATGGATGAACGAAATAGACAGATCGCTGAGATAGGTGCCTCACTG
ATTAAGCATTGGTAACTGTCAGACCAAGTTTACTCATATATACTTTAGATTGATTT
AAAACCTCATTTTTTAATTTAAAAGGATCTAGGTGAAGATCCTTTTTGATAATCTCA
TGACCAAATCCCTTAACGTGAGTTTTTCGTTCCACTGAGCGTCAGACCCCGTAG
AAAAGATCAAAGGATCTTCTTGAGATCCTTTTTTTCTGCGCGTAATCTGCTGCTT
GCAAACAAAAAACCACCGCTACCAGCGGTGGTTTGTGGCCGGATCAAGAGCT
ACCAACTCTTTTTCCGAAGGTAACCTGGCTTACAGCAGAGCGCAGATACCAAATAC
TGTCTTCTAGTGTAGCCGTAGTTAGGCCACCACTTCAAGAACTCTGTAGCACC
GCCTACATACCTCGCTCTGCTAATCCTGTTACCAGTGGCTGCTGCCAGTGGCGA
TAAGTCGTGTCTTACCGGGTTGGACTCAAGACGATAGTTACCGGATAAGGCGCA
GCGGTCCGGCTGAACGGGGGGTTCGTGCACACAGCCAGCTTGGAGCGAACG
ACCTACACCGAACTGAGATACCTACAGCGTGAGCTATGAGAAAGCGCCACGCTT
CCCGAAGGGAGAAAGGCGGACAGGTATCCGGTAAGCGGCAGGGTCGGAACAG
GAGAGCGCACGAGGGAGCTTCCAGGGGGAAACGCCTGGTATCTTTATAGTCCT
GTCGGGTTTTCGCCACCTCTGACTTGAAGCGTCGATTTTTGTGATGCTCGTCAGGG

GGGCGGAGCCTATGGAAAAACGCCAGCAACGCGGCCTTTTTACGGTTCCTGGC
CTTTTGCTGGCCTTTTGCTCACATGTTCTTTCCTGCGTTATCCCCTGATTCTGTG
GATAACCGTATTACCGCCTTTGAGTGAGCTGATACCGCTCGCCGCAGCCGAAC
GACCGAGCGCAGCGAGTCAGTGAGCGAGGAAGCGGAAGAGCGCCTGATGCGG
TATTTTCTCCTTACGCATCTGTGCGGTATTTACACCCGCATATATGGTGCACTCT
CAGTACAATCTGCTCTGATGCCGCATAGTTAAGCCAGTATACTCCGCTATCG
CTACGTGACTGGGTCATGGCTGCGCCCCGACACCCGCCAACACCCGCTGACGC
GCCCTGACGGGCTTGTCTGCTCCCGGCATCCGCTTACAGACAAGCTGTGACCG
TCTCCGGGAGCTGCATGTGTCAGAGGTTTTACCGTCATCACCGAAACGCGCG
AGGCAGCTGCGGTAAAGCTCATCAGCGTGGTCGTGAAGCGATTCACAGATGTC
TGCTGTTTCATCCGCGTCCAGCTCGTTGAGTTTCTCCAGAAGCGTTAATGTCTG
GCTTCTGATAAAGCGGGCCATGTTAAGGGCGGTTTTTTCCTGTTTGGTCACTGA
TGCTCCGTGTAAGGGGGATTTCTGTTTCATGGGGGTAATGATACCGATGAAACG
AGAGAGGATGCTCACGATACGGGTTACTGATGATGAACATGCCCGGTTACTGGA
ACGTTGTGAGGGTAAACAACCTGGCGGTATGGATGCGGGCGGGACCAGAGAAAA
TCACTCAGGGTCAATGCCAGCGCTTCGTTAATACAGATGTAGGTGTTCCACAGG
GTAGCCAGCAGCATCCTGCGATGCAGATCCGGAACATAATGGTGCAGGGCGCT
GACTTCCGCGTTTTCCAGACTTTACGAAACACGGAAACCGAAGACCATTTCATGTT
GTTGCTCAGGTCGCAGACGTTTTGCAGCAGCAGTCGCTTACGTTTCGCTCGCG
TATCGGTGATTCATTCTGCTAACCAGTAAGGCAACCCCGCCAGCCTAGCCGGGT
CCTCAACGACAGGAGCACGATCATGCGCACCCGTGGCCAGGACCCAACGCTGC
CCGAGATCTCGATCCCGCGAAATTAATACGACTCACTATAGGGAGACCACAACG
GTTTCCCTCTAGAAATAATTTTGTTTAACTTTAAGAAGGAGATATACATATGGCTA
GCATGACTGGTGGACAGCAAATGGGTGCGGGATCCGAATTCCTGAAGAAGAAG
CGCAAAGTACTGGTACCGGTCGCCACCATGGTGAGCAAGGGCGAGGAGCTGTT
CACCGGGGTGGTGCCCATCCTGGTTCGAGCTGGACGGCGACGTAAACGGCCAC
AAGTTCAGCGTGTCCGGCGAGGGCGAGGGCGATGCCACCTACGGCAAGCTGA
CCCTGAAGTTCATCTGCACCACCGGCAAGCTGCCCGTGCCCTGGCCCACCCTC
GTGACCACCCTGACCTACGGCGTGCAGTGCTTCAGCCGCTACCCCGACCACAT
GAAGCAGCACGACTTCTTCAAGTCCGCCATGCCCGAAGGCTACGTCCAGGAGC
GCACCATCTTCTTCAAGGACGACGGCAACTACAAGACCCGCGCCGAGGTGAAG
TTCGAGGGCGACACCCTGGTGAACCGCATCGAGCTGAAGGGCATCGACTTCAA
GGAGGACGGCAACATCCTGGGGCACAAGCTGGAGTACAACACTACAACAGCCACA
ACGTCTATATCATGGCCGACAAGCAGAAGAACGGCATCAAGGCCAACTTCAAGA

TCCGCCACAACATCGAGGACGGCAGCGTGCAGCTCGCCGACCACTACCAGCAG
AACACCCCCATCGGCGACGGCCCCGTGCTGCTGCCCGACAACCACTACCTGAG
CACCCAGTCCGCCCTGAGCAAAGACCCCAACGAGAAGCGCGATCACATGGTCC
TGCTGGAGTTCGTGACCGCCGCCGGGATCACTCTCGGCATGGACGAGCTTTAC
AAGA

9.1.4 pET 23a(+)-SV40nls-EGFP-HIVTAT



Scheme 9.4: Plasmid pET-23a(+)-SV40nls-EGFP-HIVTAT

Base Sequence:

AGCTTGGTTATGGGCGCAAAAACGCCGTGAGCGCCGTCGGGGCCTCGAGCAC
CACCACCACCACCACTGAGATCCGGCTGCTAACAAAGCCCGAAAGGAAGCTGA
GTTGGCTGCTGCCACCGCTGAGCAATAACTAGCATAACCCCTTGGGGCCTCTAA
ACGGGTCTTGAGGGGTTTTTGGCTGAAAGGAGGAAGTATATCCGGATTGGCGAA
TGGGACGCGCCCTGTAGCGGCGCATTAAAGCGCGGCGGGTGTGGTGGTTACGC
GCAGCGTGACCGCTACACTTGCCAGCGCCCTAGCGCCCGCTCCTTTTCGCTTTC

TTCCCTTCCTTTCTCGCCACGTTTCGCCGGCTTTCCCCGTCAAGCTCTAAATCGG
GGGCTCCCTTTAGGGTTCCGATTTAGTGCTTTACGGCACCTCGACCCCAAAAA
CTTGATTAGGGTGATGGTTCACGTAGTGGGCCATCGCCCTGATAGACGGTTTTT
CGCCCTTTGACGTTGGAGTCCACGTTCTTTAATAGTGGACTCTTGTTCCAAACTG
GAACAACACTCAACCCTATCTCGGTCTATTCTTTTGATTTATAAGGGATTTTGCC
GATTTTCGGCCTATTGGTTAAAAAATGAGCTGATTTAACAAAAATTTAACGCGAAT
TTTAACAAAATATTAACGTTTACAATTTTCAGGTGGCACTTTTCGGGGAAATGTGC
GCGGAACCCCTATTTGTTTATTTTTCTAAATACATTCAAATATGTATCCGCTCATG
AGACAATAACCCTGATAAATGCTTCAATAATATTGAAAAAGGAAGAGTATGAGTA
TTCAACATTTCCGTGTCGCCCTTATTCCCTTTTTTGCGGCATTTTGCCTTCCTGTT
TTTGCTCACCCAGAAACGCTGGTGAAAGTAAAAGATGCTGAAGATCAGTTGGGT
GCACGAGTGGGTACATCGAACTGGATCTCAACAGCGGTAAGATCCTTGAGAGT
TTTCGCCCCGAAGAACGTTTTCCAATGATGAGCACTTTTAAAGTTCTGCTATGTG
GCGCGGTATTATCCCGTATTGACGCCGGCAAGAGCAACTCGGTGCGCCGCATA
CACTATTCTCAGAATGACTTGGTTGAGTACTACCAGTCACAGAAAAGCATCTTA
CGGATGGCATGACAGTAAGAGAATTATGCAGTGCTGCCATAACCATGAGTGATA
ACACTGCGGCCAACTTACTTCTGACAACGATCGGAGGACCGAAGGAGCTAACC
GCTTTTTTGCACAACATGGGGGATCATGTAACCTCGCCTTGATCGTTGGGAACCG
GAGCTGAATGAAGCCATACCAAACGACGAGCGTGACACCACGATGCCTGCAGC
AATGGCAACAACGTTGCGCAAACCTATTAACCTGGCGAACTACTTACTCTAGCTTCC
CGGCAACAATTAATAGACTGGATGGAGGCGGATAAAGTTGCAGGACCACTTCTG
CGCTCGGCCCTTCCGGCTGGCTGGTTTATTGCTGATAAATCTGGAGCCGGTGA
GCGTGGGTCTCGCGGTATCATTGCAGCACTGGGGCCAGATGGTAAGCCCTCCC
GTATCGTAGTTATCTACACGACGGGGAGTCAGGCAACTATGGATGAACGAAATA
GACAGATCGCTGAGATAGGTGCCTCACTGATTAAGCATTGGTAACTGTCAGACC
AAGTTTACTCATATATACTTTAGATTGATTTAAAACCTTCATTTTTAATTTAAAAGGA
TCTAGGTGAAGATCCTTTTTGATAATCTCATGACCAAATCCCTTAACGTGAGTT
TTCGTTCCACTGAGCGTCAGACCCCGTAGAAAAGATCAAAGGATCTTCTTGAGA
TCCTTTTTTTCTGCGCGTAATCTGCTGCTTGCAAACAAAAAAACCACCGCTACCA
GCGGTGGTTTGTGGCCGATCAAGAGCTACCAACTCTTTTTCCGAAGGTAAC
GGCTTCAGCAGAGCGCAGATAACCAAATACTGTCCTTCTAGTGTAGCCGTAGTTA
GGCCACCACTTCAAGAACTCTGTAGCACCGCCTACATACCTCGCTCTGCTAATC
CTGTTACCAGTGGCTGCTGCCAGTGGCGATAAGTCGTGTCTTACCGGGTTGGA
CTCAAGACGATAGTTACCGGATAAGGCGCAGCGGTGCGGGCTGAACGGGGGGTT

CGTGCACACAGCCCAGCTTGGAGCGAACGACCTACACCGAACTGAGATACCTA
CAGCGTGAGCTATGAGAAAGCGCCACGCTTCCCGAAGGGAGAAAGGCGGACA
GGTATCCGGTAAGCGGCAGGGTCGGAACAGGAGAGCGCACGAGGGAGCTTCC
AGGGGGAAACGCCTGGTATCTTTATAGTCCTGTCTGGGTTTCGCCACCTCTGACT
TGAGCGTCGATTTTTGTGATGCTCGTCAGGGGGGCGGAGCCTATGGAAAAACG
CCAGCAACGCGGCCTTTTTACGGTTCCTGGCCTTTTGCTGGCCTTTTGCTCACA
TGTTCTTTCCTGCGTTATCCCCTGATTCTGTGGATAACCGTATTACCGCCTTTGA
GTGAGCTGATACCGCTCGCCGCAGCCGAACGACCGAGCGCAGCGAGTCAGTG
AGCGAGGAAGCGGAAGAGCGCCTGATGCGGTATTTTCTCCTTACGCATCTGTG
CGGTATTTACACCCGCATATATGGTGCACCTCTCAGTACAATCTGCTCTGATGCC
GCATAGTTAAGCCAGTATACTCCGCTATCGCTACGTGACTGGGTCATGGCTG
CGCCCCGACACCCGCCAACACCCGCTGACGCGCCCTGACGGGCTTGTCTGCT
CCCGGCATCCGCTTACAGACAAGCTGTGACCGTCTCCGGGAGCTGCATGTGTC
AGAGGTTTTACCGTCATCACCGAAACGCGCGAGGCAGCTGCGGTAAAGCTCA
TCAGCGTGGTCGTGAAGCGATTACAGATGTCTGCCTGTTTCATCCGCGTCCAGC
TCGTTGAGTTTCTCCAGAAGCGTTAATGTCTGGCTTCTGATAAAGCGGGCCATG
TTAAGGGCGGTTTTTTCCTGTTTGGTCACTGATGCCTCCGTGTAAGGGGGATTT
CTGTTTCATGGGGGTAATGATACCGATGAAACGAGAGAGGATGCTCACGATACG
GGTTACTGATGATGAACATGCCCGTTACTGGAACGTTGTGAGGGTAAACA
GGCGGTATGGATGCGGCGGGACCAGAGAAAAATCACTCAGGGTCAATGCCAGC
GCTTCGTTAATACAGATGTAGGTGTTCCACAGGGTAGCCAGCAGCATCCTGCGA
TGCAGATCCGGAACATAATGGTGCAGGGCGCTGACTTCCGCGTTTCCAGACTTT
ACGAAACACGGAAACCGAAGACCATTTCATGTTGTTGCTCAGGTCGCAGACGTTT
TGCAGCAGCAGTCGCTTACGTTTCGCTCGCGTATCGGTGATTCATTCTGCTAAC
CAGTAAGGCAACCCCGCCAGCCTAGCCGGGTCTCAACGACAGGAGCACGATC
ATGCGCACCCGTGGCCAGGACCCAACGCTGCCCGAGATCTCGATCCCGCGAAA
TTAATACGACTCACTATAGGGAGACCACAACGGTTTTCCCTCTAGAAATAATTTTG
TTTAACTTTAAGAAGGAGATATACATATGGCTAGCATGACTGGTGGACAGCAAAT
GGGTCGCGGATCCGAATTCCCGAAGAAGAAGCGCAAAGTACTGGTACCGGTCCG
CCACCATGGTGAGCAAGGGCGAGGAGCTGTTACCGGGGTGGTGCCCATCCT
GGTCGAGCTGGACGGCGACGTAAACGGCCACAAGTTCAGCGTGTCCGGCGAG
GGCGAGGGCGATGCCACCTACGGCAAGCTGACCCTGAAGTTCATCTGCACCAC
CGGCAAGCTGCCCGTGCCCTGGCCCACCCTCGTGACCACCCTGACCTACGGC
GTGCAGTGCTTCAGCCGCTACCCCGACCACATGAAGCAGCACGACTTCTTCAA

GTCCGCCATGCCCCGAAGGCTACGTCCAGGAGCGCACCATCTTCTTCAAGGACG
ACGGCAACTACAAGACCCGCGCCGAGGTGAAGTTCGAGGGCGACACCCTGGT
GAACCGCATCGAGCTGAAGGGCATCGACTTCAAGGAGGACGGCAACATCCTGG
GGCACAAGCTGGAGTACAACAGCCACAACGTCTATATCATGGCCGACA
AGCAGAAGAACGGCATCAAGGCCAACTTCAAGATCCGCCACAACATCGAGGAC
GGCAGCGTGCAGCTCGCCGACCACTACCAGCAGAACACCCCATCGGGCAGC
GCCCCGTGCTGCTGCCCCGACAACCACTACCTGAGCACCCAGTCCGCCCTGAGC
AAAGACCCCAACGAGAAGCGCGATCACATGGTCCTGCTGGAGTTCGTGACCGC
CGCCGGGATCACTCTCGGCATGGACGAGCTTTACAAGA

9.2 Amino acid sequences

9.2.1 SV40nls-EGFP

MASMTGGQQMGRGSEFPKKRKRKVLVPVATMVSKGEELFTGVVPILVELDGDVNGH
KFSVSGEGEGDATYGKLTCLKFICTTGKLPVPWPTLVTTLTYGVCFSRYPDHMKQH
DFFKSAMPEGYVQERTIFFKDDGNYKTRAEVKFEGDTLVNRIELKGIDFKEDGNILG
HKLEYNYNSHNVYIMADKQKNGIKANFKIRHNIEDGSVQLADHYQQNTPIGDGPVLL
PDNHYLSTQSALSKDPNEKRDHMLLEFVTAAGITLGMDELYKKLAAALEHHHHHH

9.2.2 SV40nls-EGFP-HIVTAT

MASMTGGQQMGRGSEFPKKRKRKVLVPVATMVSKGEELFTGVVPILVELDGDVNGH
KFSVSGEGEGDATYGKLTCLKFICTTGKLPVPWPTLVTTLTYGVCFSRYPDHMKQH
DFFKSAMPEGYVQERTIFFKDDGNYKTRAEVKFEGDTLVNRIELKGIDFKEDGNILG
HKLEYNYNSHNVYIMADKQKNGIKANFKIRHNIEDGSVQLADHYQQNTPIGDGPVLL
PDNHYLSTQSALSKDPNEKRDHMLLEFVTAAGITLGMDELYKKLGYGRKKRRRQR
RGLEHHHHHH

9.2.3 β -galactosidase

MTMITDSLAVVLQRRDWENPGVTQLNRLAAHPPFASWRNSEEARTDRPSQQLRSL
NGEWRFAWFPAPEAVPESWLECDLPEADTVVPSNWQMHGYDAPIYTNVTYPITV
NPPFVPTENPTGCYSLTFNVDES WLQEGQTRIIFDGVNSAFHLWCNGRWVGYGQD
SRLPSEFDLSAFLRAGENRLAVMVLRWSDGSYLEDQDMWRMSGIFRDVSLHKPT

TQISDFHVATR FNDDFSRAVLEAEVQMC GELRDYLRVTVSLWQGETQVASGTAPF
GGEIIDERGGYADRVT LRLNVENPKLWSAEIPNLYRAVVELHTADGTLIEAEACDVG
FREVRIENGLLLLNGKPLLIRGVNRHEHHPLHGQVMDEQTMVQDILLMKQNNFNAV
RCSHYPNHPLWYTLCDRYGLYVVDEANIETHGMVPMNRLTDDPRWLPAMSERVTR
MVQRDRNHPSVIIWSLGNESGHGANHDALYRWIKSVDPSPRPVQYEGGGADTTATD
IICPMYARVDEDQPFP AVPKWSIKKWLSLPGETRPLILCEYAHAMGNSLGGFAKYW
QAFRQYPRLQGGFVWDWVDQSLIKYDENG NPWSAYGGDFGDTPNDRQFCMNGL
VFADRTPHPALTEAKHQQQFFQFRLSGQTIEVTSEYLF RHSDNELLHWMVALDGKP
LASGEVPLDVAPQGKQLIELPELPQPESAGQLWLTVRVVQPNATAWSEAGHISAW
QQWRLAENLSVTLP AASHAIPHLTTSEMDFCIELGNKRWQFN RQSGFLSQMWIGD
KKQLLTPLRDQFTRAPLDNDIGVSEATR IDPNAWVERWKAAGHYQAEAALLQCTAD
TLADAVLITTAHAWQH QGKTLFISRKTYRIDGSGQMAITVDVEVASDTPHPARIGLNC
QLAQVAERVNWLGLGPQENYPDRLTAACFDRWDLPLSDMYTPYVFPS ENGLRCG
TRELNYGPHQWRGDFQFNISRYSSQQQLMETSHRHLLHAE EGTWLNIDGFHMGIGG
DDSWSPSVSAEFQLSAGRYHYQLVWCQK

9.3 Analytic spectra

9.3.1 Alkyne hemicyanine dye

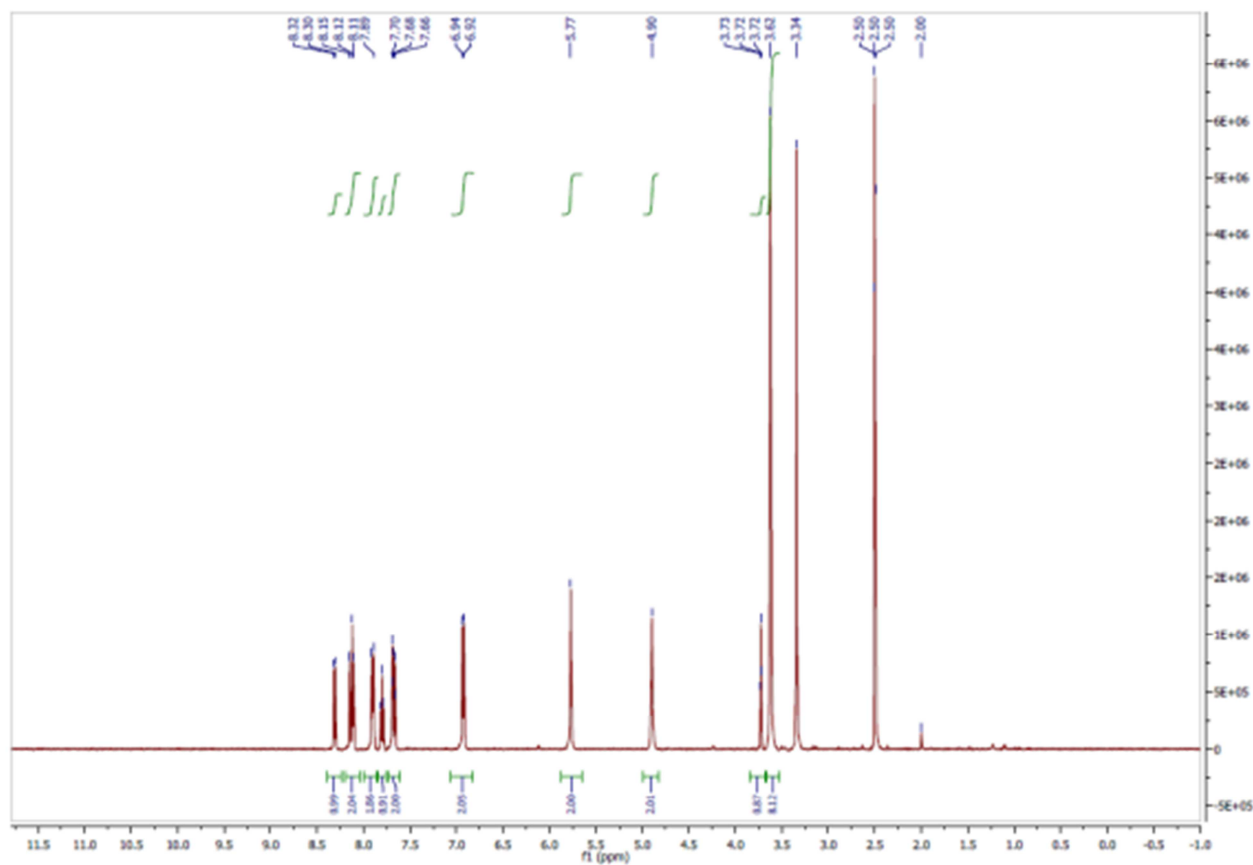


Figure 9.1: ^1H NMR of 2-[2-(4-Dihydroxyethylamino-phenyl)-vinyl]-3-prop-2-ynyl-benzothiazol-3-ium bromide 12.

9.3.2 AzMMMan linker

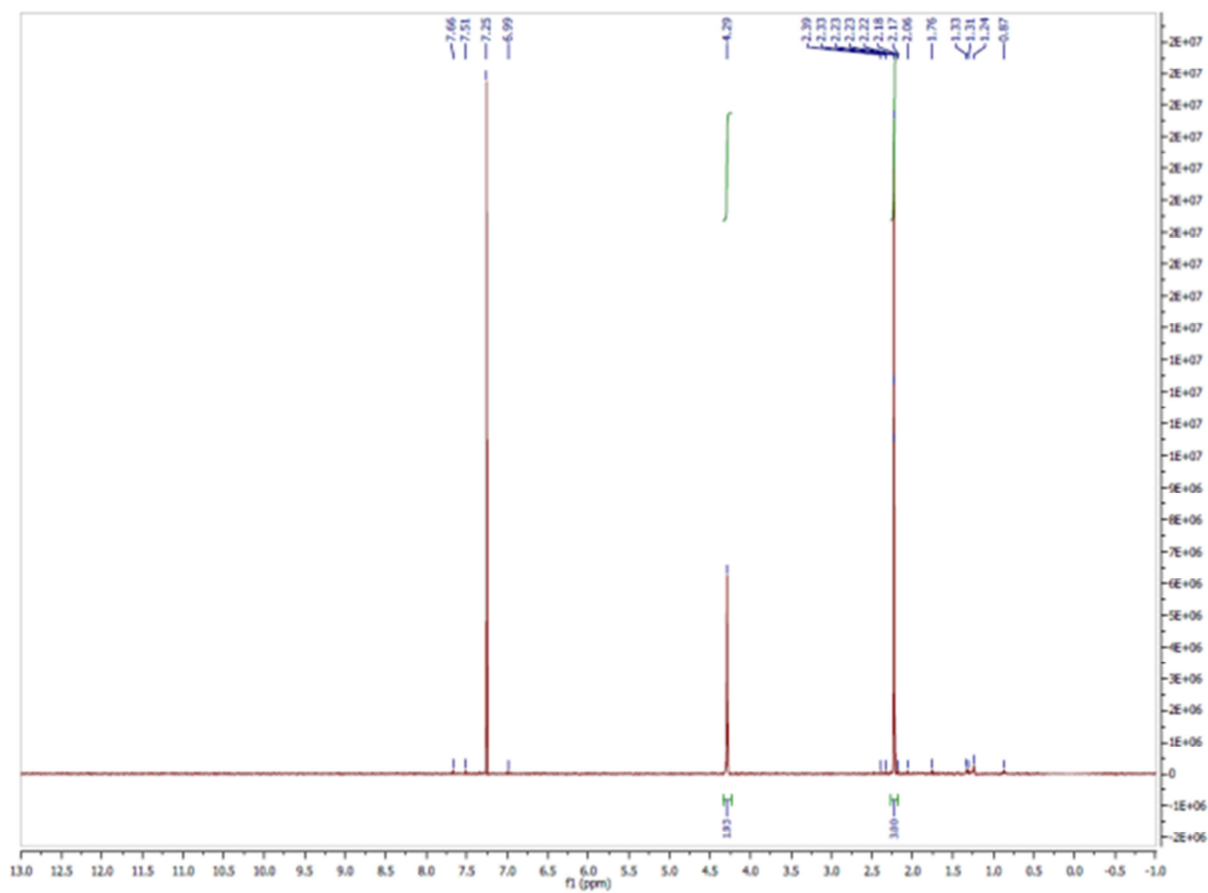


Figure 9.2: ¹H NMR of 3-(azidomethyl)-4-methyl-2,5-furandione.

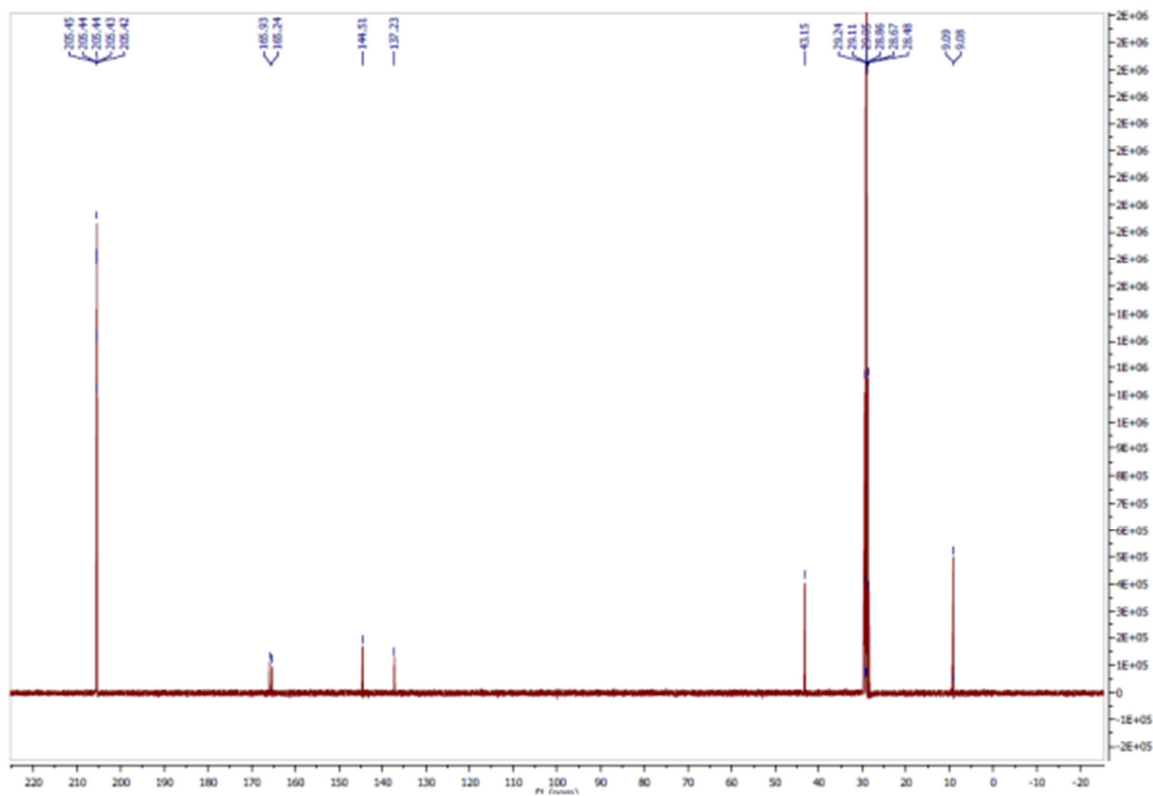


Figure 9.3: ^{13}C NMR of 3-(azidomethyl)-4-methyl-2,5-furandione.

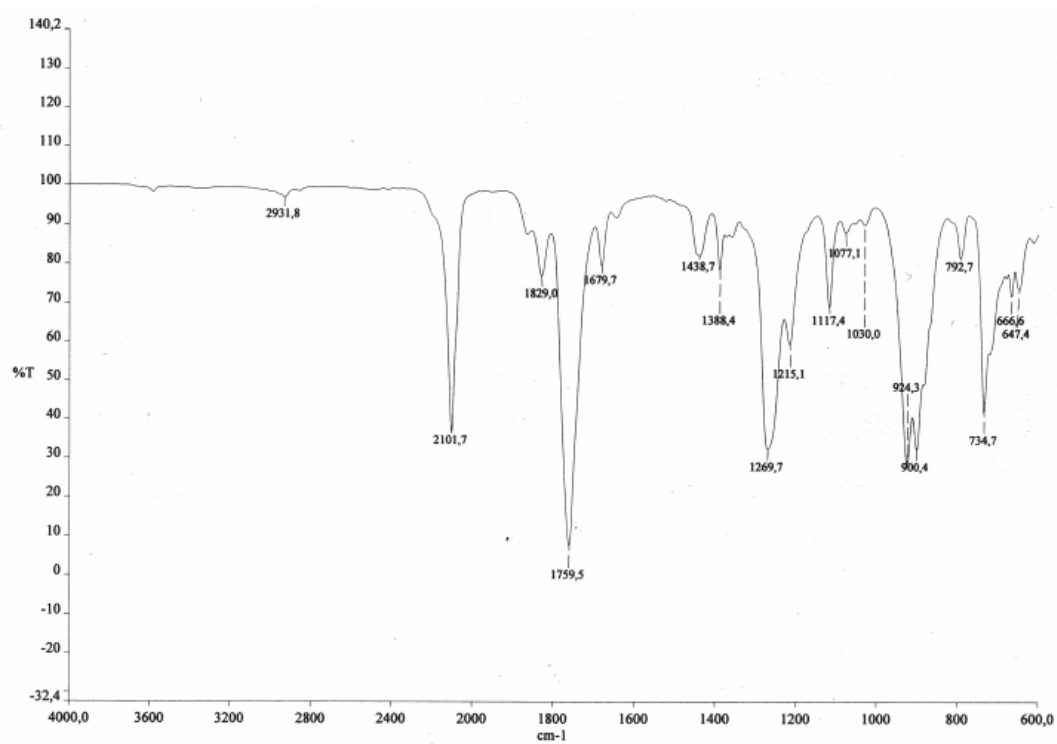


Figure 9.4: IR spectrum of 3-(azidomethyl)-4-methyl-2,5-furandione.

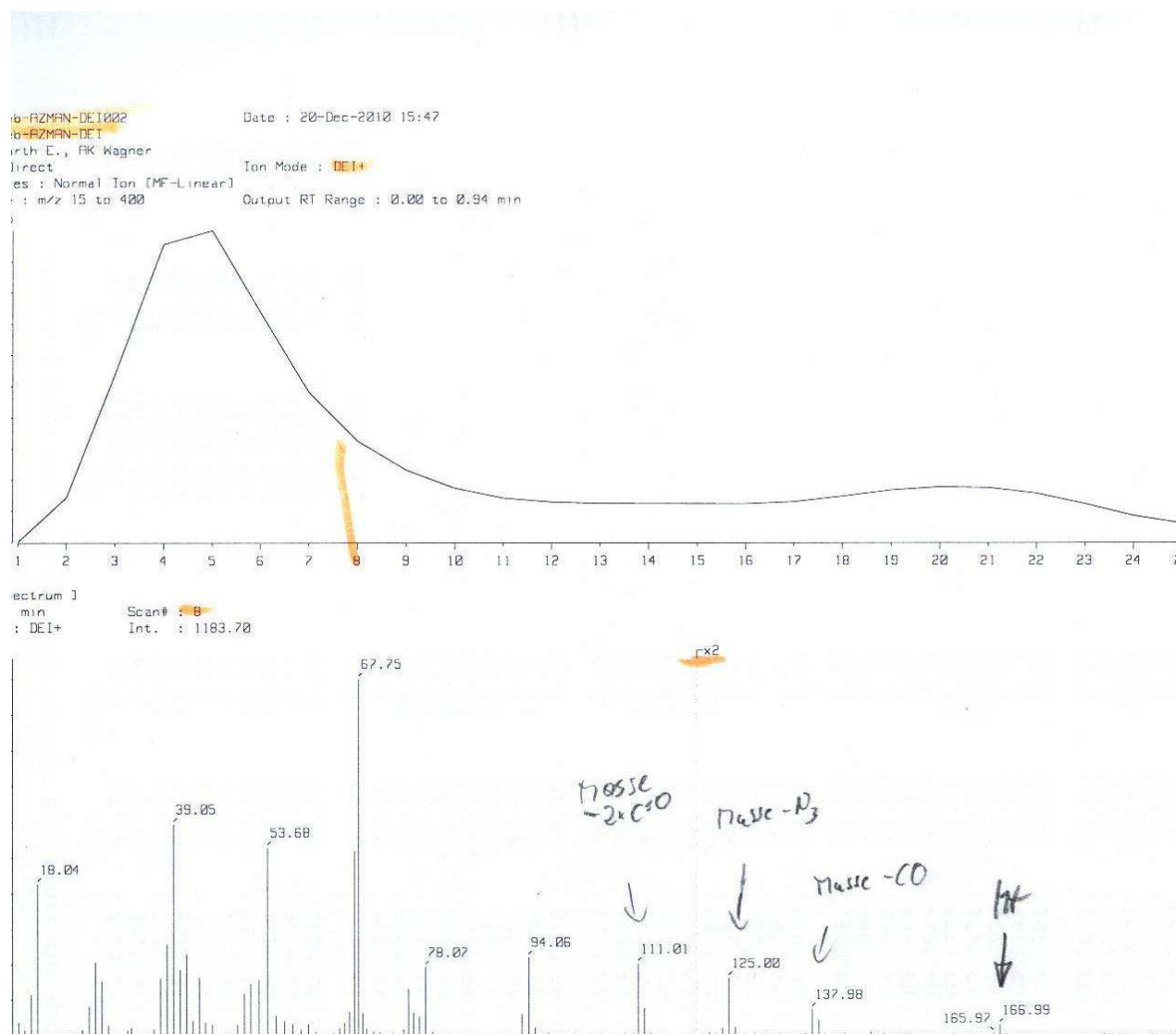


Figure 9.5: DE1⁺ mass spectra of AzMMMan.

9.3.3 PentyneMMan linker

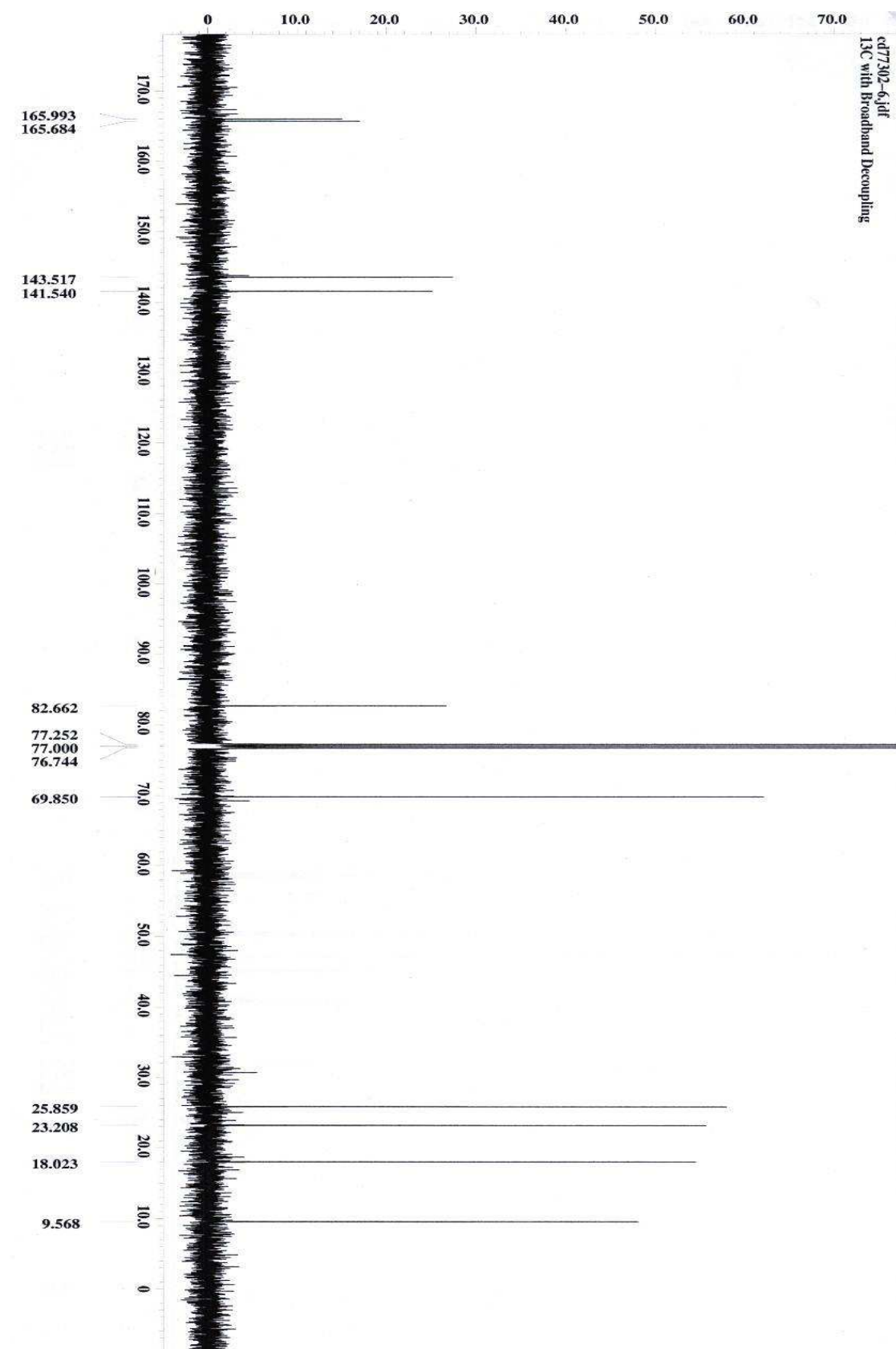


Figure 9.6: ^{13}C NMR of PentyneMMan.

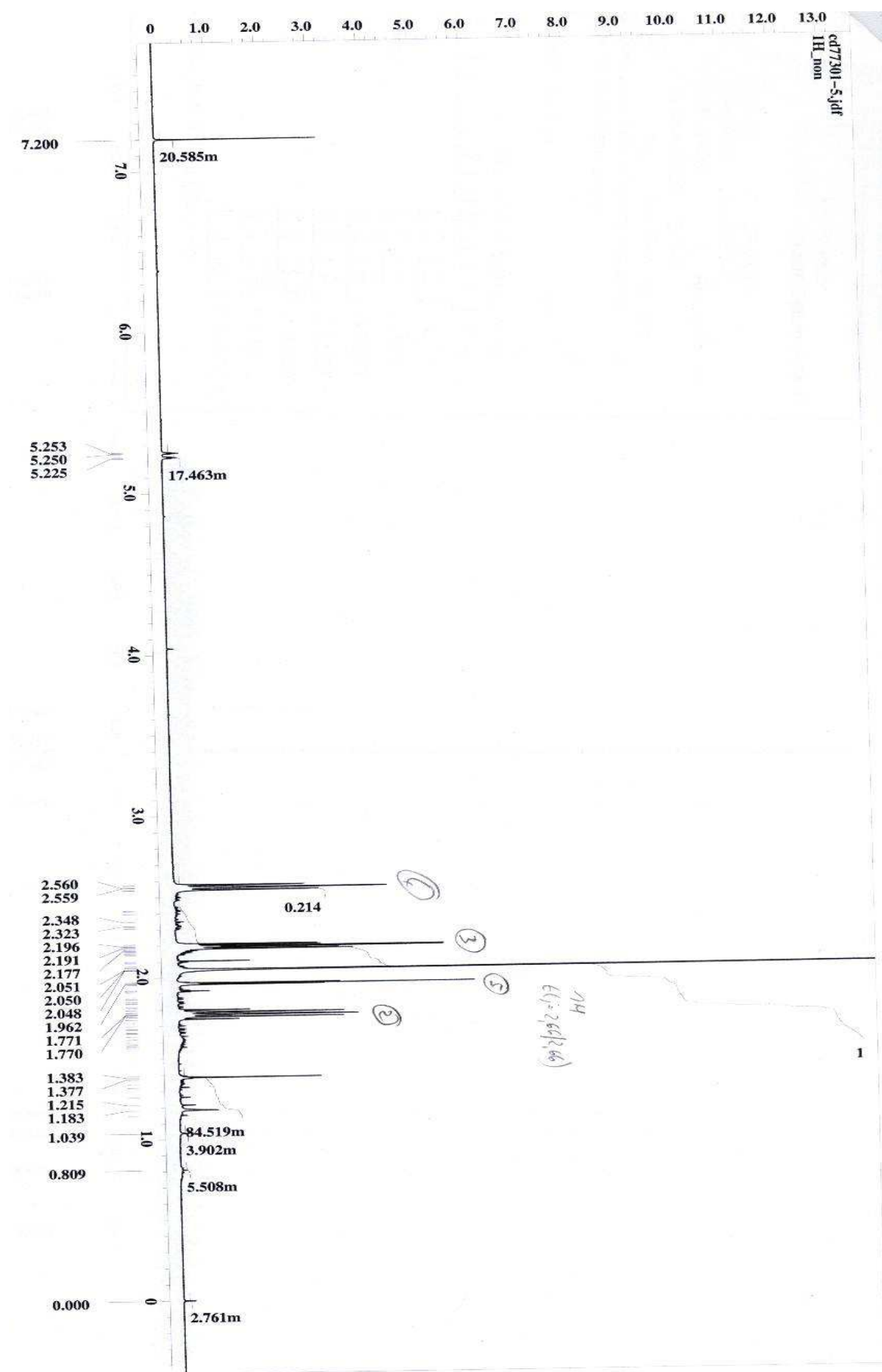


Figure 9.7: ¹H NMR of PentyneMMan

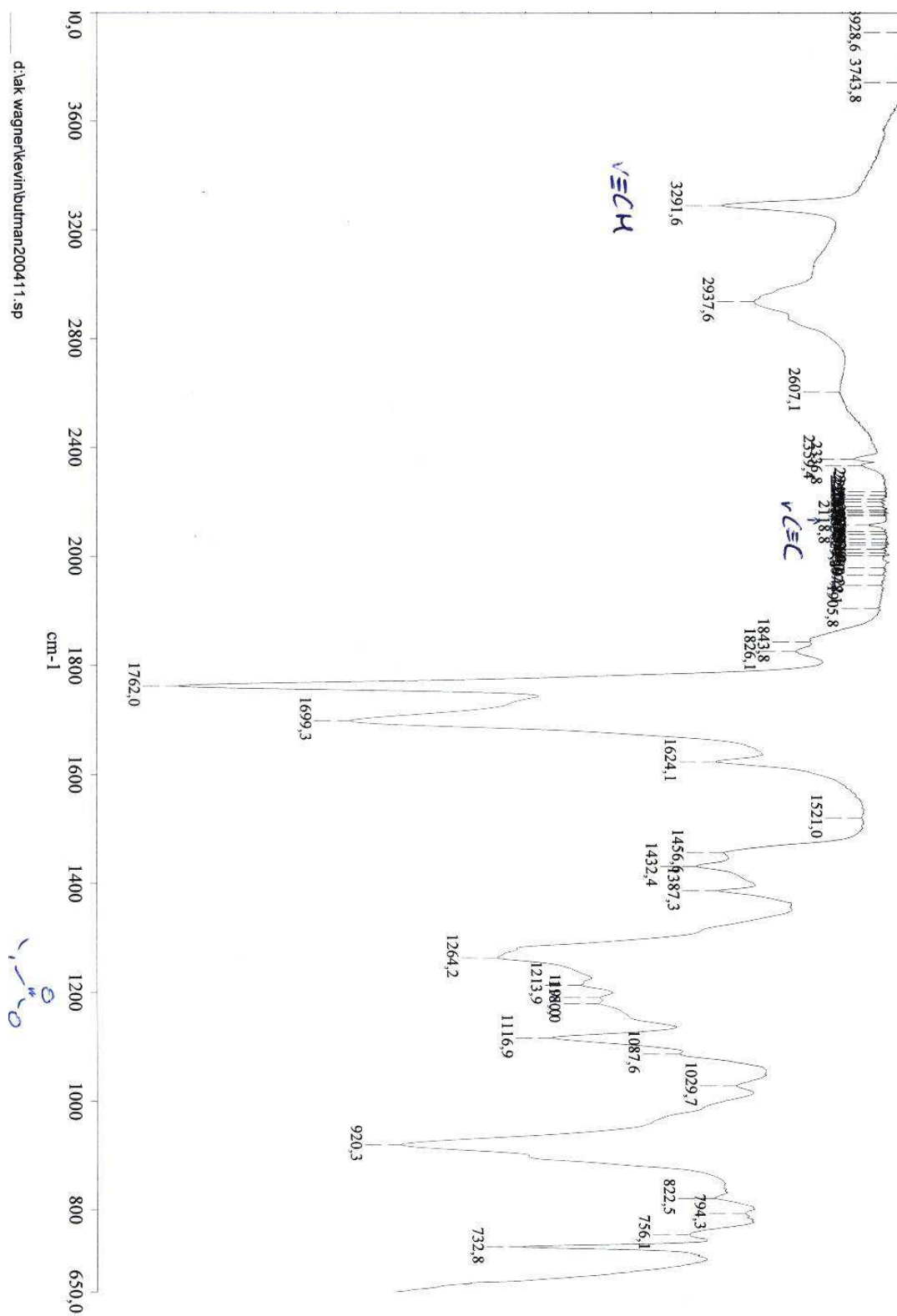


Figure 9.8: IR spectra of PentyneMMan.

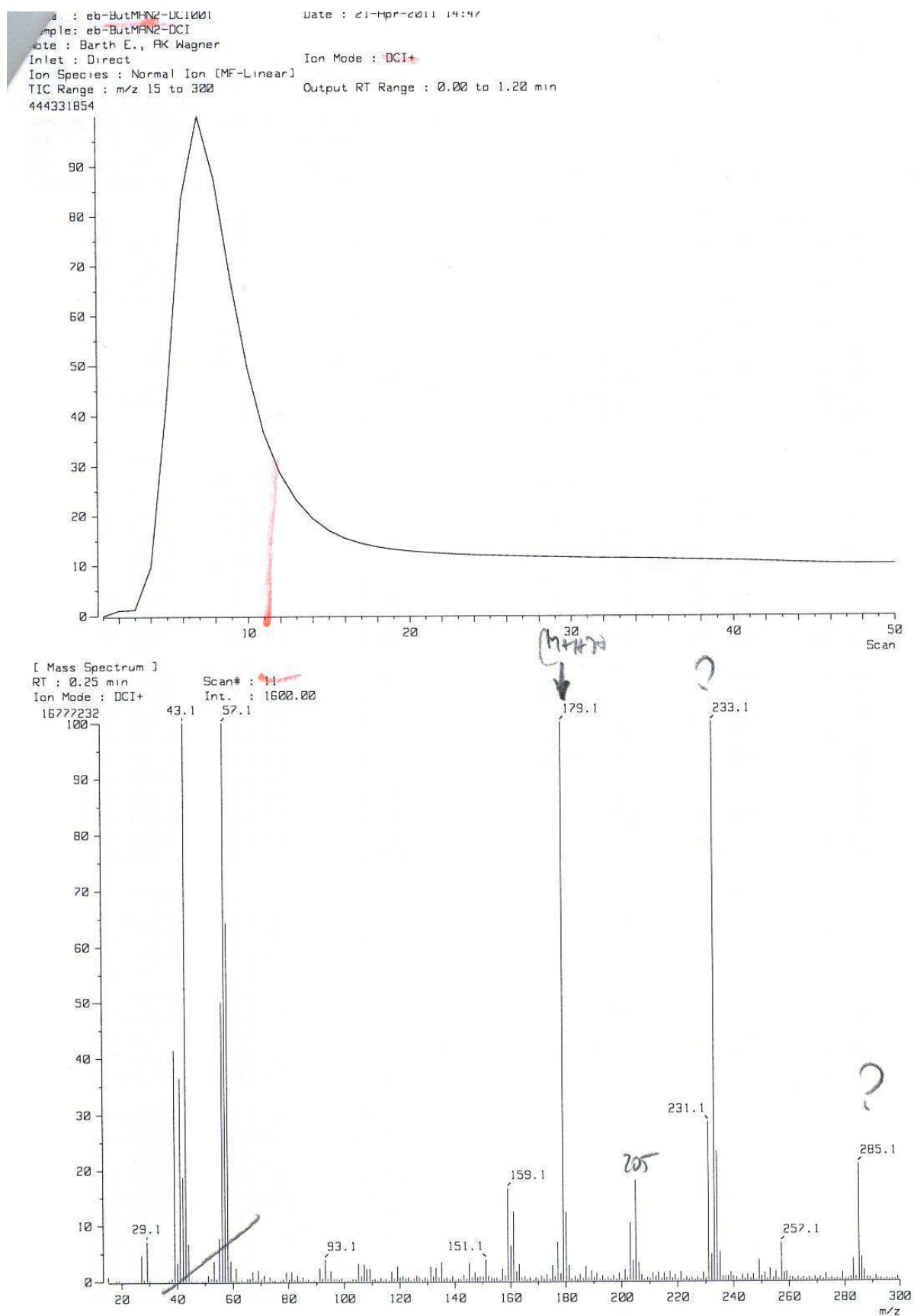


Figure 9.9: DCI⁺ mass spectra of PentyneMMan.

10 References

1. C.A. Lipinski, F. Lombardo, B.W. Dominy, and P.J. Feeney. Experimental and computational approaches to estimate solubility and permeability in drug discovery and development settings. *Adv Drug Deliv Rev.* 46:3-26 (2001).
2. B. Leader, Q.J. Baca, and D.E. Golan. Protein therapeutics: a summary and pharmacological classification. *Nat Rev Drug Discov.* 7:21-39 (2008).
3. J.L. Rosado, N.W. Solomons, R. Lisker, and H. Bourges. Enzyme replacement therapy for primary adult lactase deficiency. Effective reduction of lactose malabsorption and milk intolerance by direct addition of beta-galactosidase to milk at mealtime. *Gastroenterology.* 87:1072-1082 (1984).
4. H.L. Corwin, A. Gettinger, R.G. Pearl, M.P. Fink, M.M. Levy, M.J. Shapiro, M.J. Corwin, and T. Colton. Efficacy of recombinant human erythropoietin in critically ill patients: a randomized controlled trial. *JAMA.* 288:2827-2835 (2002).
5. H.J. Out, S.G. Driessen, B.M. Mannaerts, and H.J. Coelingh Bennink. Recombinant follicle-stimulating hormone (follitropin beta, Puregon) yields higher pregnancy rates in in vitro fertilization than urinary gonadotropins. *Fertil Steril.* 68:138-142 (1997).
6. M.P. Manns, J.G. McHutchison, S.C. Gordon, V.K. Rustgi, M. Shiffman, R. Reindollar, Z.D. Goodman, K. Koury, M. Ling, and J.K. Albrecht. Peginterferon alfa-2b plus ribavirin compared with interferon alfa-2b plus ribavirin for initial treatment of chronic hepatitis C: a randomised trial. *Lancet.* 358:958-965 (2001).
7. J. Blasi, E.R. Chapman, E. Link, T. Binz, S. Yamasaki, P. De Camilli, T.C. Sudhof, H. Niemann, and R. Jahn. Botulinum neurotoxin A selectively cleaves the synaptic protein SNAP-25. *Nature.* 365:160-163 (1993).
8. F.G. Banting, C.H. Best, J.B. Collip, W.R. Campbell, and A.A. Fletcher. Pancreatic extracts in the treatment of diabetes mellitus: preliminary report. 1922. *CMAJ.* 145:1281-1286 (1991).
9. A. Isaacs and J. Lindenmann. Virus interference. I. The interferon. *Proc R Soc Lond B Biol Sci.* 147:258-267 (1957).
10. S. Cohen. The stimulation of epidermal proliferation by a specific protein (EGF). *Dev Biol.* 12:394-407 (1965).
11. T. Friedmann. A brief history of gene therapy. *Nat Genet.* 2:93-98 (1992).
12. M.J. Cline, H. Stang, K. Mercola, L. Morse, R. Ruprecht, J. Brown, and W. Salser. Gene transfer in intact animals. *Nature.* 284:422-425 (1980).
13. S.A. Rosenberg, P. Aebersold, K. Cornetta, A. Kasid, R.A. Morgan, R. Moen, E.M. Karson, M.T. Lotze, J.C. Yang, S.L. Topalian, and et al. Gene transfer into humans--immunotherapy of patients with advanced melanoma, using tumor-infiltrating lymphocytes modified by retroviral gene transduction. *N Engl J Med.* 323:570-578 (1990).
14. D. Mahadevan, P. Chalasani, D. Rensvold, S. Kurtin, C. Pretzinger, J. Jolivet, R.K. Ramanathan, D.D. Von Hoff, and G.J. Weiss. Phase I Trial of AEG35156

- an Antisense Oligonucleotide to XIAP Plus Gemcitabine in Patients With Metastatic Pancreatic Ductal Adenocarcinoma. *Am J Clin Oncol* (2012).
15. B. Weide, S. Pascolo, B. Scheel, E. Derhovanessian, A. Pflugfelder, T.K. Eigentler, G. Pawelec, I. Hoerr, H.G. Rammensee, and C. Garbe. Direct injection of protamine-protected mRNA: results of a phase 1/2 vaccination trial in metastatic melanoma patients. *J Immunother.* 32:498-507 (2009).
 16. H.X. Chen, J.L. Marshall, E. Ness, R.R. Martin, B. Dvorchik, N. Rizvi, J. Marquis, M. McKinlay, W. Dahut, and M.J. Hawkins. A safety and pharmacokinetic study of a mixed-backbone oligonucleotide (GEM231) targeting the type I protein kinase A by two-hour infusions in patients with refractory solid tumors. *Clin Cancer Res.* 6:1259-1266 (2000).
 17. Z. Ni and P. Hui. Emerging pharmacologic therapies for wet age-related macular degeneration. *Ophthalmologica.* 223:401-410 (2009).
 18. M.D. de Smet, C.J. Meenken, and G.J. van den Horn. Fomivirsen - a phosphorothioate oligonucleotide for the treatment of CMV retinitis. *Ocul Immunol Inflamm.* 7:189-198 (1999).
 19. A. Shir, M. Ogris, E. Wagner, and A. Levitzki. EGF receptor-targeted synthetic double-stranded RNA eliminates glioblastoma, breast cancer, and adenocarcinoma tumors in mice. *PLoS Med.* 3:e6 (2006).
 20. N. Tomita, H. Azuma, Y. Kaneda, T. Ogihara, and R. Morishita. Application of decoy oligodeoxynucleotides-based approach to renal diseases. *Curr Drug Targets.* 5:717-733 (2004).
 21. E.S. Hildebrandt-Eriksen, V. Aarup, R. Persson, H.F. Hansen, M.E. Munk, and H. Orum. A Locked Nucleic Acid Oligonucleotide Targeting MicroRNA 122 Is Well-Tolerated in Cynomolgus Monkeys. *Nucleic Acid Ther* (2012).
 22. J. Stenvang and S. Kauppinen. MicroRNAs as targets for antisense-based therapeutics. *Expert Opin Biol Ther.* 8:59-81 (2008).
 23. S.M. Elbashir, J. Harborth, W. Lendeckel, A. Yalcin, K. Weber, and T. Tuschl. Duplexes of 21-nucleotide RNAs mediate RNA interference in cultured mammalian cells. *Nature.* 411:494-498 (2001).
 24. J.C. Burnett, J.J. Rossi, and K. Tiemann. Current progress of siRNA/shRNA therapeutics in clinical trials. *Biotechnol J.* 6:1130-1146 (2011).
 25. S. Hacein-Bey-Abina, C. Von Kalle, M. Schmidt, M.P. McCormack, N. Wulffraat, P. Leboulch, A. Lim, C.S. Osborne, R. Pawliuk, E. Morillon, R. Sorensen, A. Forster, P. Fraser, J.I. Cohen, G. de Saint Basile, I. Alexander, U. Wintergerst, T. Frebourg, A. Aurias, D. Stoppa-Lyonnet, S. Romana, I. Radford-Weiss, F. Gross, F. Valensi, E. Delabesse, E. Macintyre, F. Sigaux, J. Soulier, L.E. Leiva, M. Wissler, C. Prinz, T.H. Rabbitts, F. Le Deist, A. Fischer, and M. Cavazzana-Calvo. LMO2-associated clonal T cell proliferation in two patients after gene therapy for SCID-X1. *Science.* 302:415-419 (2003).
 26. S.R. Schwarze, A. Ho, A. Vocero-Akbani, and S.F. Dowdy. In vivo protein transduction: delivery of a biologically active protein into the mouse. *Science.* 285:1569-1572 (1999).
 27. R.K. June, K. Gogoi, A. Eguchi, X.S. Cui, and S.F. Dowdy. Synthesis of a pH-sensitive nitrilotriacetic linker to peptide transduction domains to enable

- intracellular delivery of histidine imidazole ring-containing macromolecules. *J Am Chem Soc.* 132:10680-10682 (2010).
28. I.M. Verma and N. Somia. Gene therapy -- promises, problems and prospects. *Nature.* 389:239-242 (1997).
 29. G. Walsh. Biopharmaceutical benchmarks 2010. *Nat Biotechnol.* 28:917-924 (2010).
 30. A.D. Frankel and C.O. Pabo. Cellular uptake of the tat protein from human immunodeficiency virus. *Cell.* 55:1189-1193 (1988).
 31. M. Green and P.M. Loewenstein. Autonomous functional domains of chemically synthesized human immunodeficiency virus tat trans-activator protein. *Cell.* 55:1179-1188 (1988).
 32. A. Joliot, C. Pernelle, H. Deagostini-Bazin, and A. Prochiantz. Antennapedia homeobox peptide regulates neural morphogenesis. *Proc Natl Acad Sci U S A.* 88:1864-1868 (1991).
 33. E. Dupont, A. Prochiantz, and A. Joliot. Penetratin story: an overview. *Methods Mol Biol.* 683:21-29 (2011).
 34. M. Lindgren and U. Langel. Classes and prediction of cell-penetrating peptides. *Methods Mol Biol.* 683:3-19 (2011).
 35. L. Chatelin, M. Volovitch, A.H. Joliot, F. Perez, and A. Prochiantz. Transcription factor *hoxa-5* is taken up by cells in culture and conveyed to their nuclei. *Mech Dev.* 55:111-117 (1996).
 36. K. Kilk, M. Magzoub, M. Pooga, L.E. Eriksson, U. Langel, and A. Graslund. Cellular internalization of a cargo complex with a novel peptide derived from the third helix of the islet-1 homeodomain. Comparison with the penetratin peptide. *Bioconjug Chem.* 12:911-916 (2001).
 37. S.R. Schwarze, A. Ho, A. Vocero-Akbani, and S.F. Dowdy. In vivo protein transduction: delivery of a biologically active protein into the mouse. *Science.* 285:1569-1572 (1999).
 38. A. van den Berg and S.F. Dowdy. Protein transduction domain delivery of therapeutic macromolecules. *Curr Opin Biotechnol.* 22:888-893 (2011).
 39. M.J. Tolentino, A.J. Brucker, J. Fosnot, G.S. Ying, I.H. Wu, G. Malik, S. Wan, and S.J. Reich. Intravitreal injection of vascular endothelial growth factor small interfering RNA inhibits growth and leakage in a nonhuman primate, laser-induced model of choroidal neovascularization. *Retina.* 24:132-138 (2004).
 40. A. Abuchowski, J.R. McCoy, N.C. Palczuk, T. van Es, and F.F. Davis. Effect of covalent attachment of polyethylene glycol on immunogenicity and circulating life of bovine liver catalase. *J Biol Chem.* 252:3582-3586 (1977).
 41. M. Ogris, S. Brunner, S. Schuller, R. Kircheis, and E. Wagner. PEGylated DNA/transferrin-PEI complexes: reduced interaction with blood components, extended circulation in blood and potential for systemic gene delivery. *Gene Ther.* 6:595-605 (1999).
 42. P.R. Dash, M.L. Read, L.B. Barrett, M.A. Wolfert, and L.W. Seymour. Factors affecting blood clearance and in vivo distribution of polyelectrolyte complexes for gene delivery. *Gene Ther.* 6:643-650 (1999).

43. J. DeRouchey, C. Schmidt, G.F. Walker, C. Koch, C. Plank, E. Wagner, and J.O. Radler. Monomolecular assembly of siRNA and poly(ethylene glycol)-peptide copolymers. *Biomacromolecules*. 9:724-732 (2008).
44. M. Bidlingmaier and C.J. Strasburger. Growth hormone. *Handb Exp Pharmacol*:187-200 (2010).
45. J.F. Mouser and J.S. Hyams. Infliximab: a novel chimeric monoclonal antibody for the treatment of Crohn's disease. *Clin Ther*. 21:932-942; discussion 931 (1999).
46. M.C. Cardoso and H. Leonhardt. Protein transduction: a novel tool for tissue regeneration. *Biol Chem*. 383:1593-1599 (2002).
47. H. Li and Z.M. Qian. Transferrin/transferrin receptor-mediated drug delivery. *Med Res Rev*. 22:225-250 (2002).
48. N. Tietze, J. Pelisek, A. Philipp, W. Roedl, T. Merdan, P. Tarcha, M. Ogris, and E. Wagner. Induction of apoptosis in murine neuroblastoma by systemic delivery of transferrin-shielded siRNA polyplexes for downregulation of Ran. *Oligonucleotides*. 18:161-174 (2008).
49. C. Dohmen, T. Frohlich, U. Lachelt, I. Rohl, H.-P. Vornlocher, P. Hadwiger, and E. Wagner. Defined Folate-PEG-siRNA Conjugates for Receptor-specific Gene Silencing. *Mol Ther Nucleic Acids*. 1:e7 (2012).
50. J. Kloeckner, L. Prasmickaite, A. Hogset, K. Berg, and E. Wagner. Photochemically enhanced gene delivery of EGF receptor-targeted DNA polyplexes. *J Drug Target*. 12:205-213 (2004).
51. I. Martin, C. Dohmen, C. Mas-Moruno, C. Troiber, P. Kos, D. Schaffert, U. Lachelt, M. Teixido, M. Gunther, H. Kessler, E. Giralt, and E. Wagner. Solid-phase-assisted synthesis of targeting peptide-PEG-oligo(ethane amino)amides for receptor-mediated gene delivery. *Org Biomol Chem*. 10:3258-3268 (2012).
52. Z. Li, R. Zhao, X. Wu, Y. Sun, M. Yao, J. Li, Y. Xu, and J. Gu. Identification and characterization of a novel peptide ligand of epidermal growth factor receptor for targeted delivery of therapeutics. *FASEB J*. 19:1978-1985 (2005).
53. S.D. Conner and S.L. Schmid. Regulated portals of entry into the cell. *Nature*. 422:37-44 (2003).
54. A. Subtil, A. Hemar, and A. Dautry-Varsat. Rapid endocytosis of interleukin 2 receptors when clathrin-coated pit endocytosis is inhibited. *J Cell Sci*. 107 (Pt 12):3461-3468 (1994).
55. I.M. Kaplan, J.S. Wadia, and S.F. Dowdy. Cationic TAT peptide transduction domain enters cells by macropinocytosis. *J Control Release*. 102:247-253 (2005).
56. K. von Gersdorff, N.N. Sanders, R. Vandenbroucke, S.C. De Smedt, E. Wagner, and M. Ogris. The internalization route resulting in successful gene expression depends on both cell line and polyethylenimine polyplex type. *Mol Ther*. 14:745-753 (2006).
57. A. Ferrari, V. Pellegrini, C. Arcangeli, A. Fittipaldi, M. Giacca, and F. Beltram. Caveolae-mediated internalization of extracellular HIV-1 tat fusion proteins visualized in real time. *Mol Ther*. 8:284-294 (2003).

58. J.-P. Behr. The Proton Sponge: a Trick to Enter Cells the Viruses Did Not Exploit. *CHIMIA International Journal for Chemistry*. 51:34-36 (1997).
59. D. Schaffert, C. Troiber, E.E. Salcher, T. Frohlich, I. Martin, N. Badgular, C. Dohmen, D. Edinger, R. Klager, G. Maiwald, K. Farkasova, S. Seeber, K. Jahn-Hofmann, P. Hadwiger, and E. Wagner. Solid-phase synthesis of sequence-defined T-, i-, and U-shape polymers for pDNA and siRNA delivery. *Angew Chem Int Ed Engl*. 50:8986-8989 (2011).
60. I.S. Zuhorn and D. Hoekstra. On the mechanism of cationic amphiphile-mediated transfection. To fuse or not to fuse: is that the question? *J Membr Biol*. 189:167-179 (2002).
61. Y. Xu and F.C. Szoka, Jr. Mechanism of DNA release from cationic liposome/DNA complexes used in cell transfection. *Biochemistry*. 35:5616-5623 (1996).
62. M. Meyer, A. Zintchenko, M. Ogris, and E. Wagner. A dimethylmaleic acid-melittin-polylysine conjugate with reduced toxicity, pH-triggered endosomolytic activity and enhanced gene transfer potential. *J Gene Med*. 9:797-805 (2007).
63. C. Dohmen, D. Edinger, T. Frohlich, L. Schreiner, U. Lachelt, C. Troiber, J. Radler, P. Hadwiger, H.P. Vornlocher, and E. Wagner. Nanosized Multifunctional Polyplexes for Receptor-Mediated SiRNA Delivery. *ACS Nano*. 6:5198-5208 (2012).
64. P. Guterstam, F. Madani, H. Hirose, T. Takeuchi, S. Futaki, S. El Andaloussi, A. Graslund, and U. Langel. Elucidating cell-penetrating peptide mechanisms of action for membrane interaction, cellular uptake, and translocation utilizing the hydrophobic counter-anion pyrenebutyrate. *Biochim Biophys Acta*. 1788:2509-2517 (2009).
65. M. Magzoub, A. Pramanik, and A. Graslund. Modeling the endosomal escape of cell-penetrating peptides: transmembrane pH gradient driven translocation across phospholipid bilayers. *Biochemistry*. 44:14890-14897 (2005).
66. C.M. Lee and I.F. Tannock. Inhibition of endosomal sequestration of basic anticancer drugs: influence on cytotoxicity and tissue penetration. *Br J Cancer*. 94:863-869 (2006).
67. A. Subramanian, P. Ranganathan, and S.L. Diamond. Nuclear targeting peptide scaffolds for lipofection of nondividing mammalian cells. *Nat Biotechnol*. 17:873-877 (1999).
68. E.A. Nigg. Nucleocytoplasmic transport: signals, mechanisms and regulation. *Nature*. 386:779-787 (1997).
69. D. Schaffert. Precise Oligoethyleneimine-based Carriers for Nucleic Acid Delivery, *Department of Pharmacy*, Vol. phd, Ludwig-Maximilians-University Munich, 2010, p. 161.
70. B.E. Houk, G. Hochhaus, and J.A. Hughes. Kinetic modeling of plasmid DNA degradation in rat plasma. *AAPS PharmSci*. 1:E9 (1999).
71. M. Werle and A. Bernkop-Schnurch. Strategies to improve plasma half life time of peptide and protein drugs. *Amino Acids*. 30:351-367 (2006).
72. M.S. Kormann, G. Hasenpusch, M.K. Aneja, G. Nica, A.W. Flemmer, S. Herber-Jonat, M. Huppmann, L.E. Mays, M. Illenyi, A. Schams, M. Griese, I.

- Bittmann, R. Handgretinger, D. Hartl, J. Rosenecker, and C. Rudolph. Expression of therapeutic proteins after delivery of chemically modified mRNA in mice. *Nat Biotechnol.* 29:154-157 (2011).
73. A.G. Harris. Somatostatin and somatostatin analogues: pharmacokinetics and pharmacodynamic effects. *Gut.* 35:S1-4 (1994).
74. C. Scholz and E. Wagner. Therapeutic plasmid DNA versus siRNA delivery: Common and different tasks for synthetic carriers. *J Control Release* (2011).
75. Y. Lee, T. Ishii, H. Cabral, H.J. Kim, J.H. Seo, N. Nishiyama, H. Oshima, K. Osada, and K. Kataoka. Charge-conversional polyionic complex micelles-efficient nanocarriers for protein delivery into cytoplasm. *Angew Chem Int Ed Engl.* 48:5309-5312 (2009).
76. T. Magnusson, R. Haase, M. Schleef, E. Wagner, and M. Ogris. Sustained, high transgene expression in liver with plasmid vectors using optimized promoter-enhancer combinations. *J Gene Med.* 13:382-391 (2011).
77. J.K. McClung and R.F. Kletzien. Analysis of BHK cell growth kinetics after microinjection of catalytic subunit of cyclic AMP-dependent protein kinase. *Mol Cell Biol.* 4:1079-1085 (1984).
78. M. Fenton, N. Bone, and A.J. Sinclair. The efficient and rapid import of a peptide into primary B and T lymphocytes and a lymphoblastoid cell line. *J Immunol Methods.* 212:41-48 (1998).
79. R. Thummel, T.J. Bailey, and D.R. Hyde. In vivo electroporation of morpholinos into the adult zebrafish retina. *J Vis Exp:e3603* (2011).
80. C. Voelkel, M. Galla, T. Maetzig, E. Warlich, J. Kuehle, D. Zychlinski, J. Bode, T. Cantz, A. Schambach, and C. Baum. Protein transduction from retroviral Gag precursors. *Proc Natl Acad Sci U S A.* 107:7805-7810 (2010).
81. C. Muratori, R. Bona, and M. Federico. Lentivirus-based virus-like particles as a new protein delivery tool. *Methods Mol Biol.* 614:111-124 (2010).
82. S.J. Kaczmarczyk, K. Sitaraman, H.A. Young, S.H. Hughes, and D.K. Chatterjee. Protein delivery using engineered virus-like particles. *Proc Natl Acad Sci U S A.* 108:16998-17003 (2011).
83. N.W. Kam, Z. Liu, and H. Dai. Carbon nanotubes as intracellular transporters for proteins and DNA: an investigation of the uptake mechanism and pathway. *Angew Chem Int Ed Engl.* 45:577-581 (2006).
84. N.W. Shi Kam, T.C. Jessop, P.A. Wender, and H. Dai. Nanotube molecular transporters: internalization of carbon nanotube-protein conjugates into Mammalian cells. *J Am Chem Soc.* 126:6850-6851 (2004).
85. N.W. Kam and H. Dai. Carbon nanotubes as intracellular protein transporters: generality and biological functionality. *J Am Chem Soc.* 127:6021-6026 (2005).
86. Slowing, II, B.G. Trewyn, and V.S. Lin. Mesoporous silica nanoparticles for intracellular delivery of membrane-impermeable proteins. *J Am Chem Soc.* 129:8845-8849 (2007).
87. S.S. Bale, S.J. Kwon, D.A. Shah, A. Banerjee, J.S. Dordick, and R.S. Kane. Nanoparticle-mediated cytoplasmic delivery of proteins to target cellular machinery. *ACS Nano.* 4:1493-1500 (2010).

88. P. Ghosh, X. Yang, R. Arvizo, Z.J. Zhu, S.S. Agasti, Z. Mo, and V.M. Rotello. Intracellular delivery of a membrane-impermeable enzyme in active form using functionalized gold nanoparticles. *J Am Chem Soc.* 132:2642-2645 (2010).
89. L. Liguori, B. Marques, A. Villegas-Mendez, R. Rothe, and J.L. Lenormand. Liposomes-mediated delivery of pro-apoptotic therapeutic membrane proteins. *J Control Release.* 126:217-227 (2008).
90. R.J. Debs, L.P. Freedman, S. Edmunds, K.L. Gaensler, N. Duzgunes, and K.R. Yamamoto. Regulation of gene expression in vivo by liposome-mediated delivery of a purified transcription factor. *J Biol Chem.* 265:10189-10192 (1990).
91. C.O. Weill, S. Biri, A. Adib, and P. Erbacher. A practical approach for intracellular protein delivery. *Cytotechnology.* 56:41-48 (2008).
92. L.Y. Chou, K. Ming, and W.C. Chan. Strategies for the intracellular delivery of nanoparticles. *Chem Soc Rev.* 40:233-245 (2011).
93. D. Dalkara, C. Chandrashekhar, and G. Zuber. Intracellular protein delivery with a dimerizable amphiphile for improved complex stability and prolonged protein release in the cytoplasm of adherent cell lines. *J Control Release.* 116:353-359 (2006).
94. N.A. Lissy, P.K. Davis, M. Irwin, W.G. Kaelin, and S.F. Dowdy. A common E2F-1 and p73 pathway mediates cell death induced by TCR activation. *Nature.* 407:642-645 (2000).
95. D. Jo, D. Liu, S. Yao, R.D. Collins, and J. Hawiger. Intracellular protein therapy with SOCS3 inhibits inflammation and apoptosis. *Nat Med.* 11:892-898 (2005).
96. R. Sawant and V. Torchilin. Intracellular transduction using cell-penetrating peptides. *Mol Biosyst.* 6:628-640 (2010).
97. J.M. Gump, R.K. June, and S.F. Dowdy. Revised role of glycosaminoglycans in TAT protein transduction domain-mediated cellular transduction. *J Biol Chem.* 285:1500-1507 (2010).
98. J.C. Mai, H. Shen, S.C. Watkins, T. Cheng, and P.D. Robbins. Efficiency of protein transduction is cell type-dependent and is enhanced by dextran sulfate. *J Biol Chem.* 277:30208-30218 (2002).
99. I. Nakase, T. Takeuchi, G. Tanaka, and S. Futaki. Methodological and cellular aspects that govern the internalization mechanisms of arginine-rich cell-penetrating peptides. *Adv Drug Deliv Rev.* 60:598-607 (2008).
100. F. Duchardt, M. Fotin-Mleczek, H. Schwarz, R. Fischer, and R. Brock. A comprehensive model for the cellular uptake of cationic cell-penetrating peptides. *Traffic.* 8:848-866 (2007).
101. K.M. Stewart, K.L. Horton, and S.O. Kelley. Cell-penetrating peptides as delivery vehicles for biology and medicine. *Org Biomol Chem.* 6:2242-2255 (2008).
102. F. Madani, S. Lindberg, U. Langel, S. Futaki, and A. Graslund. Mechanisms of cellular uptake of cell-penetrating peptides. *J Biophys.* 2011:414729 (2011).
103. L.N. Patel, J.L. Zaro, and W.C. Shen. Cell penetrating peptides: intracellular pathways and pharmaceutical perspectives. *Pharm Res.* 24:1977-1992 (2007).

104. I. Green, R. Christison, C.J. Voyce, K.R. Bundell, and M.A. Lindsay. Protein transduction domains: are they delivering? *Trends Pharmacol Sci.* 24:213-215 (2003).
105. M. Okuyama, H. Laman, S.R. Kingsbury, C. Visintin, E. Leo, K.L. Eward, K. Stoeber, C. Boshoff, G.H. Williams, and D.L. Selwood. Small-molecule mimics of an alpha-helix for efficient transport of proteins into cells. *Nat Methods.* 4:153-159 (2007).
106. H. Murata, J. Futami, M. Kitazoe, T. Yonehara, H. Nakanishi, M. Kosaka, H. Tada, M. Sakaguchi, Y. Yagi, M. Seno, N.H. Huh, and H. Yamada. Intracellular delivery of glutathione S-transferase-fused proteins into mammalian cells by polyethylenimine-glutathione conjugates. *J Biochem.* 144:447-455 (2008).
107. J. Futami, M. Kitazoe, T. Maeda, E. Nukui, M. Sakaguchi, J. Kosaka, M. Miyazaki, M. Kosaka, H. Tada, M. Seno, J. Sasaki, N.H. Huh, M. Namba, and H. Yamada. Intracellular delivery of proteins into mammalian living cells by polyethylenimine-cationization. *J Biosci Bioeng.* 99:95-103 (2005).
108. Y. Lee, T. Ishii, H.J. Kim, N. Nishiyama, Y. Hayakawa, K. Itaka, and K. Kataoka. Efficient delivery of bioactive antibodies into the cytoplasm of living cells by charge-conversional polyion complex micelles. *Angew Chem Int Ed Engl.* 49:2552-2555 (2010).
109. V.V. Didenko, H. Ngo, and D.S. Baskin. Polyethylenimine as a transmembrane carrier of fluorescently labeled proteins and antibodies. *Anal Biochem.* 344:168-173 (2005).
110. E. Wagner. *Polymers for siRNA Delivery: Inspired by Viruses to be Targeted, Dynamic, and Precise.* *Acc Chem Res* (2011).
111. D. Dalkara, G. Zuber, and J.P. Behr. Intracytoplasmic delivery of anionic proteins. *Mol Ther.* 9:964-969 (2004).
112. J. Browning and A. Ribolini. Studies on the differing effects of tumor necrosis factor and lymphotoxin on the growth of several human tumor lines. *J Immunol.* 143:1859-1867 (1989).
113. V. Russ, M. Gunther, A. Halama, M. Ogris, and E. Wagner. Oligoethylenimine-grafted polypropylenimine dendrimers as degradable and biocompatible synthetic vectors for gene delivery. *J Control Release.* 132:131-140 (2008).
114. L.S. Park, D. Friend, S. Gillis, and D.L. Urdal. Characterization of the cell surface receptor for a multi-lineage colony-stimulating factor (CSF-2 alpha). *J Biol Chem.* 261:205-210 (1986).
115. T.C. Farries and J.P. Atkinson. Biosynthesis of properdin. *J Immunol.* 142:842-847 (1989).
116. D.A. Zarling, A. Watson, and F.H. Bach. Mapping of lymphocyte surface polypeptide antigens by chemical cross-linking with BSOCOES. *J Immunol.* 124:913-920 (1980).
117. Z. Bouizar, M. Fouchereau-Peron, J. Taboulet, M.S. Moukhtar, and G. Milhaud. Purification and characterization of calcitonin receptors in rat kidney membranes by covalent cross-linking techniques. *Eur J Biochem.* 155:141-147 (1986).

118. A.D. Howard, S. de La Baume, T.L. Gioannini, J.M. Hiller, and E.J. Simon. Covalent labeling of opioid receptors with radioiodinated human beta-endorphin. Identification of binding site subunit. *J Biol Chem.* 260:10833-10839 (1985).
119. J. Carlsson, H. Drevin, and R. Axen. Protein thiolation and reversible protein-protein conjugation. N-Succinimidyl 3-(2-pyridyldithio)propionate, a new heterobifunctional reagent. *Biochem J.* 173:723-737 (1978).
120. L.L. Chen, J.J. Rosa, S. Turner, and R.B. Pepinsky. Production of multimeric forms of CD4 through a sugar-based cross-linking strategy. *J Biol Chem.* 266:18237-18243 (1991).
121. S. Joshi and R. Burrows. ATP synthase complex from bovine heart mitochondria. Subunit arrangement as revealed by nearest neighbor analysis and susceptibility to trypsin. *J Biol Chem.* 265:14518-14525 (1990).
122. L.C. Packman and R.N. Perham. Quaternary structure of the pyruvate dehydrogenase multienzyme complex of *Bacillus stearothermophilus* studied by a new reversible cross-linking procedure with bis(imidoesters). *Biochemistry.* 21:5171-5175 (1982).
123. M.P. Barnes and W.C. Shen. Disulfide and thioether linked cytochrome c-oligoarginine conjugates in HeLa cells. *Int J Pharm.* 369:79-84 (2009).
124. J. Mendez, A. Monteagudo, and K. Griebenow. Stimulus-responsive controlled release system by covalent immobilization of an enzyme into mesoporous silica nanoparticles. *Bioconjug Chem.* 23:698-704 (2012).
125. M. Meyer, C. Dohmen, A. Philipp, D. Kiener, G. Maiwald, C. Scheu, M. Ogris, and E. Wagner. Synthesis and biological evaluation of a bioresponsive and endosomolytic siRNA-polymer conjugate. *Mol Pharm.* 6:752-762 (2009).
126. D. Schaffert, M. Kiss, W. Rodl, A. Shir, A. Levitzki, M. Ogris, and E. Wagner. Poly(I:C)-mediated tumor growth suppression in EGF-receptor overexpressing tumors using EGF-polyethylene glycol-linear polyethylenimine as carrier. *Pharm Res.* 28:731-741 (2011).
127. H. Murata, M. Sakaguchi, J. Futami, M. Kitazoe, T. Maeda, H. Doura, M. Kosaka, H. Tada, M. Seno, N.H. Huh, and H. Yamada. Denatured and reversibly cationized p53 readily enters cells and simultaneously folds to the functional protein in the cells. *Biochemistry.* 45:6124-6132 (2006).
128. D. Saran and D.H. Burke. A versatile photocleavable bifunctional linker for facile synthesis of substrate-DNA conjugates for the selection of nucleic acid catalysts. *Bioconjug Chem.* 18:275-279 (2007).
129. J. Ottl, D. Gabriel, and G. Marriott. Preparation and photoactivation of caged fluorophores and caged proteins using a new class of heterobifunctional, photocleavable cross-linking reagents. *Bioconjug Chem.* 9:143-151 (1998).
130. X. Tang and I.J. Dmochowski. Synthesis of light-activated antisense oligodeoxynucleotide. *Nat Protoc.* 1:3041-3048 (2006).
131. V. Knorr, V. Russ, L. Allmendinger, M. Ogris, and E. Wagner. Acetal linked oligoethylenimines for use as pH-sensitive gene carriers. *Bioconjug Chem.* 19:1625-1634 (2008).

132. K. Engin, D.B. Leeper, J.R. Cater, A.J. Thistlethwaite, L. Tupchong, and J.D. McFarlane. Extracellular pH distribution in human tumours. *Int J Hyperthermia*. 11:211-216 (1995).
133. R.F. Murphy, S. Powers, and C.R. Cantor. Endosome pH measured in single cells by dual fluorescence flow cytometry: rapid acidification of insulin to pH 6. *J Cell Biol*. 98:1757-1762 (1984).
134. W.A. Blattler, B.S. Kuenzi, J.M. Lambert, and P.D. Senter. New heterobifunctional protein crosslinking reagent that forms an acid-labile link. *Biochemistry*. 24:1517-1524 (1985).
135. E. Saxon and C.R. Bertozzi. Cell surface engineering by a modified Staudinger reaction. *Science*. 287:2007-2010 (2000).
136. H. Yu, Y. Nie, C. Dohmen, Y. Li, and E. Wagner. Epidermal growth factor-PEG functionalized PAMAM-pentaethylenehexamine dendron for targeted gene delivery produced by click chemistry. *Biomacromolecules*. 12:2039-2047 (2011).
137. M.R. Vallee, P. Majkut, I. Wilkening, C. Weise, G. Muller, and C.P. Hackenberger. Staudinger-phosphonite reactions for the chemoselective transformation of azido-containing peptides and proteins. *Org Lett*. 13:5440-5443 (2011).
138. K. Maier and E. Wagner. Acid-labile traceless click linker for protein transduction. *J Am Chem Soc*. 134:10169-10173 (2012).
139. D. Pedersen and C. Rosenbohm. Dry Column Vacuum Chromatography. *Synthesis*. 2001:2431-2434 (2001).
140. C. Still, M. Kahn, and A. Mitra. Rapid chromatographic technique for preparative separations with moderate resolution. *The Journal of Organic Chemistry*. 43:2923-2925 (1978).
141. W.-h. Zhan, H.N. Barnhill, K. Sivakumar, H. Tian, and Q. Wang. Synthesis of hemicyanine dyes for 'click' bioconjugation. *Tetrahedron Letters*. 46:1691-1695 (2005).
142. S. Ciampi, M. James, P. Michaels, and J.J. Gooding. Tandem "click" reactions at acetylene-terminated Si(100) monolayers. *Langmuir*. 27:6940-6949 (2011).
143. A.T. Dirks, J.J. Cornelissen, and R.J. Nolte. Monitoring protein-polymer conjugation by a fluorogenic Cu(I)-catalyzed azide-alkyne 1,3-dipolar cycloaddition. *Bioconjug Chem*. 20:1129-1138 (2009).
144. H. Xie, O. Braha, L.Q. Gu, S. Cheley, and H. Bayley. Single-molecule observation of the catalytic subunit of cAMP-dependent protein kinase binding to an inhibitor peptide. *Chem Biol*. 12:109-120 (2005).
145. A.M. Deshpande, A.A. Natu, and N.P. Argade. Chemoselective Carbon-Carbon Coupling of Organocuprates with (Bromomethyl)methylmaleic Anhydride: Synthesis of Chaetomelic Acid A†. *The Journal of Organic Chemistry*. 63:9557-9558 (1998).
146. H.P. Acharya, K. Miyoshi, and Y. Kobayashi. Mercury-free preparation and selective reactions of propargyl (and propargylic) Grignard reagents. *Org Lett*. 9:3535-3538 (2007).

147. S. Tada, E.H. Chowdhury, C.S. Cho, and T. Akaike. pH-sensitive carbonate apatite as an intracellular protein transporter. *Biomaterials*. 31:1453-1459 (2010).
148. M. Yan, J. Du, Z. Gu, M. Liang, Y. Hu, W. Zhang, S. Priceman, L. Wu, Z.H. Zhou, Z. Liu, T. Segura, Y. Tang, and Y. Lu. A novel intracellular protein delivery platform based on single-protein nanocapsules. *Nat Nanotechnol*. 5:48-53 (2010).
149. J.B. McGuire, T.J. James, C.J. Imber, S.D. St Peter, P.J. Friend, and R.P. Taylor. Optimisation of an enzymatic method for beta-galactosidase. *Clin Chim Acta*. 326:123-129 (2002).
150. S.T. Henriques, J. Costa, and M.A. Castanho. Translocation of beta-galactosidase mediated by the cell-penetrating peptide pep-1 into lipid vesicles and human HeLa cells is driven by membrane electrostatic potential. *Biochemistry*. 44:10189-10198 (2005).
151. M. Kneen, J. Farinas, Y. Li, and A.S. Verkman. Green fluorescent protein as a noninvasive intracellular pH indicator. *Biophys J*. 74:1591-1599 (1998).
152. H. Ayame, N. Morimoto, and K. Akiyoshi. Self-assembled cationic nanogels for intracellular protein delivery. *Bioconjug Chem*. 19:882-890 (2008).
153. D. Ponti, M. Troiano, G.C. Bellenchi, P.A. Battaglia, and F. Gigliani. The HIV Tat protein affects processing of ribosomal RNA precursor. *BMC Cell Biol*. 9:32 (2008).
154. A. Efthymiadis, L.J. Briggs, and D.A. Jans. The HIV-1 Tat nuclear localization sequence confers novel nuclear import properties. *J Biol Chem*. 273:1623-1628 (1998).
155. V. Russ, T. Frohlich, Y. Li, A. Halama, M. Ogris, and E. Wagner. Improved in vivo gene transfer into tumor tissue by stabilization of pseudodendritic oligoethylenimine-based polyplexes. *J Gene Med*. 12:180-193 (2010).
156. T. Frohlich, D. Edinger, R. Klager, C. Troiber, E. Salcher, N. Badgujar, I. Martin, D. Schaffert, A. Cengizeroglu, P. Hadwiger, H.P. Vornlocher, and E. Wagner. Structure-activity relationships of siRNA carriers based on sequence-defined oligo (ethane amino) amides. *J Control Release* (2012).
157. J. Mueller, I. Kretzschmar, R. Volkmer, and P. Boisguerin. Comparison of cellular uptake using 22 CPPs in 4 different cell lines. *Bioconjug Chem*. 19:2363-2374 (2008).
158. J. Rejman, V. Oberle, I.S. Zuhorn, and D. Hoekstra. Size-dependent internalization of particles via the pathways of clathrin- and caveolae-mediated endocytosis. *Biochem J*. 377:159-169 (2004).
159. Y. Aoyama, T. Kanamori, T. Nakai, T. Sasaki, S. Horiuchi, S. Sando, and T. Niidome. Artificial viruses and their application to gene delivery. Size-controlled gene coating with glycocluster nanoparticles. *J Am Chem Soc*. 125:3455-3457 (2003).
160. T. Nakai, T. Kanamori, S. Sando, and Y. Aoyama. Remarkably size-regulated cell invasion by artificial viruses. Saccharide-dependent self-aggregation of glycoviruses and its consequences in glycoviral gene delivery. *J Am Chem Soc*. 125:8465-8475 (2003).

161. F. Osaki, T. Kanamori, S. Sando, T. Sera, and Y. Aoyama. A quantum dot conjugated sugar ball and its cellular uptake. On the size effects of endocytosis in the subviral region. *J Am Chem Soc.* 126:6520-6521 (2004).
162. J.P. Horwitz, J. Chua, R.J. Curby, A.J. Tomson, M.A. Da Rooze, B.E. Fisher, J. Mauricio, and I. Klundt. Substrates for Cytochemical Demonstration of Enzyme Activity. I. Some Substituted 3-Indolyl- β -D-glycopyranosides1a. *Journal of Medicinal Chemistry.* 7:574-575 (1964).
163. M. Meyer, A. Philipp, R. Oskuee, C. Schmidt, and E. Wagner. Breathing life into polycations: functionalization with pH-responsive endosomolytic peptides and polyethylene glycol enables siRNA delivery. *J Am Chem Soc.* 130:3272-3273 (2008).
164. M.A. Nieto and E. Palacian. Effects of temperature and pH on the regeneration of the amino groups of ovalbumin after modification with citraconic and dimethylmaleic anhydrides. *Biochim Biophys Acta.* 749:204-210 (1983).
165. D.B. Rozema, D.L. Lewis, D.H. Wakefield, S.C. Wong, J.J. Klein, P.L. Roesch, S.L. Bertin, T.W. Reppen, Q. Chu, A.V. Blokhin, J.E. Hagstrom, and J.A. Wolff. Dynamic PolyConjugates for targeted in vivo delivery of siRNA to hepatocytes. *Proc Natl Acad Sci U S A.* 104:12982-12987 (2007).
166. D.B. Rozema, K. Ekena, D.L. Lewis, A.G. Loomis, and J.A. Wolff. Endosomolysis by masking of a membrane-active agent (EMMA) for cytoplasmic release of macromolecules. *Bioconjug Chem.* 14:51-57 (2003).
167. E.M. Bachelder, T.T. Beaudette, K.E. Broaders, J. Dashe, and J.M. Frechet. Acetal-derivatized dextran: an acid-responsive biodegradable material for therapeutic applications. *J Am Chem Soc.* 130:10494-10495 (2008).
168. N. Murthy, J. Campbell, N. Fausto, A.S. Hoffman, and P.S. Stayton. Bioinspired pH-responsive polymers for the intracellular delivery of biomolecular drugs. *Bioconjug Chem.* 14:412-419 (2003).
169. K. Miyata, N. Nishiyama, and K. Kataoka. Rational design of smart supramolecular assemblies for gene delivery: chemical challenges in the creation of artificial viruses. *Chem Soc Rev.* 41:2562-2574 (2012).
170. A. Biswas, K.I. Joo, J. Liu, M. Zhao, G. Fan, P. Wang, Z. Gu, and Y. Tang. Endoprotease-mediated intracellular protein delivery using nanocapsules. *ACS Nano.* 5:1385-1394 (2011).
171. A. Zintchenko, A. Philipp, A. Dehshahri, and E. Wagner. Simple modifications of branched PEI lead to highly efficient siRNA carriers with low toxicity. *Bioconjug Chem.* 19:1448-1455 (2008).
172. A. Luong, T. Issarapanichkit, S.D. Kong, R. Fong, and J. Yang. pH-Sensitive, N-ethoxybenzylimidazole (NEBI) bifunctional crosslinkers enable triggered release of therapeutics from drug delivery carriers. *Org Biomol Chem.* 8:5105-5109 (2010).
173. V. Knorr, M. Ogris, and E. Wagner. An acid sensitive ketal-based polyethylene glycol-oligoethylenimine copolymer mediates improved transfection efficiency at reduced toxicity. *Pharm Res.* 25:2937-2945 (2008).
174. B.D. Mather, S.R. Williams, and T.E. Long. Synthesis of an Acid-Labile Diacrylate Crosslinker for Cleavable Michael Addition Networks. *Macromolecular Chemistry and Physics.* 208:1949-1955 (2007).

11 Publications

11.1 Original papers

K. Maier, I. Martin and E. Wagner. Sequence Defined Disulfide-linked Protein Transduction Shuttle. Submitted to Molecular Pharmaceutics.

K. Maier and E. Wagner. Acid-labile traceless click linker for protein transduction. J Am Chem Soc. 134:10169-10173 (2012).

M. Ackermann, M. Kubitza, K. Maier, A. Brawanski, G. Hauska, and A.L. Pina. The vertebrate homolog of sulfide-quinone reductase is expressed in mitochondria of neuronal tissues. Neuroscience. 199:1-12 (2011).

S. Abke, M. Neumeier, J. Weigert, G. Wehrwein, E. Eggenhofer, A. Schaffler, K. Maier, C. Aslanidis, J. Scholmerich, and C. Buechler. Adiponectin-induced secretion of interleukin-6 (IL-6), monocyte chemotactic protein-1 (MCP-1, CCL2) and interleukin-8 (IL-8, CXCL8) is impaired in monocytes from patients with type I diabetes. Cardiovasc Diabetol. 5:17 (2006).

11.2 Book chapters

K. Maier and E. Wagner. Intracellular Fate of Plasmid DNA Polyplexes. In V. Weissig and G.G.M. D`Souza (eds.), Organelle-Specific Pharmaceutical Nanotechnology, Wiley, New Jersey, 2010, pp. 123-143.

11.3 Poster presentations

Maier K, Fröhlich T, Russ V, Li Y, Halama A, Ogris M, Schaffert D, Schlossbauer A, Bein T and Wagner E. Biocompatible Nanosystems for Nucleic Acid & Protein Delivery. Third Annual Symposium on Nanobiotechnology: New Directions in NanoHealth, 2009, California NanoSystems Institute, UCLA, Los Angeles, USA.

Schlossbauer A, Bein T, Ruthardt N, Bräuchle C, Plank C, Schmidt C, Rädler J, Schaffert D, Dohmen C, Maier K, Meyer M, Ogris M and Wagner E. NIM workshop 2009. Nanosystems: from Information Technology to Life Science. Nanosystems Initiative Munich, LMU, Munich, Germany.

12 Acknowledgements

First of all, I would like to thank all my colleagues; without you this thesis would have never been possible. It was a pleasure to work together with each single member of the team. Thanks for your support and the fun we had over the last four years inside and also outside the lab. I want to thank my supervisor Professor Dr. Ernst Wagner for giving me the opportunity to perform this work in his research group. Thank you for giving me time and trust to develop new ideas and to bring them to fruition, as well as for scientific support and helpful discussions. My lab-mate Christian Dohmen deserves a big thank not just for numerous scientific discussions but rather for being a friend from the first minute we met. Thanks to my other lab-mates Edith Salcher and Claudia Scholz for keeping the place on their window ledge reserved for me. This oasis of tranquility and socialization made work much easier. Uli Lächelt my lab-mate during the last few days in the lab deserves a special thanks for being the most likeable scientist in the world. I am also very grateful to Thomas Froehlich for the phenomenal work trip to L.A, for buying me shoes and for many more. Thanks to David Schaffert for getting a biologist introduced in the secrets of organic chemistry and to Arzu Cengizeroglu for introducing me to cell culture. I also owe gratitude to Wolfgang Roedl for helping me with computer problems, broken machines and so much more. I have to thank Ursula Biebl (my lower bavarian countryman) for the delicious birthday cakes and so on. Without the help of our technicians Miriam Hoehn, Anna Kulinyak, Markus Kovac and Melinda Kiss who keep the lab running serious research would be impossible – thank you not only for that. I appreciate Dr. Martina Rüffer showing me how to teach students and what pleasure this can be. I am grateful to Manfred Ogris, Prajakta Oak, Christian Marfels, Rebekka Kubisch, Alexandra Vetter for helping me fighting with the microscope and FACS machines and... Thanks to Christina Troiber for synthesizing the transduction carrier molecule 71 and showing me how to keep cleanliness in a lab. Irene Martin, thanks for synthesizing polymer 386 and for bringing southern European lightheartedness into our lab. I will never forget the amazing evenings I spent with the phd room clique (Florian, Petra,...) – thanks a lot. Furthermore I want to thank Rafaela Kläger for sweetening me the last days of my phd work in the Schreibkammer. I would also like to say a big thank you to all master students who did an excellent job, namely Alice Pahnke, Evelyn Hartung, Verena Staudacher and Kathrin Abstiens.

But most of all I have to thank my family: My sisters Nadja and Martina for always having a sympathetic ear. Regina, Alois and Bernd for taking care of our children hectic times. My parents for their unconditional love, for my beautiful childhood, for my education, for their indefatigable support and for numerous other things. Christina for always being there, for bearing my moods and for the two most wonderful girls in the world. Mona and Paula for always making me happy and showing me the meaning of life on every day.